MODELING APPLICATION OF HYDROGEN RELEASE COMPOUND TO EFFECT *IN SITU* BIOREMEDIATION OF CHLORINATED SOLVENT – CONTAMINATED GROUNDWATER

THESIS

Ryan C. Wood, 1st Lieutenant, USAF

AFIT/GEM/ENV/05M-14

DEPARTMENT OF THE AIR FORCE
AIR UNIVERSITY

AIR FORCE INSTITUTE OF TECHNOLOGY

Wright-Patterson Air Force Base, Ohio

The views expressed in this thesis are those of the author and do not reflect the official policy or position of the United States Air Force, Department of Defense, or the United States government.

AFIT/GEM/ENV/05M-14

MODELING APPLICATION OF HYDROGEN RELEASE COMPOUND TO EFFECT *IN SITU* BIOREMEDIATION OF CHLORINATED SOLVENT-CONTAMINATED GROUNDWATER

THESIS

Presented to the Faculty

Department of Systems and Engineering Management

Graduate School of Engineering and Management

Air Force Institute of Technology

Air University

Air Education and Training Command

In Partial Fulfillment of the Requirements for the

Degree of Master of Science in Engineering Management

Ryan C. Wood, B.S.

1st Lieutenant, USAF

March 2005

AFIT/GEM/ENV/05M-14

MODELING APPLICATION OF HYDROGEN RELEASE COMPOUND TO EFFECT *IN SITU* BIOREMEDIATION OF CHLORINATED SOLVENT-CONTAMINATED GROUNDWATER

Ryan C. Wood, B.S.
1st Lieutenant, USAF

Approved:

_____/signed/_____	9 March 2005
Dr. Mark N. Goltz	date
Chairman, Advisory Committee	
_____/signed/_____	9 March 2005
Dr. Charles Bleckmann	date
Member, Advisory Committee	
_____/signed/_____	9 March 2005
Dr. Junqi Huang	date
Member, Advisory Committee	

Abstract

Chlorinated solvents like tetrachloroethene (PCE) and trichloroethylene (TCE) are common groundwater contaminants at military installations and industrial sites across the United States. Natural attenuation of chlorinated solvents is a promising alternative to traditional remediation methods. As natural attenuation processes have become better understood, efforts have intensified to find ways to enhance their efficiency. In recent years, a number of chlorinated solvent remedial efforts have involved enhancement of natural attenuation through addition of electron donors to facilitate reductive dechlorination, a major process contributing to the attenuation of chlorinated solvents. One popular method of adding electron donor in the field involves use of a product called Hydrogen Release Compound (HRC®).

This study investigates how application of HRC® might be implemented to remediate a site contaminated with PCE or its daughter products, under varying site conditions. The 3-D reactive transport model RT3D was coupled with a dual-Monod biodegradation submodel to simulate the effect of the hydrogen generated by HRC® on accelerating the biodegradation of dissolved chlorinated solvents. Varying site conditions and injection well configurations were investigated to determine the effect of these environmental and design conditions on overall treatment efficiency. The model was applied to data obtained at a chlorinated solvent contaminated site at Vandenberg AFB, where a pilot study of HRC® injection was conducted. Historical data were initially used to calibrate the model, under the assumption that natural reductive dehalogenation processes are

occurring at the site. The model was then applied to predict how HRC® injection enhances natural attenuation processes. Model predictions were compared to the results of the pilot study. The model-simulated concentrations were relatively consistent with concentrations measured at the site, indicating the model may be a useful design tool, as well as an aid to help us better understand how HRC® injection may enhance natural attenuation of chlorinated solvents.

Acknowledgements

This thesis was made possible through the guidance and assistance of many individuals. First and foremost, I must thank Dr. Mark Goltz for his tireless assistance and his insightful guidance. I would also like to thank Dr. Junqi Huang for his amazing technical and theoretical abilities and assistance in designing the model. I also appreciate the instruction I received by Dr. Charles Bleckmann, who brought the amazing world of microbiology into a new light allowing me to understand better many of the processes significant to this thesis. I am also grateful to Ms. Clarissa Hansen at the COE Waterways Experimentation Station for the instruction and assistance she provided with GMS. Thanks also to Regenesis, Tetra Tech, and Vandenberg AFB Environmental Flight for all the support. Thanks to AFCEE for sponsoring this research. This study was partially supported by the Strategic Environmental Research and Development Program through Project CU-1295, Impact of DNAPL Source Zone Treatment: Experimental and Modeling Assessment of Benefits of Partial Source Removal.

Ryan C. Wood

Table of Contents

Page

Page

Page

List of Figures

Page

Page

Page

List of Tables

Page

MODELING APPLICATION OF HYDROGEN RELEASE COMPOUND TO EFFECT *IN SITU* BIOREMEDIATION OF CHLORINATED SOLVENT-CONTAMINATED GROUNDWATER

1.0 Introduction

1.1 Motivation

The United States faces a very large groundwater contamination problem. Although the total number of contaminated groundwater sites is not known, estimates range from 300,000 to 400,000 (NRC, 1994). The money needed to clean up these sites over the next 30 years has been estimated to exceed $1 trillion (NRC, 1994).

Beginning with the 1962 publication of Silent Spring by Rachel Carson, the public began to gain awareness of a potential connection between man-made (anthropogenic) pollution and impacts to human health and the environment. This connection was confirmed in the public mind with the news of problems at an elementary school and residential housing development that had been constructed on a former chemical waste disposal site in Love Canal, NY (LaGrega *et al.,* 1994). Residents in the area were exposed to hazardous chemicals that were disposed of at the site and had leaked into the earth beneath this neighborhood. A reporter following up on stories of a few diseases among neighborhood children that seemed to be linked to indoor fumes discovered more than 100 examples of chemically induced illness and himself smelled the fumes in many neighborhood basements (LaGrega *et al.,* 1994). The threat of these pollutants to human health and safety was now apparent.

It has been said that Love Canal was the pivotal event that eventually resulted in the passage of the Comprehensive Environmental Response, Compensation, and Liability Act (CERCLA) in 1980 by the U.S. Congress (LaGrega *et al.,* 1994). CERCLA established a "Superfund" and a remedial process to cleanup contaminated sites that posed a threat to human health and the environment. While the Act initially provided $1.6 billion, this proved to be a gross underestimate of remediation costs. A decade later, the National Research Council (NRC) would estimate the total cost to cleanup the nation's hazardous waste sites as $1 trillion over 30 years (NRC, 1994; Lee *et al.,* 1998). In addition to the huge cost, another obstacle to completion of the remediation required by CERCLA was due to the fact that environmental cleanup technologies were in their infancy in 1980, and in many cases technologies simply were not available to attain the remediation goals in a reasonable amount of time (Travis and Doty, 1990).

The CERCLA remedial process requires that potentially hazardous sites be characterized, so that the risks posed by the sites could be quantified. As a result of these site characterizations, which were conducted nationwide, it was found that chlorinated solvents and their natural degradation byproducts represent the most prevalent organic groundwater contaminants in the country (McCarty and Semprini, 1994). Two chlorinated solvents, trichloroethylene (TCE) and tetrachloroethylene (PCE), are ranked first and third, respectively, in a listing of the 25 most frequently detected groundwater contaminants (NRC, 1994). TCE and PCE are chlorinated aliphatic hydrocarbons (CAHs), widely used as industrial solvents for cleaning and degreasing. From 1925 to 1970, TCE was used throughout the country without regulation, leaving a legacy of TCE

contamination at countless former industrial sites and at most military installations in the U.S. (Stiber *et al.,* 1999). An example of the widespread occurrence of both TCE and PCE was seen in a survey in New Jersey of over 1,000 wells, of which 58% and 43% were contaminated by TCE and PCE, respectively (Pankow and Cherry, 1996).

Chlorinated solvents such as TCE and PCE are classified as dense non-aqueous phase liquids (DNAPLs) as they are denser than water. Thus, if spilled on the ground or leaked from underground storage tanks, they percolate as separate phase liquids through the unsaturated zone, eventually reaching the water table. Because the DNAPLs are denser than water, they continue to travel down through the water table, leaving behind residual DNAPL as illustrated in Figure 1.1.

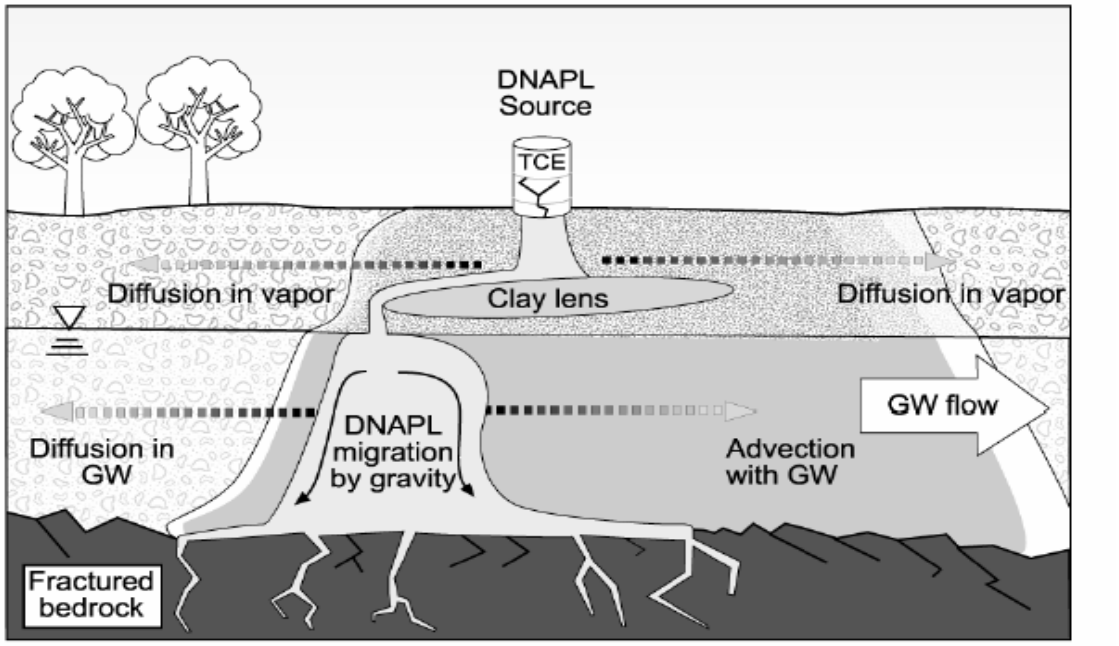

Figure 1.1 DNAPL Behavior in the Subsurface (U.S. EPA, 2001)

When the DNAPLs encounter low permeability lenses or confining layers, they spread laterally, creating DNAPL pools. These DNAPL residuals and pools slowly dissolve into the groundwater, resulting in plumes that can extend for miles. Because of the relatively low solubility of both TCE and PCE, the DNAPL source area can persist for decades (Pankow and Cherry, 1996).

There are currently no proven technologies to remediate DNAPL source zones (Pankow and Cherry, 1996), which leaves us with the management option of dealing with CAHs in the dissolved phase. In the 1980's, pump-and-treat was the chosen treatment method for thousands of DNAPL sites throughout the United States (Pankow and Cherry, 1996). It is now well established that pump-and-treat is not an effective method for remediating CAH-contaminated groundwater, as it could take many decades or longer to reach cleanup goals (Pankow and Cherry, 1996).

The nature of DNAPLs and the limitations of conventional technologies have motivated development of innovative technologies to help manage CAH-contaminated sites to meet remediation goals (Pankow and Cherry, 1996). Some innovative technologies that are applicable to manage CAH-contaminated groundwater include permeable reactive barriers (PRBs) (NRC, 1994), monitored natural attenuation (MNA) (Suthersan, 2002), and enhanced *in situ* bioremediation (Suthersan, 2002).

A permeable reactive barrier consists of a zone of reactive material installed in the path of a plume of contaminated groundwater. The material in the barrier chemically,

biologically, or physically treats the contaminant as it passes through. The reactive material may consist of granular iron or some other reduced metal, lime, an electron donor-releasing compound, or an electron acceptor-releasing compound (Richardson and Nicklow, 2002). The active component of the PRB can be varied in order to treat a wide variety of contaminants.

As PRBs are typically installed using trenching equipment, the depths of PRBs are limited, and they may be unsuitable to manage deep contamination. Depending on the emplacement technique, the maximum depth of a PRB ranges from 25 to 200 feet with costs ranging from $5 to $200 per square foot (see Table 1.1). (Richardson and Nicklow, 2002).

Table 1.1 Summary of Barrier Emplacement Techniques (from Gavaskar *et al.* (2000) as seen in Richardson and Nicklow (2002))

Emplacement Technique	Maximum Depth (ft)	Cost	Comments
Caisson-Based Emplacement	50	$50-$300/ vertical ft	Relatively inexpensive
Mandrel-Based Emplacement	40-50	$10-$25/sf	Relatively inexpensive and fast production rate; a 3-5 in-thick zone can be installed in a single pass
Continuous Trenching	25	$5-$12/sf	High production rate High mobilization cost
Jetting	200	$40-$200/sf	Ability to install barrier around existing buried utilities
Deep Soil Mixing	150	$80-$200/sf	May not be cost-effective for permeable barriers; columns are 3-5 ft in diameter
Hydraulic Fracturing	80-120	$2,300 per fracture	Can be emplaced at deep sites Fractures are only up to 3 in thick
Vibrating Beam	100	$8/sf	Driven beam is only 6 in wide

As PRBs are a passive technology, changing groundwater flow conditions may permit contaminants to bypass the barrier. Another possible limitation is the longevity of the reactive media. Due to a lack of long-term experience with these systems, the schedule to replenish the reactive media, which would entail considerable expense, is unknown (AFCEE, 2004).

MNA is defined as the use of natural processes to achieve site remediation goals (NRC, 2000). These natural processes generally include all physical, chemical, and biological mechanisms that can reduce the concentration and mass of a contaminant in groundwater, though most commonly MNA relies on indigenous microorganisms to biodegrade the contaminant. It has been shown that under the right biogeochemical conditions, natural attenuation can be an effective method for the remediation of CAH-contaminated groundwater (Clement *et al.,* 2000). Unfortunately, in many instances, although site conditions may promote some degree of CAH attenuation, attenuation falls short of being "acceptable", where acceptable is typically defined as achievement of remedial objectives within a specified time frame. Other disadvantages of MNA are that it can be seen by the public as the "do nothing" solution (NRC, 1994), it can be difficult to assess the efficiency of the process (NRC, 2000), and with certain contaminants, natural attenuation can create a compound that is more toxic than the original (NRC, 2000).

Biostimulation and bioaugmentation are two techniques that can be used to accelerate the process of natural attenuation, in order to address the problems of MNA noted above. The use of such techniques is termed enhanced *in situ* bioremediation (EISB). It has been shown that naturally occurring microorganisms can use hydrogen as an electron donor to reductively dechlorinate CAHs (Smatlack *et al.,* 1996). Reductive dechlorination is recognized as one of the primary attenuation mechanisms by which chlorinated solvent groundwater plumes can be contained and/or remediated. The bacteria necessary for reductive dechlorination are called halorespirors. The dehalogenation process is shown

in Figure 1.2:

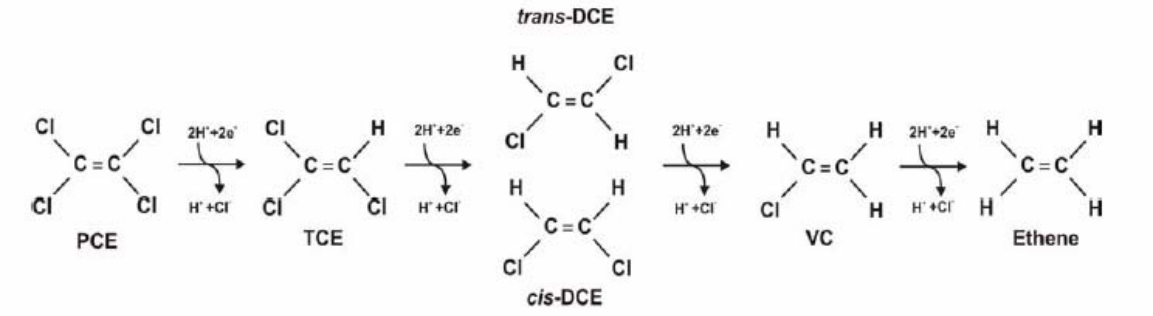

Figure 1.2 Sequential Reduction of PCE to Ethene by Reductive Dehalogenation (AFCEE, 2004)

Halorespirors appear to be common, although not ubiquitous in nature. When bacteria at a site prove incapable of completely dehalogenating the target CAH contaminant, bioaugmentation may be used to introduce halorespiring organisms that are able to achieve complete dehalogenation (Major *et al.,* 2002). Bioaugmentation is performed by injecting a consortium of laboratory-grown halorespirors into the subsurface. It is hoped that the introduced microorganisms will adjust to the subsurface environment and begin using the target CAHs as electron acceptors (in the presence of either introduced or natural electron donors). Bioaugmentation has been used successfully in a number of laboratory and field studies, but there have been instances where the injected bacteria could not adapt to the subsurface environment and the process failed (Nyer, 2003).

Unfortunately, even if they are present at a site, halorespiring organisms may be unable to completely dehalogenate PCE or TCE to ethene (Hendrickson *et al.,* 2002; He *et al.,* 2003). As seen in figure 1.2, hydrogen plays an important role in reductive

dehalogenation. Hydrogen can be the limiting factor to the success of MNA. A common technique for enhancing *in situ* bioremediation by reductive dehalogenation is to add substrates to the subsurface. These substrates serve as the electron donor by providing the hydrogen necessary for reductive dehalogenation to proceed. Table 1.2 describes many of the different substrates that have been used for EISB, to stimulate reductive dehalogenation of CAHs by indigenous microorganisms.

Table 1.2 Substrates used for enhanced anaerobic bioremediation (AFCEE, 2004)

Substrate	Typical Delivery Techniques	Form of Application	Frequency of Injection
Soluble Substrates			
Lactate and Butyrate	Injection wells or circulation systems	Acids or salts diluted in water	Continuous to monthly
Methanol and Ethanol	Injection wells or circulation systems	Diluted in water	Continuous to monthly
Sodium Benzoate	Injection wells or circulation systems	Dissolved in water	Continuous to monthly
Molasses, High Fructose Corn Syrup	Injection wells	Dissolved in water	Continuous to monthly
Viscous Fluid Substrates			
HRC® or HRC-X™	Direct injection	Straight injection	Annually to bi-annually for HRC® (typical); Every 3 to 4 years for HRC-X™; potential for one-time application
Vegetable Oils	Direct injection or injection wells	Straight oil injection with water push, or high oil:water content (>20 percent oil) emulsions	One-time application (typical)
Low-Viscosity Fluid Substrates			
Vegetable Oil Emulsions	Direct injection or injection wells	Low oil content (<10 percent) microemulsions suspended in water	Every 2 to 3 years (typical); potential for one-time application
Solid Substrates			
Mulch and Compost	Trenching or excavation	Trenches, excavations, or surface amendments	One-time application (typical)
Experimental (few applications)			
Whey (soluble)	Direct injection or injection wells	Dissolved in water or slurry	Monthly to annually
Chitin (solid)	Trenching or injection of a chitin slurry	Solid or slurry	Annually to biannually; potential for one-time application
Hydrogen (gas)	Biosparging wells	Gas injection	Pulsed injection (daily to weekly)
Humic Acids (electron shuttles)	Direct injection or injection wells	Dissolved in water	Unknown; potentially semi-annually to annually

One biostimulation technique that has been successfully applied involves use of Hydrogen Release Compound (HRC®) to provide indigenous microorganisms with hydrogen, which serves as an electron donor (Koenigsberg, 2002). HRC® is a polylactate esther designed to slowly release lactic acid to groundwater over a period of many months. The lactic acid is then biotransformed to pyruvic acid and subsequently to acetic

and propionic acids, releasing hydrogen in both steps (Faron *et al.,* 1999). HRC® has a number of advantages when compared to other potential electron donors. First, HRC® is a viscous product that can be formulated to reside in the subsurface for a period of many months to a couple years. This provides an advantage over many of the alternative substrates as the number of applications can be reduced. HRC® can be injected directly into the subsurface, with no need for excavation or a circulating system. HRC® has also been used successfully at many sites for the remediation of PCE, TCE and their daughter products, which are frequently the contaminants of concern at Superfund and DoD sites. Another advantage of HRC® is it is an engineered product that comes with professional support and application design. This can be a great help in the design of the treatment process, including determination of well locations and amounts of donor to be injected.

HRC® has been used to successfully accelerate reductive dechlorination of PCE and TCE at hundreds of sites (Koenigsberg, 2002). At a site in Sunnyvale, California, where a manufacturing operation resulted in substantial amounts of PCE, TCE, cis-1,2-dichloroethylene (DCE) and vinyl chloride (VC) in the soil and groundwater, HRC® was applied as an alternative to the expensive and ineffective pump-and-treat system that was in use. The HRC® proved effective in stimulating indigenous organisms to reductively dechlorinate the CAH contaminants to ethene (Vique and Koenigsberg, 2003). Contaminant reductions were to such an extent that regulatory permission was granted to shut down the pump-and-treat system.

Based on its potential to help the DoD manage CAH-contaminated sites, the effectiveness and applicability of HRC® is being evaluated at some installations. A pilot study of EISB is currently underway at a CAH-contaminated site at Vandenberg Air Force Base. The site was contaminated by a former rocket launch facility that had used large amounts of TCE to degrease engines prior to launch. HRC® was chosen as the method of treatment for the Vandenberg site because it promised to be a cost effective method of remediation that could produce results quicker than by relying on MNA alone. In addition, HRC® was the substrate of choice because it had gained regulatory acceptance in California, and there was more documented evidence of success with HRC® than was available at the time for other substrates that were under consideration (TetraTech, personal communications).

When choosing EISB as a remediation method, it is very important to design the injection scheme properly, and to provide evidence that the method is working. HRC® injection schemes are currently designed using a simple model that is used to determine the mass of HRC® necessary to meet remediation objectives (Regenesis, 2002). This model calculates the amount of HRC® that would be needed to provide enough hydrogen to accommodate the competing electron acceptor load and calculated mass of CAHs in the targeted treatment zone. A more advanced model of HRC® that includes reactive transport can be useful in system design. The model can be used to quickly run through a number of alternative designs of HRC® injection schemes and quantities. The effect of the site's hydrology on the HRC® injection scheme can be determined and the design can be adjusted accordingly.

Models can also be used to provide evidence that EISB is achieving remedial objectives. For example, at the Vandenberg site, the data from sampling wells are the only information available to the project managers to answer questions about the performance of the HRC®. These data can be misleading if the area near the wells is more (or less) effectively remediated than surrounding areas. The ability to model the performance of the HRC® based upon monitoring data will give the decision maker additional information regarding treatment effectiveness.

Models have been used successfully in the past to demonstrate the success of MNA in achieving remedial objectives at many sites contaminated with CAHs. Clement et al. (2002) successfully used the U.S. Environmental Protection Agency's (1998) MNA screening protocol along with the computer model BIOCHLOR to determine if the contamination at a Louisiana Superfund site was being degraded via MNA at an acceptable rate. BIOCHLOR along with other computer models such as BIOSCREEN were developed to show natural attenuation of CAHs. On the other hand, the benefits of modeling have not been demonstrated for EISB using HRC®. Just as models have been used to demonstrate that MNA has achieved remedial objectives, modeling can be used to provide evidence that HRC® application is achieving remedial objectives.

In addition to helping remedial project managers design a remediation technology application and determine whether the technology is achieving remedial objectives, models are also useful in helping managers gain an understanding of the remediation problem and the important processes that affect contaminant fate and transport in order to

formulate a site conceptual model. For instance, the accumulation of DCE at a site can give the impression that the reductive dehalogenation process is not proceeding favorably. In fact, this might not be the case. DCE might be accumulating because: 1) unknown sources are providing a constant source of parent material such as PCE or TCE, 2) degradation rates of the parent compounds are faster than those of the daughter compounds ("kinetic disparity"), resulting in accumulation of the daughter compound, and/or 3) differences in solubility of the parent and daughter compounds could make the daughter compounds more prevalent in the dissolved phase (Koenigsberg, 2002). Modeling can be helpful in determining the cause of DCE accumulation, thereby helping the remedial project manager make a decision with regard to the best course of action to deal with the problem. When the contaminated site is improperly understood, bad decisions may be made and failure may result. Modeling helps understanding; fostering better management decisions.

The objective of this research is to develop a model of the HRC® technology in order to accurately simulate real-world applications of HRC® to biodegrade CAHs in the subsurface. The model will then be validated by comparing its output to the real-world data available at the Vandenberg site.

1.2 Research Questions

1. Is HRC® an effective additive to stimulate the degradation of CAHs to the degree required in a reasonable time?
2. Does HRC® aid in the complete reduction of TCE and PCE to innocuous end-products or does the reduction stop short, producing a large amount of equally or even more harmful by-product such as vinyl chloride?

3. What subsurface conditions are favorable or unfavorable to the use of HRC® to accelerate natural attenuation?

4. How may an HRC® injection system be designed to ensure a CAH-plume is effectively treated to meet remediation goals?

1.3 Methodology

A review of current literature will focus on 1) the properties and function of HRC® in the subsurface as well as prior field applications, 2) reductive dechlorination of PCE and TCE to ethene and the challenges to avoiding a stall at DCE or VC, 3) numerical models with the ability to simulate both natural and enhanced reductive dehalogenation, 4) bioaugmentation to implement reductive dechlorination, and 5) ways by which modeling can aid in understanding technology and in designing treatment strategies. A model will then be selected and applied to the Vandenberg site. In order to assess the impact of the HRC® on the site, a comparison will be made between the real-world CAH concentrations obtained from monitoring the HRC® pilot study, and model simulations of CAH concentrations for a scenario where the HRC® pilot study never took place. This comparison will help answer research question 1. Research question 2 will be answered by modeling the pilot study site as if there were no HRC® injected. The resulting data will then be compared to the actual pilot study monitoring data. If TCE is reduced further with the addition of HRC® than the model assuming no HRC® use predicts, we have evidence that HRC® does effectively speed up the degradation of TCE. In addition, we will also compare the model-simulated and actual build-up of byproducts such as VC to determine if more VC is generated when HRC® is used than when it is not used. In order to answer research question 3, some model sensitivity studies will be conducted.

Key parameters will be varied over a predetermined range to see the effect they have on the degradation of TCE. This will make it possible to discover which parameters are the most important and which have little impact on determining CAH fate and transport. Research question 4 can be answered using the model to vary injection well locations and HRC® amounts, and observe the resultant impact on CAH concentrations.

By modeling the most significant processes that affect CAH fate and transport in a contaminated system being treated with HRC®, it is hoped that we can gain understanding into the effectiveness of the HRC® treatment. For given site conditions and HRC® design parameters (amounts and locations of HRC® injection), the model can be used to predict the extent to which remedial objectives are achieved.

1.4 Scope and Limitations

Although this research deals with enhanced reductive dechlorination of chlorinated solvents with the addition of electron donor, it was performed focusing on HRC, and therefore is not applicable for other electron donor producing substrates. There are a number of limitations to this study. Section 3.3.4 includes a list of specific assumptions made for the model used in this study. Other limitations are listed below:

1. The soil matrix at the site was assumed to be homogeneous.
2. When conducting the natural attenuation modeling, the CAHs were assumed to decay according to first-order kinetics.
3. Initial conditions throughout the model domain had to be estimated from concentration measurements made at a relatively few discrete sampling points.

These concentration measurements were extrapolated to define the initial concentration distribution of contaminant. 4. Model validation depended on comparing model predictions with a number of data points that were limited in both space and time.

5. In this modeling study, it was assumed that certain processes (*e.g.* fermentation and NAPL dissolution) were fast with respect to other processes (*e.g.* advection, reductive dechlorination). Based on this assumption, the kinetics of the fast processes were not modeled.

2.0 Literature Review

2.1 Overview

Chlorinated organic compounds are considered serious groundwater contaminants because of their persistence and mobility in the subsurface, their widespread use, and their effects on human health (Sleep, 2004). When a DNAPL (e.g., chlorinated solvent like PCE and TCE) is released to the subsurface it will penetrate downward through the vadose zone. Because the DNAPL is denser than water, it will continue down through the saturated zone. As it travels, the DNAPL breaks up and forms residual DNAPL in the vadose and saturated zones, or remains in DNAPL pools in areas of the aquifer where capillary pressure was such that the DNAPL could not penetrate. As groundwater flows past residual DNAPL in the saturated zone, or flows over pools, soluble chlorinated solvents will slowly dissolve into the flowing groundwater (Wiedemeier *et al.,* 1999). Thus, residual DNAPL throughout the saturated zone will act as a long term, continuous source of dissolved contaminants. This residual DNAPL can persist as a source of contaminant for decades (Sleep, 2004).

2.2 Treatment Alternatives

The nature of DNAPLs is such that traditional approaches to groundwater cleanup will generally not succeed. Accordingly, a number of alternatives have been suggested to deal with the problem of chlorinated solvents in the subsurface. Thus far, no technology has been developed that is effective in removing the DNAPL source, so there has been a focus on developing alternative technologies and strategies to manage the dissolved contaminant plume that emanates from the source. These alternatives vary from

installation intensive methods such as emplacement of permeable reactive barriers, to less intrusive methods like monitored natural attenuation or enhanced bioremediation. Each alternative has advantages and disadvantages, and may or may not be appropriate for application at a site, depending on site specific characteristics. Due to the limitations mentioned in Ch. 1, PRBs will not be investigated further. A closer investigation follows of two techniques that show promise as low-impact, low-cost solutions.

2.2.1 Monitored Natural Attenuation

Monitored natural attenuation is defined by the Environmental Protection Agency (EPA) as follows:

> [The] reliance on natural attenuation processes (within the context of a carefully controlled and monitored site cleanup approach) to achieve site-specific remediation objectives within a time frame that is reasonable compared to that offered by other more active methods. The 'natural attenuation processes' that are at work in such a remediation approach include a variety of physical, chemical, or biological processes that, under favorable conditions, act without human intervention to reduce the mass, toxicity, mobility, volume, or concentration of contaminants in soil or groundwater. These in-situ processes include biodegradation; dispersion; dilution; sorption; volatilization; radioactive decay; and chemical or biological stabilization, transformation, or destruction of contaminants. (EPA, 1999)

Due to the complex and often poorly understood nature of contaminants in the subsurface, monitored natural attenuation (MNA) has been difficult to rely on as sole means of restoration. However, significant progress has been made in quantifying the role of MNA in groundwater contaminant remediation in the past decade (Wiedemeier *et al.,* 1999). MNA affects the fate and transport of chlorinated aliphatic hydrocarbons (CAHs) in many ways. For this study, the process of *in situ* biodegradation will be examined. The main subsurface biological processes resulting in CAH degradation are reductive dechlorination (Vogel and McCarty, 1985; McCarty and Semprini, 1994),

direct oxidation (Bradley and Chapelle, 1996), and aerobic cometabolism (McCarty and Semprini, 1994). Of these three processes, reductive dehalogenation is thought to be the most important resutling in the natural destruction of CAHs in the subsurface (Sleep, 2004).

2.2.1.1 Reductive Dehalogenation

Reductive dehalogenation can occur in two different ways. The first process is termed halorespiration because the CAH is used as an electron acceptor, in effect allowing the microorganism to "breathe" the CAH the way aerobic organisms use oxygen (McCarty, 1997). Acting as an electron acceptor, the chlorinated solvent is reduced, with a hydrogen ion replacing a chloride ion. The second process by which reductive dehalogenation can occur is cometabolic. In anaerobic cometabolic reductive dehalogenation constituents of groundwater such as carbon dioxide, ferric iron or sulfate act as electron acceptors. Indigenous microorganisms utilize electron donors such as dissolved organic carbon that may also be present as a source of energy and carbon. In the process of metabolizing the donor, the microorganisms produce enzymes that fortuitously degrade the chlorinated compounds (Wiedemeier *et al.,* 1999). The microorganism gains no benefit from the reductive dehalogenation of the CAH, which usually results in a slow and often insignificant contribution to the degradation of chlorinated solvents at a site (Wiedemeier *et al.,* 1999). Because of the slow and incomplete nature of cometabolic reductive dehalogenation, the largest contribution to the natural attenuation of a chlorinated solvent is usually from halorespiration.

Anaerobic reductive dehalogenation of PCE and TCE has been studied as a potential remediation tool since the early 1980's (Fennell *et al.,* 1995). CAHs can be classified as relatively oxidized compounds because of the presence of electronegative chlorine atoms, and as a result they can act as electron acceptors (Vogel *et al.,* 1987). Figure 2.1 below illustrates the reduction potential of some CAHs compared to common groundwater electron acceptors such as nitrate, Fe(III), carbon dioxide, and sulfate.

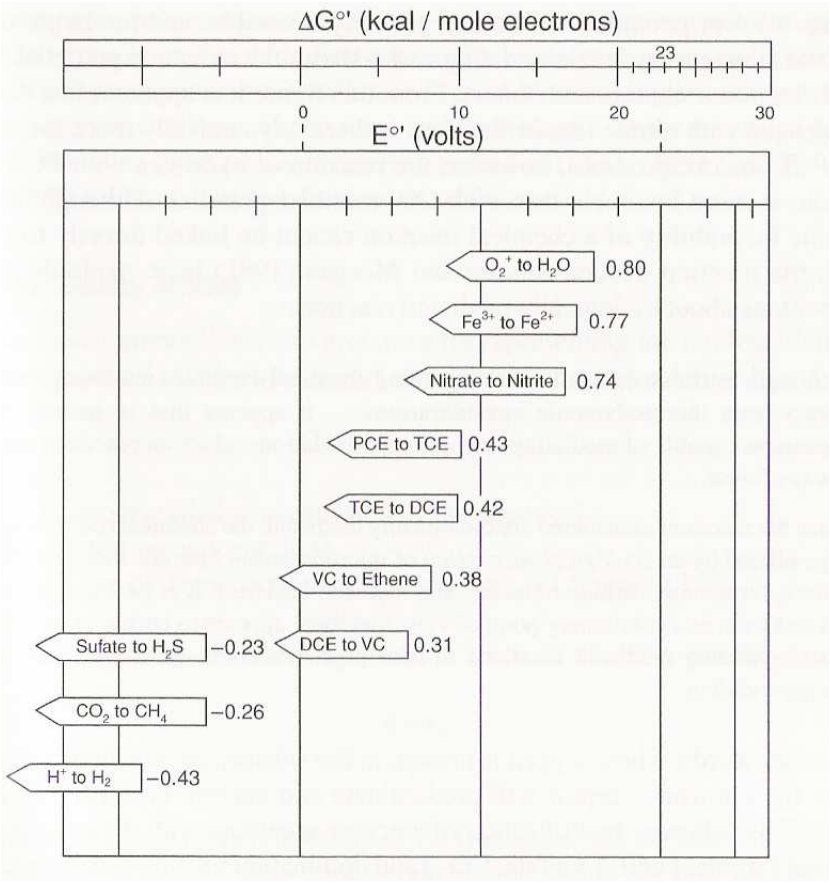

Figure 2.1 Reduction potential for various half-cell reactions (Stumm and Morgan, 1981)

The key electron donor for CAH halorespiration is molecular hydrogen (Hollinger *et al.,* 1993; Smatlack *et al.,* 1996; Ballapragada *et al.,* 1997; Wiedemeier *et al.,* 1999). The efficiency of reductive dehalogenation is directly related to the availability of molecular

hydrogen (USGS, 2003). Because hydrogen plays such an important role in the reductive process of halorespiration, it is important to understand the sources of hydrogen and the concentrations of hydrogen that are most favorable for halorespiring microorganisms.

In natural groundwater, concentrations of H_2 are controlled by ambient microbial terminal electron-accepting processes (TEAPs) (USGS, 2003). Under anaerobic conditions, H_2 is produced continuously by microorganisms fermenting available organic matter. This H_2 is then utilized in a number of TEAPs, most commonly using Fe(III), SO_4, or CO_2 as terminal electron acceptors (USGS, 2003). Each TEAP has a different affinity for H_2 uptake. Thus, the concentration of H_2 in the aquifer depends on the dominant TEAP at the site. The reduction potential of the aquifer can be described using the dominant terminal electron acceptor at the site. If Fe(III) is dominant, aquifer conditions are referred to as iron- or Fe(III)-reducing. If the available iron is exhausted and SO_4 becomes the dominant terminal electron acceptor, then we have sulfate-reducing conditions. Figure 2.2 below shows the characteristic H_2 concentrations associated with different TEAPs.

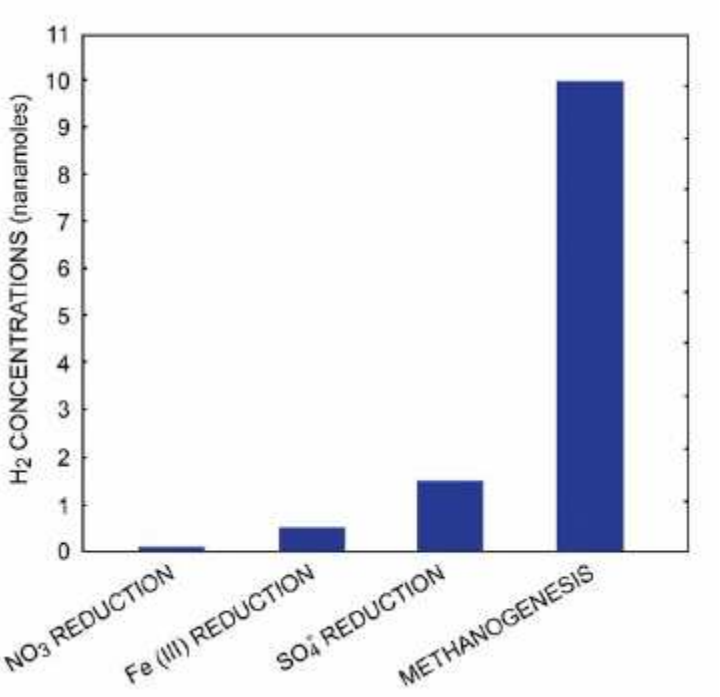

Figure 2.2 Characteristic hydrogen concentrations associated with different terminal electron-accepting processes

Microorganisms that use CO_2 as an electron acceptor (methanogens), have the lowest affinity for H_2, and therefore steady-state H_2 concentrations in methanogenic aquifers are relatively high at around 10 nanomoles per liter (nM) (Figure 2.2) (USGS, 2003). Smatlack *et al.,* (1996) reported that the increased reductive dechlorination activity seen under methanogenic conditions compared to other less reducing conditions such as Fe(III) or SO_4 reduction was due to the greater availability of H_2 for reductive dechlorination, and not the specific activity of the methanogenic microorganisms.

With the proper electron donor and microorganism present, hydrogen can replace a chlorine atom on a CAH molecule (USGS, 2003). Gossett and Zinder (1996) reported that "the success or failure of natural attenuation can be linked to the specific type of

dechlorinator present, as well as to the relative supply of H_2 precursors compared with the supply of chlorinated ethene that must be reduced." Figure 2.3 shows how molecular hydrogen drives reductive dehalogenation of PCE to TCE producing a hydrogen and chloride ion (USGS, 2003).

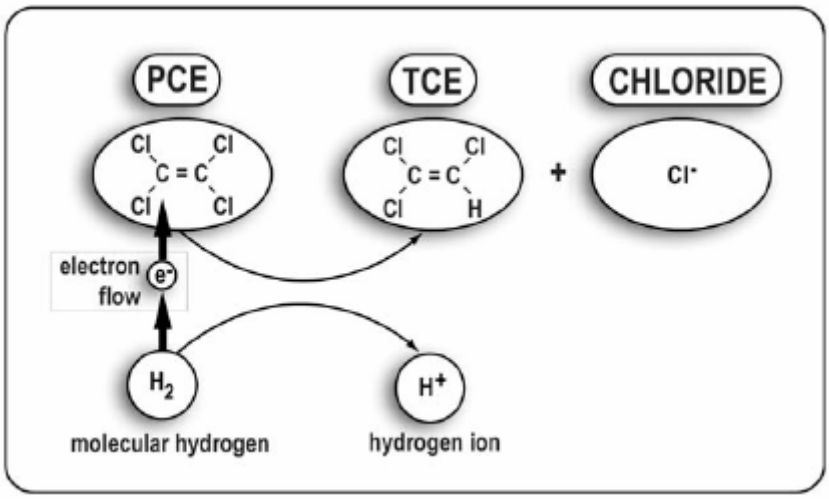

Figure 2.3 Role of hydrogen in reductive dehalogenation of PCE

The number of chlorines present in a CAH molecule plays a direct role in the rate and extent to which reductive dehalogenation will be carried out (Vogel *et al.,* 1987). PCE, which consists of four chlorine atoms, readily undergoes reductive dehalogenation to TCE in an anaerobic environment because it is a stronger oxidant than all electron-accepting species naturally occurring in groundwater besides oxygen gas (see Figure 2.4) (Vogel *et al.,* 1987).

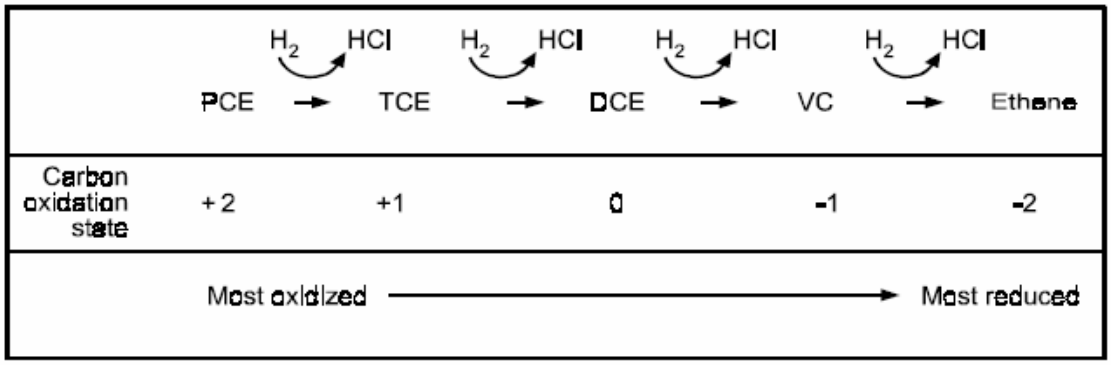

Figure 2.4 Oxidation state of chlorinated ethenes

TCE, with its three chlorine atoms, is reduced to DCE under Fe(III) and stronger-reducing conditions. DCE can take on three forms: *cis*-1,2-DCE, *trans*-1,2-DCE, and 1,1-DCE, with *cis*-1,2-DCE being the most common daughter product of the reductive dehalogenation of TCE (Klier *et al.,* 1999). In order for DCE to be reductively dehalogenated to yield VC, reducing conditions must be as strong as those required for sulfate (SO_4)-reducing conditions. Finally, the most stubborn of the chlorinated ethenes, VC, is characteristically slow and reductive dehalogenation is significant only under highly reducing, methanogenic conditions (Vogel and McCarty, 1985; Fennel *et al.,* 1995). The final product of VC reductive dehalogenation is ethene, an innocuous end product. Figure 2.5 shows the reductive dehalogenation pathway for chlorinated ethenes.

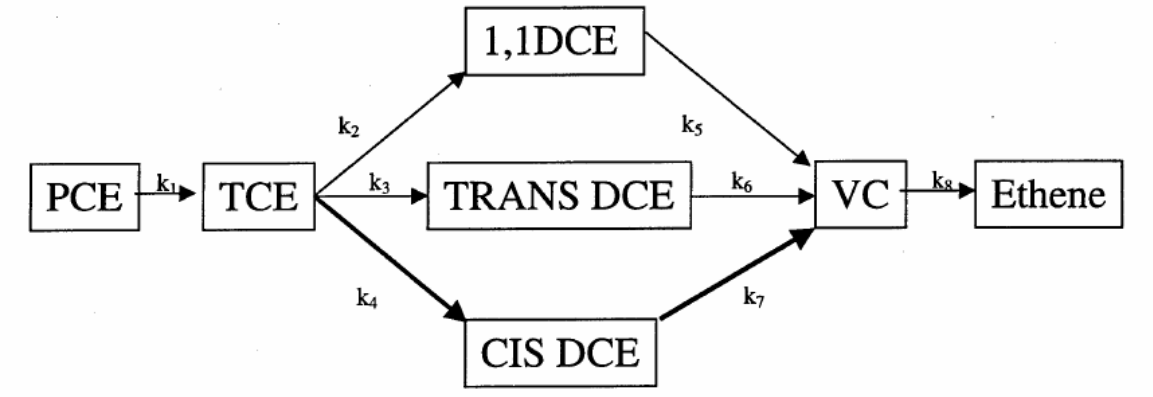

Figure 2.5 Reductive dehalogenation of PCE to Ethene (Freedman and Gossett, 1989)

Due to the stronger, less common reductive conditions required for the complete dehalogenation of PCE to ethene, there is commonly a build-up of DCE and VC seen at chlorinated solvent spill sites. It is this knowledge of the difficulty of achieving complete reduction to nonchlorinated products that has motivated reductive dehalogenation-specific research in the area of enhanced *in situ* bioremediation.

2.2.2 Enhanced *In Situ* Bioremediation

When natural attenuation does not occur, or occurs at a rate that will not meet site cleanup objectives in a reasonable timeframe, steps must be taken to stimulate the indigenous microbial population to increase the rate of biological activity (Suthersan, 2002). For reductive dehalogenation to take place, the following conditions are necessary (Lee et al, 1998): 1) a microbial consortium capable of dehalogenating the chlorinated solvent must be present or added by bioaugmentation, 2) contaminant concentrations must be within an acceptable range that the microorganisms can degrade, 3) the aquifer must be under appropriately reducing conditions, 4) electron donor must be present in

adequate concentrations, and 5) the required nutrients must be available, along with other favorable environmental conditions such as pH. When any of these required conditions is missing, natural attenuation will not occur. The microorganisms capable of reductive dehalogenation are thought to be present at a majority of contaminated groundwater sites (Suthersan, 2002). When it is determined that they are not present, bioaugmentation can be used to introduce the needed microorganisms into the contaminated aquifer. If it is determined that the necessary microorganisms are present, they can be stimulated to reproduce, grow, and destroy the contaminants if the required additional reagents are introduced into the system (Suthersan, 2002). A limiting factor common to reductive dehalogenation is electron donor. A steady source of electron donor is necessary to create the reducing conditions essential to reductive dehalogenation. Hydrogen Release Compound was created to overcome this limitation by producing a steady supply of electron donor.

2.2.2.1 Hydrogen Release Compound

HRC® was developed for use in EISB systems where it has been determined that the obstacle to the reductive dehalogenation of CAH is the shortage of hydrogen for use as an electron donor. Hydrogen gas (H_2) is a byproduct of fermentation; however, it is a highly reduced molecule, which makes it an excellent electron donor (Wiedemeier et al, 1999).

HRC® is a proprietary, environmentally safe, food quality, polylactate ester formulated for the slow release of lactic acid upon contact with water (see Figure 2.6). Microbes in

the subsurface will metabolize the lactic acid producing hydrogen which can then be used by halorespirors to dechlorinate CAHs.

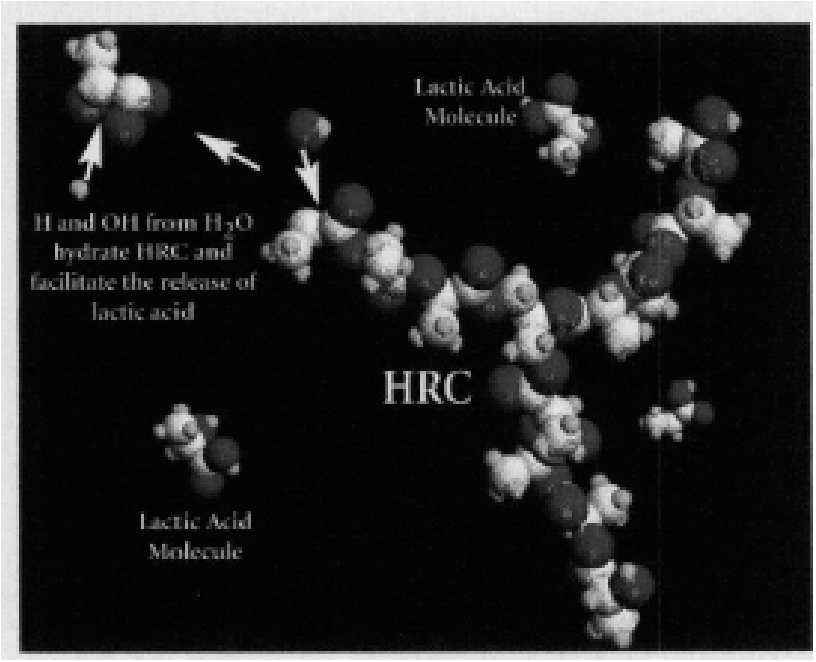

Figure 2.6 Glycerol polylactate (GPL) - the active ingredient in HRC®

The purpose of HRC® is to slowly release lactic acid so as to provide a constant source of H_2 which facilitates reductive dechlorination.

2.2.2.2 Bioaugmentation

Microorganisms capable of reductive dechlorination were once thought to be missing from many groundwater contamination sites. The consensus today is that reductive dehalogenating microorganisms are ubiquitous in anaerobic, CAH-contaminated aquifers, but the rate and extent of dechlorination is site specific depending on a number of variables (McCarty and Semprini, 1994; USGS, 2003). Of particular interest are microorganisms capable of reducing DCE and VC to ethene. The debate among

remediation experts continues today over the microorganisms responsible for cometabolic degradation and halorespiration (Suthersan, 2002; Nyer *et al.,* 2003). The debate is between those who believe the necessary bacteria for degradation can be isolated and applied to various sites where they are not indigenous and those who believe that the key to achieving degradation is to understand and create the correct environment in which the native bacteria will thrive (Nyer *et al.,* 2003). The current belief is that dehalogenating organisms are nearly ubiquitous in nature (Suthersan, 2002) though some sites exist that do not have these native dehalogenating microorganisms present. Thus, some sites may require bioaugmentation. Bioaugmentation is the selection of exogenous microorganisms for their capability to metabolize the target contaminant and subsequent injection of these microorganisms along with the essential nutrients directly into the contaminated zone (Suthersan, 2002). The success of bioaugmentation has been varied. A number of successes have been reported, both in the laboratory and field, and a number of failures have also occurred. Looking at the number of abiotic and biotic stresses that an introduced microorganism faces, it is no surprise that bioaugmentation has suffered a fair amount of failure. Suthersan (2002) describes the reasons for frequent failures of bioaugmentation as follows: limiting nutrients and growth factors in the natural environment, predators and parasites, inability of the introduced bacteria to spread throughout the subsurface, metabolism of nontarget organic compounds present, too low a concentration of target compound to support microbial growth, and other inhibitory conditions such as pH, temperature, salinity, and toxins. As noted earlier, despite the many obstacles to success, bioaugmentation has been used successfully. Zinder and Gossett of Cornell were able to isolate a microorganism called *Dehalococcoides*

ethenogenes that is presently the only isolated organism known to be capable of dechlorinating PCE to ethene, a process that stalls out at *cis*-DCE at many sites (Maymo-Gatell *et al.,* 2001).

2.2.3 Field Applications

2.2.3.1 MNA Field Applications

Natural attenuation is recognized by the EPA as a viable method of remediation for CAH-contaminated groundwater (U.S. EPA, 1999). The director of EPA's Federal Facilities Restoration and Reuse Office, Jim Woolford, said "Under certain site conditions, and if properly documented, natural attenuation can be a viable option for remediating sites as a stand-alone option or in conjunction with other engineered remediation" (U.S. EPA, 1999). MNA for remediation of CAH-contaminated groundwater is not yet as pervasive as that of MNA of dissolved benzene, toluene, ethyl benzene, and xylene (BTEX) plumes, but it is becoming more common and will be a viable option for at least a portion of the dissolved CAH plumes at many sites (AFCEE, 1999). Monitored natural attenuation has been chosen as a component of the remediation strategy at many sites and as the sole method for site remediation at a lesser number of sites. Of 14 sites studied in one report (AFCEE, 1999), natural attenuation processes at two sites were sufficiently efficient to warrant the use of MNA as the sole remedial alternative.

One site where MNA was tested as a possible remediation alternative was the Cape Canaveral, Florida Facility 1381 (SWMU 21). The groundwater at this site was

contaminated with CAHs such as TCE. It was determined that the conditions in the groundwater were such that TCE was being reductively dehalogenated to DCE. The dissolved oxygen and reduction potential were sufficiently low, and the amount of organic carbon found in the soil was sufficiently high that reductive dehalogenation could occur (AFCEE, 1999). However, due to the highly anaerobic conditions at the site, the VC was degrading very slowly. MNA was recommended as a viable alternative for treatment of the CAH-contaminated groundwater at the site. It was, however, noted that MNA should be used as a part of an overall site remediation strategy that included source removal.

Models have been used to aid in the analysis of natural attenuation design at chlorinated solvent sites. One such model was developed by Clement *et al.* (2000) and applied to analyze field-scale transport and biodegradation processes occurring at the Area-6 site in Dover Air Force Base, Delaware. The calibrated model was able to reproduce the general groundwater flow patterns, as well as successfully recreate the observed distribution of PCE, TCE, DCE, and VC at the site. Model simulations were able to give the site managers a great deal of information about the site and how the contaminants were behaving. The ability to model the site and gain understanding as to what is happening in the subsurface is very important when deciding to employ monitored natural attenuation as a remediation alternative.

2.2.3.2 EISB Field Applications

Regulatory acceptance of enhanced *in situ* bioremediation has grown over the last several years (AFCEE, 2004). EISB has been implemented under various federal programs, including CERCLA and the Resource Conservation and Recovery Act. The technology has been applied in over 32 states (AFCEE, 2004). While the use of enhanced bioremediation has been approved by the EPA and the majority of the states, it has yet to gain widespread acceptance as a proven technology, primarily due to a lack of consistency in achieving remedial objectives (AFCEE, 2004). The substrate of choice to aid in the enhancing of bioremediation has varied from corn syrup, cheese whey, and molasses, to HRC®.

One example of the use of HRC® to remediate a chlorinated solvent plume took place in Fisherville, Massachusetts. The site was home to a mill producing steel racks, machine tool parts, and aluminum lawn furniture. During operation of the mill, an unknown amount of chlorinated solvents including PCE and TCE was spilled and found its way into the subsurface. A pump and treat system was installed in late 1996 which operated until it was destroyed in a fire in 1999. The pump and treat system was not repaired and the site still exhibited a significant contamination problem. TCE levels were still found to exceed 2,500 µg/L in many sampling wells. It was decided that HRC® could be used to passively reduce the levels of CAH contamination in the groundwater. The pilot test was initiated by injecting HRC® into a barrier perpendicular to the groundwater flow direction. The barrier consists of three staggered rows of five injection points each. Within each row, the points are spaced approximately 7 ft apart, and the rows are

separated by approximately 5 ft. Thus, the barrier consists of 15 injection points in an area that is approximately 10 ft long in the direction of groundwater flow, and, due to the staggered positioning of the individual rows, is approximately 35 ft wide perpendicular to the flow. The staggering of the rows gives the approaching groundwater flow little chance of migrating through the barrier without contacting the bioactive zone created by the HRC®. HRC® was injected into each injection point at the rate of approximately 6 pounds per vertical foot. Several months after HRC® injection, the concentration of TCE was reduced by 88% to 98% in all but one sampling well. The worst performing well was reduced by 62%. DCE was noted to increase in concentration as the TCE was degraded, but DCE and VC were later noted to decrease in concentration. From this HRC® application several conclusions were made. It was concluded that HRC® addition can effectively accelerate reductive dehalogenation of CAHs through ethene. It was also noted that HRC® addition can be effective for as long as 27 months. Finally, it was said that a second application of HRC® would be required to maintain the barrier for an extended period of time.

2.3 Modeling

A model is a representation of the real world (Anderson and Woessner, 1992). This research will make use of mathematical models which simulate groundwater flow and contaminant fate and transport by means of governing equations thought to represent the important physical, chemical, and biological processes that occur in the system (Anderson and Woessner, 1992). Mathematical models can be solved analytically or numerically. Analytical models are exact solutions to the governing equations. In order

to obtain an analytical solution, a number of simplifications are required, limiting the utility of these solutions to simulate complex real-world problems. Numerical models use approximations of the governing mathematical equations to simulate a system. These models are able to solve more complex problems, minimizing the need for numerous simplifying assumptions. Reliable and accurate fate and transport models are needed to assess the risks posed by spills of contaminants to the subsurface and to aid in designing remediation programs to address these spills (Sleep, 2004). Models can be used to predict how far and in what direction a groundwater contaminant will travel in a specified timeframe. Models can also be used to predict the concentration of contaminant anywhere along the dissolved contaminant plume. Another important aspect of models is that they can be used to quickly test the effectiveness of alternative remediation methods. Models are essential in helping the decision maker better understand site specific processes. When dealing with CAHs, modeling can play a major role in determining whether or not monitored natural attenuation will be able to remediate the plume in an acceptable timeframe.

2.3.1 Mathematical Modeling of subsurface fate and transport of CAHs

2.3.2 Important fate and transport processes

One important feature of a good model is that it represents only those processes necessary to provide a useful representation of reality. In this study, the physiochemical processes of advection, dispersion, and sorption will be modeled along with the biological processes significant to HRC® fermentation and CAH biodegradation. The general

equations describing the fate and transport of contaminant in the aqueous and solid phase, respectively, are represented below (Clement, 1997).

$$\frac{\partial C_k}{\partial t} = \frac{\partial}{\partial x_i}\left(D_{ij} \frac{\partial C_k}{\partial x_j} \right) - \frac{\partial}{\partial x_i}\left(v_i C_k\right) + \frac{q_s}{\phi} C_{s_k} + r_c \text{, where k = 1,2, … m} \qquad (2.1)$$

$$\frac{d\,\tilde{C}_{im}}{dt} = \tilde{r}_c \text{, where, im = 1,2,…,(n-m)} \qquad (2.2)$$

where

n = total number of species

m = total number of aqueous phase species (thus, n-m is the total number of solid phase species

C_k = aqueous phase concentration of the k^{th} species [M/L^3]

$\tilde{C}_{im}$ = solid phase concentration of the immobile species [M/M]

D_{ij} = hydrodynamic dispersion coefficient [L^2/T]

v = pore velocity [L/T]

ϕ = soil porosity [-]

q_s = volumetric flux of water per unit volume of aquifer representing sources and sinks [1/T]

C_{s_k} = concentration of source/sink [M/L^3]

r_c = rate of all reactions occurring in the aqueous phase [M/L^3T]

$\tilde{r}_c$ = rate of all reactions occurring in the soil phase [M/MT]

In the sections below, we discuss each of the terms in equations 2.1 and 2.2 in more detail.

2.3.2.1 Advection

Advection is the transport of mass due to the flow of the water in which the mass is dissolved (Domenico and Schwartz, 1998). Advection is typically considered the primary transport mechanism for dissolved solutes. Darcy's Law is used to calculate the average linear velocity of a fluid flowing in a porous medium (Domenico and Schwartz, 1998).

$$v_i = \frac{Ki}{\phi} \tag{2.3}$$

where:

K = the hydraulic conductivity of the porous medium [L/T]

i = the hydraulic gradient [L/L]

The hydraulic conductivity and porosity are properties of the aquifer material unique to each site. The hydraulic gradient can be calculated using the equations of flow, with the necessary initial and boundary conditions, as presented in Domenico and Schwartz, (1998). The contaminants in question are assumed to move with the flow of groundwater in the same direction and at the same velocity. Advection is represented in the general contaminant fate and transport equations by the following (Clement, 1997):

$$\frac{\partial C_k}{\partial t} = -\frac{\partial (v_i C_k)}{\partial x_i} \tag{2.4}$$

2.3.2.2 Dispersion

Dispersion is the spreading of mass transverse to or along the path of advective movement. Two distinct processes are responsible for dispersion. The first is molecular diffusion, which is caused by movement of molecules from an area of high concentration to one of lower concentration. Diffusion is usually considered negligible due to the microscopic scale of its occurrence. It is usually only considered important in cases of extremely slow groundwater movement (Clark, 1996). The second mechanism of dispersion is the mechanical mixing that occurs as the groundwater travels through tortuous pathways in the soil matrix. Contaminant molecules travel through different pathways causing some to move at a rate faster than the average groundwater velocity and others slower. Mechanical dispersion can be modeled using the following equation (Clark, 1996).

$$D_{ij} = \alpha_i \nu_x \tag{2.5}$$

Where

D_{ij} = dispersion coefficient in the i^{th} direction [L^2/T]

α_i = dispersivity in the i^{th} direction [L]

ν_x = average linear groundwater velocity in the x-direction [L/T]

Dispersion is represented in the general contaminant fate and transport equation by the following expression (Clement, 1997):

$$\frac{\partial C_k}{\partial t} = \frac{\partial}{\partial x_i}\left(D_{ij} \frac{\partial C_k}{\partial x_j} \right) \tag{2.6}$$

2.3.2.3 Sorption

Sorption is the partitioning of mass between the solute and the solid. In this study the mass of concern is the CAH, which is partitioned between the groundwater and the soil matrix. Sorption can have a large impact on the transport of contaminants as it can retard, or slow the movement of the contaminants, and in some cases it can virtually immobilize them (Domenico and Schwartz, 1998). Sorption can be assumed to be either in equilibrium or rate-limited. Equilibrium sorption may be assumed when processes affecting the transport of the contaminant are slow compared to the rate of sorption. Equilibrium sorption can be modeled as either a linear or a non-linear process. Linear sorption assumes that the concentration of sorbed contaminant is directly proportional to that of the dissolved contaminant. The non-linear model does not make this assumption. Linear sorption is the simplest model to fit to data as it assumes linear partitioning. For this reason, linear equilibrium sorption will be assumed in this study. Rate-limited sorption should be assumed when the other processes affecting the transport of the contaminant are on the same order or faster than sorption.

2.3.2.4 Biodegradation

2.3.2.4.1 First-Order Decay Models

Expressing contaminant degradation as a first-order process means the rate at which the contaminant decays is proportional to the contaminant concentration. This can be expressed by the following equation:

$$r_c = \frac{dC_k}{dt} = -\lambda C_k \tag{2.7}$$

where

λ = contaminant first-order decay rate constant [1/T]

The first-order biodegradation rate constant can be an important tool for evaluating natural attenuation processes at groundwater contamination sites. The overall effectiveness of natural attenuation at a given site can be assessed by evaluating the rate at which the contaminant concentrations are decreasing (U.S. EPA, 2002). The U.S. EPA (U.S. EPA, 1997) as well as the American Society for Testing and Materials (ASTM, 1998) have approved the use of site-specific first-order attenuation rate constants for evaluating natural attenuation processes in groundwater. First-order biodegradation modeling may be applied to characterize plume trends, as well as estimate the time required for achieving remediation goals (U.S. EPA, 2002). The natural attenuation models BIOSCREEN and BIOCHLOR (Newell *et al.,* 1996; Aziz *et al.,* 1999) include the use of first-order rate constants for the simulation of the natural attenuation of dissolved contaminants. The biodegradation rate constant (λ) in units of inverse time (e.g., per day) can be estimated by a number of methods, such as by comparing contaminant transport with the transport of a conservative tracer or by calibrating a solute transport model that incorporates first-order biodegradation to field data (Figure 2.7) (U.S. EPA, 2002).

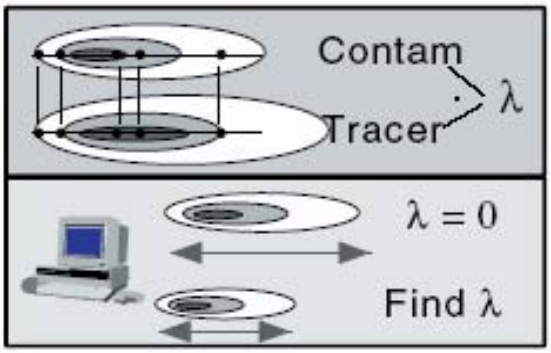

Figure 2.7 Determining the biodegradation rate constant (U.S. EPA, 2002)

Figure 2.7 shows how one could calibrate a groundwater solute contaminant transport model that includes dispersion and retardation such as BIOCHLOR, BIOSCREEN, BIOPLUME III, or RT3D, by adjusting λ until the field values closely match those generated by the model. Figure 2.8 shows the results of a series of modeling efforts using the BIOCHLOR model to estimate the biodegradation rate constant using monitoring data from a number of sites. It is apparent that a wide range of values can be calculated from site to site; therefore the values calculated are site specific. First-order biodegradation kinetics models have been shown to offer a relatively simple approximation for contaminant behavior in a plume, which can be useful in assessing the true threat of the contaminant and in making decisions regarding containment or cleanup technology.

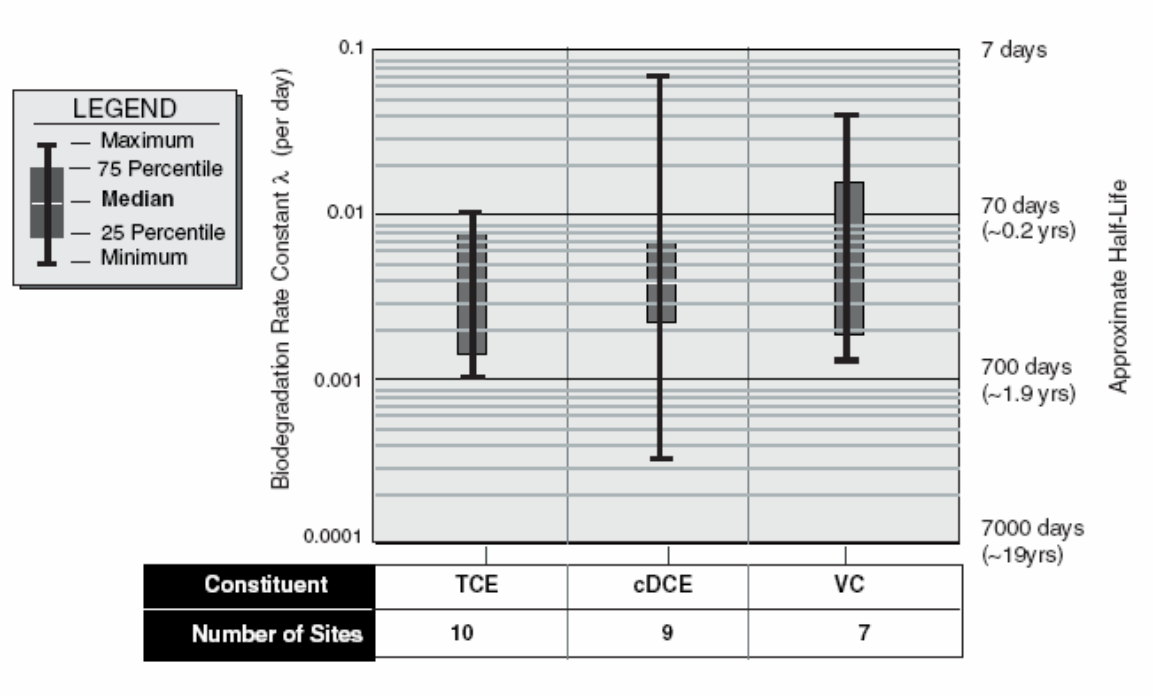

Figure 2.8 Biodegradation rate constants (λ) for Trichloroethene (TCE), cis-Dichloroethene (cDCE) and Vinyl Chloride (VC) from BIOCHLOR modeling studies (Aziz *et al.*, 2000) as seen in U.S. EPA (2002).

2.3.2.4.2 Monod Models

In some cases, a first-order model of biodegradation does not capture some important aspects of the process and a more complex model must be used. Another model used to explain the biodegradation of CAHs in contaminated groundwater is a Monod kinetic model. Monod models are based on the assumption that microbial growth is driven by consumption of a growth limiting substrate (Schwartzenbach *et al.,* 1993). When substrate is not limiting, microbial growth is exponential until it reaches some maximum growth rate, either due to the organisms intrinsic growth rate for the specific substrate, or another factor becomes limiting (Schwartzenbach *et al.,* 1993). An equation can be constructed (Equation 2.8) relating the specific growth rate of the microbes due to

synthesis (μ_{syn}) to the concentration of the growth-limiting substrate being consumed (C_k). X is the microbial concentration [biomass/liter], μ_{max} is the maximum growth rate of the microorganisms [1/T], and K_s is the Monod or half-saturation constant [μM]. Rittmann and McCarty (2001) explain that the Monod constant is the substrate concentration at which μ_{syn} is half of μ_{max}.

$$\mu_{syn} = \frac{1}{X}\frac{dX}{dt} = \mu_{\max}\left(\frac{C_k}{C_k + K_s}\right) \tag{2.8}$$

Another process that must be represented in the equation is natural microbial decay due to cell maintenance and death. If we assume first-order decay, we can define a first-order decay rate parameter b with units of 1/T (Rittmann and McCarty, 2001). Adding this decay term to equation 2.8 gives us an expression for the net growth rate of active biomass (μ), as shown in equation 2.9 below (Rittmann and McCarty, 2001).

$$\mu = \mu_{\max}\left(\frac{C_k}{C_k + K_s}\right) - b \tag{2.9}$$

Defining r_c as the overall rate of substrate utilization by biomass of concentration X, we can link microbial growth to the use of electron donor (Rittmann and McCarty, 2001):

$$r_c = -k_{\max}\left(\frac{C_k}{C_k + K_s}\right)X \tag{2.10}$$

Thus, the net rate of biomass growth, defined as r_{net}, becomes

$$r_{net} = Y_{biomass} k_{\max} \left(\frac{C_k}{C_k + K_s} \right) X - bX \qquad (2.11)$$

Where k_{max} is the maximum specific rate of substrate use [mass electron donor/(biomass*time)] and $Y_{biomass}$ is the biomass yield per mass of electron donor consumed [biomass/mass electron donor] (Rittmann and McCarty, 2001). Equation 2.11 describes the relationship between biomass growth and electron donor use, allowing the use of Monod kinetics to not only describe microbial growth kinetics (Equation 2.8), but also the kinetics of substrate utilization (Parr, 2002).

2.3.2.4.3 Dual-Monod Model

In attempts to more accurately represent real-world systems, dual-Monod kinetics has been used by a number of investigators (Semprini and McCarty, 1991; Fennell and Gossett, 1998; Lee *et al.,* 2004). Dual-Monod kinetics is used to describe microbial growth as a function of both electron acceptor and donor concentrations. The equation is written as follows (Semprini and McCarty, 1991):

$$r_X = \frac{\partial X}{\partial t} = X k_{\max} Y_{biomass} \left(\frac{C^{don}}{K_{SD} + C^{don}} \right) \left(\frac{C_k}{K_{SA} + C_k} \right) - bX \left(\frac{C_k}{K_{SA} + C_k} \right) \qquad (2.12)$$

where

C^{don} = concentration of electron donor [mg/L];

K_{SD} = electron donor half saturation concentration [mg/L]; and

K_{SA} = electron acceptor half saturation concentration [mg/L]

In this particular model, the decay rate is modified by a Monod term, assuming that the rate of microbial decay is a function of the electron acceptor concentration (Semprini and

McCarty, 1991; Parr, 2002). Other models (*e.g.* Fennell and Gossett, 1998; Lee *et al.,* 2004) do not make this assumption, and the microbial decay rate is not affected by electron acceptor concentration.

A dual-Monod model may also be used to represent the rate of electron acceptor consumption, so that the rate depends on both electron donor and acceptor concentrations, as well as the biomass concentration (which is described by Equation 2.12). Again, according to the Semprini and McCarty (1991) model, the decay rate parameter b is modified by a Monod term containing the electron acceptor concentration.

$$r_C = \frac{\partial C_k}{\partial t} = -k_{\max} FX\left(\frac{C^{don}}{K_{SD} + C^{don}}\right) * \left(\frac{C_k}{K_{SA} + C_k}\right) - bd_c f_d X\left(\frac{C_k}{K_{SA} + C_k}\right) \quad (2.13)$$

where

F = stoichiometric ration of electron acceptor to electron donor utilization for biomass synthesis [g acceptor/g donor] (Semprini and McCarty, 1991)

d_c = cell decay oxygen demand [mg oxygen/mg biomass]

f_d = fraction of cells that are biodegradable

This general model was adapted by other researchers to better suit the conditions for biodegradation of CAHs using hydrogen as an electron donor. These models will be further explored below.

2.3.3 Modeling HRC®

As far as we know, HRC® has not been modeled to simulate its effect on contaminant reductive dehalogenation. There have been, however, models that simulate the competition for hydrogen in a dechlorinating culture (Fennel and Gossett, 1998; Lee *et*

al., 2004), and PCE dechlorination via membrane delivered hydrogen (Clapp *et al.,* 2004).

2.3.3.1 Production and Competition Model

Fennell and Gossett (1998) modeled the production and competition for hydrogen in a dechlorinating culture. The biokinetic model employed dual-Monod type kinetics to describe the rate of dechlorination of the CAHs, which serve as electron acceptors, as a function of both the concentration of CAH and the concentration of the electron donor, H_2. The model also described the fermentation of electron donors to produce H_2 and the subsequent competition for H_2 between CAH dechlorinators and methanogens. The model used a single population of dechlorinators to reductively dehalogenate PCE to ethene, as well as a single population of methanogens. Growth of a donor fermenting biomass was also modeled. Competitive inhibition between CAHs was not modeled, where competitive inhibition is defined as the reduction in degradation rate of one CAH due to the presence of a second CAH. Equations describing dechlorination were developed for PCE and each of its daughter products. The equations used are exemplified by the model for PCE (Fennell and Gossett, 1998):

$$r_c = \frac{dC_{PCE}}{dt} = \frac{-k_{PCE} X_{dechlor} C_{PCE}}{K_{S(PCE)} + C_{PCE}} * \frac{\left(C_{H2} - H_2 threshold_{dechlor}\right)}{K_{S(H2)dechlor} + \left(C_{H2} - H_2 threshold_{dehclor}\right)} \quad (2.14)$$

where

k_{PCE} = maximum specific rate of the PCE utilization [μmol/mg of VSS h];

$X_{dechlor}$ = dechlorinators biomass [mg of VSS/L];

C_{PCE} = aqueous PCE concentration [μM];

$Ks_{(PCE)}$ = half-velocity coefficient for PCE degradation [μM];

C_{H2} = aqueous H_2 concentration [μM];

$Ks_{(H2)dechlor}$ = half-velocity coefficient for H_2 use by dechlorinators [μM]; and

$H_2threshold_{dechlor}$ = threshold for H_2 use by dechlorinators [μM]

Note that it was assumed that the same biomass, $X_{dechlor}$, was responsible for each step of the dechlorination. From equation 2.14, it is seen that the depletion of the PCE is controlled by the H_2 concentration (donor) as well as the PCE concentration (acceptor). The $H_2threshold_{dechlor}$ parameter plays an important role because it represents the minimum H_2 concentration at which dechlorinators gain energy, meaning that below this H_2 concentration, dechlorination does not occur.

Fennell and Gossett (1998) also modeled donor fermentation to produce H_2 as well as a kinetic model for hydrogenotrophic methanogenesis. Hydrogenotrophic methanogenesis is important to simulate, as the methanogens compete for hydrogen with the dechlorinating bacteria. The equation describing methanogenesis follows (Fennell and Gossett, 1998):

$$\left(\frac{dMt_{CH4\,fromH2}}{dt}\right)_{production} = \frac{1}{4} k_{(H2)meth} X_{hydrogenotroph} \times \frac{\left(C_{H2} - H_2threshold_{meth}\right)}{K_{S(H2)meth} + \left(C_{H2} - H_2threshold_{meth}\right)} \tag{2.15}$$

where

$Mt_{CH4\ from\ H2}$ = methane produced by hydrogenotrophs [μM];

$k_{(H2)meth}$ = maximum rate of H_2 utilization by methanogens [μmol/mg of VSS h];

$X_{hydrogenotroph}$ = biomass of hydrogenotrophic methanogens [mg of VSS/L];

$K_{S(H2)meth}$ = half-velocity coefficient for H_2 use by methanogens [μM]; and

$H_2threshold_{meth}$ = threshold for H_2 use by methanogens [μM].

Biomass growth was modeled using the following equation (Fennell and Gossett, 1998):

$$r_X = \frac{dX}{dt} = Y_{biomass}\left(\frac{-dMt}{dt}\right) - bX \qquad (2.16)$$

where

dMt/dt = the rate of substrate utilization [μmol/h]; and

$Y_{biomass}$ = organism yield [mg of VSS/L μmol substrate used]

Note here that the second term on the right, the biomass decay term, is a first-order expression, in contrast to the biomass decay term in equation 2.12, where a first-order term is modified by a Monod expression to describe biomass decay. Also, the terms $Y_{biomass}$ and b will be different for methanogens and the two types of dechlorinators.

2.3.3.2 Membrane Model

Clapp *et al.* (2004) developed a one-dimensional contaminant fate and transport model to simulate the fate and transport of the electron donor (H_2), as well as the electron acceptors PCE and reductive dechlorination byproducts TCE, DCE, VC, and ETH. Methane production by hydrogenotrophic methanogens was also simulated. The model assumed an anaerobic aquifer that was supplied with hydrogen via a gas-permeable membrane curtain. The model also assumed the hydrogen supplying membrane curtain was installed in a soil free trench, normal to groundwater flow. Due to the varying porosity and linear groundwater velocities between the trench and the aquifer porous media, different parameter values had to be used for each domain. Solute transport within the trench was described by a one-dimensional advection-dispersion equation similar to equation 2.1, but with a specific gas transfer rate out of the membranes in place

of the reaction term. Solute fate and transport in the aquifer on either side of the trench was described by the same equation, but with the reaction term (Clapp *et al.,* 2004). The biokinetic equations for dechlorination used in this model (Rittmann and McCarty, 2001) are shown below (Equations 2.17-2.21). These equations make use of dual-Monod kinetics in which electron donor and acceptor can be limiting. Although very similar to the equations used in the production and competition model described in section 2.3.3.1 above, there are several differences. First, this model tracks three separate populations of microorganisms, two populations of dechlorinators and a population of methanogens. The dechlorinating microorganisms were divided into two groups because of evidence that the reductive dehalogenation of PCE to DCE (through TCE) and that of DCE to Ethene (through VC) is performed by different populations of microorganisms (Flynn *et al.,* 2000). Secondly, this model not only takes into account competition by methanogens for available H_2, it also accounts for competitive inhibition, that is, the decrease in the rate of dechlorination of one CAH due to the presence of another CAH that is dechlorinated by the same organism.

$$r_{PCE} = -k_{PCE,dech1} X_{dech1} \left(\frac{C_{PCE}}{K_{s,PCE,dech1}\left(1 + \frac{C_{TCE}}{K_{x,TCE,dech1}}\right) + C_{PCE}} \right) \times \left(\frac{C_{H_2} - C_{H_2,th,dech}}{K_{s,H_2,dech1} + \left(C_{H_2} - C_{H_2,th,dech}\right)} \right) \qquad (2.17)$$

$$r_{TCE} = -k_{TCE,dech1} X_{dech1} \left(\frac{C_{TCE}}{K_{s,TCE,dech1}\left(1 + \frac{C_{PCE}}{K_{x,PCE,dech1}}\right) + C_{TCE}} \right) \times \left(\frac{C_{H_2} - C_{H_2,th,dech}}{K_{s,H_2,dech1} + \left(C_{H_2} - C_{H_2,th,dech}\right)} \right) \quad (2.18)$$

$$r_{DCE} = -k_{DCE,dech2} X_{dech2} \left(\frac{C_{DCE}}{K_{s,DCE,dech2}\left(1 + \frac{C_{VC}}{K_{x,VC,dech2}}\right) + C_{DCE}} \right) \times \left(\frac{C_{H_2} - C_{H_2,th,dech}}{K_{s,H_2,dech2} + \left(C_{H_2} - C_{H_2,th,dech}\right)} \right) \quad (2.19)$$

$$r_{VC} = -k_{VC,dech2} X_{dech2} \left(\frac{C_{VC}}{K_{s,VC,dech2}\left(1 + \frac{C_{DCE}}{K_{x,DCE,dech2}}\right) + C_{VC}} \right) \times \left(\frac{C_{H_2} - C_{H_2,th,dech}}{K_{s,H_2,dech2} + \left(C_{H_2} - C_{H_2,th,dech}\right)} \right) \quad (2.20)$$

where

$k_{PCE,dech1}$, etc. = maximum dechlorination rate constants [µmol mg biomass^{-1} day $^{-1}$];

$K_{s,PCE,dech1}$, etc. = respective half-saturation constants [µM];

X_{dech1} = PCE/TCE dechlorinator concentrations [mg biomass L^{-1}];

X_{dech2} = DCE/VC dechlorinators concentrations [mg biomass L^{-1}];

C_{PCE}, etc. = aqueous chloroethene concentrations [mg L^{-1}];

C_{H2} = aqueous H_2 concentration [nM];

$C_{H2,th,dech}$ = H_2 threshold concentration (assumed to be the same for both dechlorinators populations) [nM];

$K_{s,H2,dech1}$ = H_2 half-saturation constant for the PCE/TCE dechlorinators [μM]; and

$K_{s,H2,dech2}$ = H_2 half-saturation constant for the DCE/VC dechlorinators [μM]

Notice that the half-saturation constants are multiplied by an additional term that accounts for dechlorination inhibition due to competition with other chloroethenes for the actively dechlorinating sites (Clapp *et al.,* 2004). Notice also that the dechlorination rates were set to zero when the hydrogen concentration (C_{H2}) was less than $C_{H2,th,dech}$. H_2 utilization by dechlorinators was described by the following expression (Clapp *et al.,* 2004):

$$r_{H_2,dech} = F_{H_2/CE,dech}\left(r_{PCE} + r_{TCE} + r_{DCE} + r_{VC}\right) \tag{2.21}$$

where

$F_{H2/CE,dech}$ = stoichiometric coefficient relating dehalorespirer H_2 consumption to chloroethene dechlorination (Bagley, 1998).

H_2 utilization by methanogens was described by the following equation (Clapp *et al.,* 2004):

$$r_{H_2,meth} = \left(\frac{k_{meth} X_{meth}}{1 + \frac{\sum C_{PCE,TCE,DCE,VC,ETH}}{K_{I,CE,meth}}}\right) \times \left(\frac{C_{H_2} - C_{H_2,th,meth}}{K_{s,H_2,meth} + \left(C_{H_2} - C_{H_2,th,meth}\right)}\right) \tag{2.22}$$

where

$K_{I,CE,meth}$ = chloroethene noncompetitive inhibition constant for methanogens [assumed to be the same for PCE, TCE, DCE, VC, and ETH]

Finally, the biomass growth was calculated with the following equations:

$$r_{X.dech1} = -Y_{dech}(r_{PCE} + r_{TCE}) - b_{dech1} X_{dech1} \tag{2.23}$$

$$r_{X.dech2} = -Y_{dech}(r_{DCE} + r_{VC}) - b_{dech2} X_{dech2} \tag{2.24}$$

and growth of methanogens was calculated as follows:

$$r_{X.meth} = -Y_{meth} r_{H_2} - b_{dech1} X_{dech1} \quad (2.25)$$

where

Y_{dech} = dechlorinators growth yield (assumed to be the same for PCE, TCE, DCE, and VC) [mg biomass $mmol^{-1}$];

b_{dech1} = first-order endogenous decay rate constant for the PCE/TCE dechlorinators population [day^{-1}]; and

b_{dech2} = first-order endogenous decay rate constant for the DCE/VC dechlorinators population [day^{-1}]

The biomass was assumed to exist as immobile biofilms with no mass transfer limitations. In order to prevent the model estimating unrealistically high biomass concentrations near the H_2 supply membranes, biomass redistribution equations were used. The model was modified so that biomass could not accumulate above a maximum concentration ($X_{tot,max}$) of 5,000 mg VSS per L pore volume. When the biomass was calculated to exceed $X_{tot,max}$, the excess biomass would be shifted to an adjacent, downgradient node.

A literature review was performed in order to determine average values for the numerous parameters needed for the model, including physical, transport, and kinetic parameters. These parameter values are listed in Table 2.1.

Table 2.1 Microbial kinetic parameter values used in model (Clapp et al., 2004)

Symbol	Parameters and units	Average	Range	References
(a) Max. spec. utilization rates (µmol*mg VSS-1day-1)				
kPCE,dech1	PCE reduction to TCE by PCE/TCE dechlorinators	41.3	1.4-117	Maymo-Gatell et al. (1997), Hollinger et al. (1998), Hollinger et al. (1993), Tandoi et al. (1994), Fennell and Gossett (1998)
kTCE,dech1	TCE reduction to DCE by PCE/TCE dechlorinators	43.2	2.4-117	Maymo-Gatell et al. (1997), Hollinger et al. (1998), Hollinger et al. (1993), Tandoi et al. (1994), Fennell and Gossett (1998)
kH2,dech1	H2 utilization by PCE/TCE dechlorin	54.8	-	Calculated
kDCE,dech2	DCE reduction to VC by DCE/VC dechlorinators	13.2	1.7-22.2	Maymo-Gatell et al. (1997), Tandoi et al. (1994), Fennell and Gossett (1998), Rosner et al. (1997)
kVC,dech2	VC reduction to ETH by DCE/VC dechlorinators	12.7	2.6-22.2	Tandoi et al. (1994), Fennell and Gossett (1998), Rosner et al. (1997)
kH2,dech2	H2 utilization by DCE/VC dechlorina	16.8	-	Calculated
kH2,meth	H2 utilization by methanogens	346	27-1,138	Fennell and Gossett (1998), Robinson and Tiedje (1984), Weimer and Zeikus (1978), Maillacheruvu and Parkin (1996), Coates et al. (1996), Roberton and Wolfe (1970), Zehnder and Wuhrmann (1977), Westermann et al. (1989)
(b) Biomass yield coefficients (mg VSS mmol-1)				
YCE,dech	Dechlorinator growth on chloroethen	5.8	3.3-9.6	Maymo-Gattell et al. (1997), Hollinger et al. (1998), Hollinger et al. (1993), Fennell and Gossett (1998)
YH2,dech	Dechlorinator growth on H2	4.6	-	Calculated
YH2,meth	Methanogen growth on H2	0.97	0.62-1.5	Weimer and Zeikus (1978), Maillacheruvu and Parkin (1996), Roberton and Wolfe (1970), Zehander and Wuhrmann (1977), Perski et al. (1982)
(c)Maximum growth rate constants (day-1)				
µmax,dech1	PCE/TCE dechlorinators	0.245	-	Calculated
µmax,dech2	DCE/VC dechlorinators	0.075	-	Calculated
µmax,meth	Methanogens	0.336	-	Calculated
(d) Decay constants (day-1)				
bdech1	Decay rate for PCE/TCE dechlorinat	0.01	-	Assumed
bdech2	Decay rate for DCE/VC dechlorinato	0.003	-	Assumed
bmeth	Decay rate for methanogens	0.015	).007-0.02	Maillacheruvu and Parkin (1996), Kim et al. (1996), Callander et al. (1986)
(e) Half-saturation and inhibition constants (µM)				
Ks,PCE,dech1	PCE reduction to TCE by PCE/TCE dechlorinators	0.88	0.11-2.8	Tandoi et al. (1994), Fennel and Gossett (1998), Haston and McCarty (1999), Ballapragada et al. (1997)
Ks,TCE,dech1	TCE reduction to DCE by PCE/TCE dechlorinators	1.15	0.54-1.5	Tandoi et al. (1994), Fennel and Gossett (1998), Haston and McCarty (1999), Ballapragada et al. (1997)
Ks,DCE,dech2	DCE reduction to VC by DCE/VC dechlorinators	2.28	0.54-3.3	Tandoi et al. (1994), Fennel and Gossett (1998), Haston and McCarty (1999), Ballapragada et al. (1997)
Ks,VC,dech2	VC reduction to ETH by DCE/VC dechlorinators	325	2.6-360	Tandoi et al. (1994), Fennel and Gossett (1998), Haston and McCarty (1999), Ballapragada et al. (1997)
Ks,H2,dech	H2 utilization by both dehclorinator populations	0.072	).015-0.10	Fennell and Gossett (1998), Ballapragada et al. (1997), Smatlak and Gossett (1996)
Ks,H2,meth	H2 utilization by methanogens	6.1	0.5-22.2	Fennell and Gossett (1998), Robinson and Tiedje (1984), Weimer and Zeikus (1978), Maillacheruvu and Parkin (1996), Coates et al. (1996), Roberton and Wolfe (1970), Zehnder and Wuhrmann (1977), Westermann et al. (1989)
KI,CE,meth	PCE, TCE, DCE, VC, & ETH inhibitic methanogenic H2 utilization	100	100-<500	Yang and McCarty (2000), Fennell et al. (1997)
(f) H2 threshold concentrations (nM)				
CH2,th,dech	Min. H2 conc. at which dechlorinator gain energy	1.5	1.5-2.0	Fennell and Gossett (1998), Smatlak and Gossett (1996), Yang and McCarty (1998)
CH2,th,meth	Min. H2 conc. at which methanogens gain energy	33	11.0-77.0	Yang and McCarty (1998),Cord-Ruwisch et al. (1988), Conrad and Wetter (1990)
CH2,min,dech	Min H2 conc. at which dechlorinators can sustain growth	4.5	-	Calculated
CH2,min,meth	Min H2 conc. at which methanogens can sustain growth	318	-	Calculated
(g) Substrate conversion coefficients (mmol mmol-1)				
FH2/CE,dech	Moles H2 util. per mole of PCE dechlorinated to TCE, etc.	1.27	1.03-1.85	Loffler et al. (1999), Bagley (1998)
FH2/CH4,meth	Moles CH4 gen. per mole of H2 utili by methanogens	0.233	-	Bagley (1998)
(h) Maximum biomass concentration (mg VCC L-1)				
Xtot,max	Maximum ppossible total biomass concentration in aquifer	5000	-	Assumed

2.3.3.3 Glucose Model

This model developed by Lee *et al.* (2004) is the same as the membrane model above except for the method of hydrogen production or delivery. In the membrane model, hydrogen is delivered directly to the system through a membrane. In the glucose model, a fermenting population is modeled to convert glucose to hydrogen.

2.3.3.4 Regenesis Design Model

Regenesis, who sells HRC®, also provides HRC® design software to aid in designing an HRC® application. This software uses estimated plume size and concentrations to calculate an approximate amount of contaminant to be destroyed. Next, the program calculates the electron donor demand of the groundwater at the site based on the amount of contaminant present. The program also takes into account the amount of competing electron acceptors present in the groundwater that will also use the hydrogen from the HRC®. With this information, the amount of HRC® necessary for injection can be calculated. This software does a good job helping the user figure out how much HRC® will theoretically be needed to remediate the contaminant. The software also outputs the recommended injection well spacing in each row and the number of rows necessary. This recommendation is based on soil lithology and groundwater velocity. What is missing is the ability to show the user what is happening in the subsurface. This model does not account for the actual biochemical processes that are simulated in the previously mentioned models.

2.3.3.5 RT3D

Reactive Transport in 3-Dimensions (RT3D) is a computer model that solves the partial differential equations that describe the reactions and transport of multiple species, either mobile or immobile, in three-dimensional saturated groundwater systems (Clement, 1997). RT3D can describe three-dimensional advection, three-dimensional dispersion, linear, non-linear, or rate limited sorption, and biodegradation by either first-order, Monod, or dual-Monod kinetics. RT3D contains a preprogrammed module especially for first-order sequential decay reactions. This module simulates reactive transport coupled by a series of sequential degradation reactions for up to four components. RT3D also has a user defined module which allows a modeler to incorporate any relevant reaction into RT3D.

RT3D has been used numerous times to simulate CAH fate and transport (Clement *et al.,* 2000; Clement *et al.,* 1998). It has been found to be particularly useful in determining whether or not MNA is a viable remediation alternative at a particular site. At a site at Dover AFB, Delaware, RT3D was applied to analyze field-scale transport and biodegradation processes (Clement *et al.,* 2000). The model was calibrated to field data collected at the site. The calibrated model reproduced the general groundwater flow patterns, and also successfully recreated the observed distribution of PCE, TCE, DCE, and VC plumes. A great deal of information was generated from this successful modeling application, including contaminant decay rates and determination of which parameters are the most important in designing a remediation scheme.

2.3.4 Model Validation

Schlesinger (1979) defines model validation as "substantiation that a computerized model within its domain of applicability possesses a satisfactory range of accuracy consistent with the intended application of the model." It is important to be able to show that the output of a model is valuable and can be used to make decisions about a site. It is impossible to provide evidence that a model is absolutely correct, but it is possible to reach a consensus regarding the correctness of the model based on ample positive evidence (Niederer, 1990). It is with the goal of achieving consensus that the model accurately represents the site it was designed to model that the process of validation will be carried out. To validate a model, a number of steps must be performed. First, it must be verified that the structure of the model itself is correct to describe the important processes necessary. Next, the model must be applicable to the problem at hand. This can be determined by calibrating the model to observed conditions, then comparing model output to additional observed conditions that were not used in the calibration step.

3.0 Methodology

3.1 Overview

In this chapter, a model is presented that simulates the effect of HRC® application to achieve enhanced *in situ* bioremediation of TCE-contaminated groundwater. The numerical contaminant fate and transport model RT3D, supplemented with a user-defined module to model chlorinated ethene biodegradation simulated by HRC® addition, was used to simulate EISB of TCE at a contaminated site at Vandenberg Air Force Base, CA. MODFLOW was used to simulate steady-state groundwater flow at the site. Historical concentration data from the site were used to establish initial conditions for the model. RT3D used the hydraulic heads and flows from the MODFLOW model to calculate the advective/dispersive transport of the contaminants. RT3D also modeled biodegradation and sorption of TCE and its degradation daughter products, as well as the reactive transport of hydrogen, which is used as an electron donor in the reductive dehalogenation process, as it is created from the injected HRC®. Data from a pilot study at the Vandenberg site, where HRC® was injected into the TCE plume, were then used to validate the model. The validated model was subsequently used to design a full scale remediation for the Vandenberg site. To better understand the impact of site conditions and design decisions upon system performance, a sensitivity analysis was conducted.

3.2 The Vandenberg Site

The site of concern is located at Site 13 Cluster Advanced Ballistic Re-Entry Systems-A (ABRES-A) along the western edge of Vandenberg Air Force Base (see Figure 3.1). The site is a former rocket launch facility where large amounts of TCE were used to degrease

rocket engines prior to launch. The site is located in a surficial canyon which is bordered on the west by sand dunes. These sand dunes create a depression in which a small lake is located. The use of TCE has led to contamination in the lake, as well as the groundwater which flows in a subsurface canyon (paleochannel) that drains from the surficial canyon towards the ocean. TCE is found upgradient of the lake, with DCE and VC found downgradient of the lake. Anaerobic conditions favorable to TCE degradation are observed in the saturated zone resulting in a high rate of TCE degradation. However, it appears that DCE degradation occurs at a very slow rate, resulting in a buildup of DCE and VC. Monitored natural attenuation screening and groundwater contaminant fate and transport modeling at the site indicate that MNA alone could take up to 160 years to restore the site, which is not an acceptable timeframe (Tetra Tech, 2003).

A treatability study was conducted to evaluate the effectiveness of HRC® to treat chlorinated solvents in the groundwater. The objective of the HRC® injection is to increase the reduction potential of the water by increasing hydrogen concentration in the subsurface in order to accelerate degradation of DCE and VC. Upon injection of the HRC®, the groundwater was periodically monitored to evaluate the change in chlorinated solvent concentration. Data from the first 9 months of the treatability study are available for this thesis.

3.3 Model Selection and Implementation

When choosing the model equations to use in this thesis, the key criterion was to select a model that represented the important biological processes that affected the fate and

transport of the CAHs at the site. Prior research indicates that those processes are (1) the kinetics of CAH reductive dechlorination using hydrogen as an electron donor, taking into account the CAH parent-daughter compound concentrations as well as the hydrogen concentration, (2) the growth kinetics of the various microorganisms that effect and compete with the reductive dechlorination process, and (3) the competitive inhibition between CAHs. The production and competition, membrane, and glucose model each simulate the first process. Considering the second process, recent research has suggested that at least two separate dechlorinating bacteria play roles in the reduction of PCE or TCE to ethene (Flynn *et al.,* 2000). Based on these recent studies, it was felt to be important that two populations of dechlorinators be represented in the model. Both the membrane and glucose models simulated this. Another microbial population relevant to the study is the methanogens. This population can compete with dechlorinators for the limited hydrogen in the subsurface. Therefore, methanogens were also included in the model. All three models included methanogens. Finally, regarding the third process, both the membrane and glucose models simulate competitive inhibition between CAHs. The difference between the two models is that the glucose model simulates fermentation to supply hydrogen. It was decided that for the sake of simplicity, the model used in the current study would simulate hydrogen as a constant source. For this reason, fermentation was not needed in our model and the membrane model was chosen. RT3D will be used in this modeling research because of its capability to incorporate a user defined module that allows us to easily input and solve equations 2.17 – 2.25 from the membrane model. In addition, the ability of RT3D to simulate real-world CAH bioremediation has been proven (Clement *et al*., 2000). Another benefit of using RT3D

is that it is a component of the Department of Defense's Groundwater Modeling System (GMS) software, providing an easy to use visual interface for RT3D input and output.

3.3.1 The Model

The groundwater flow model described below was developed by TetraTech, Inc., and provided for use in this modeling effort. The TetraTech flow model was used as provided, without modification.

Figure 3.1 shows Site 13C at Vandenberg:

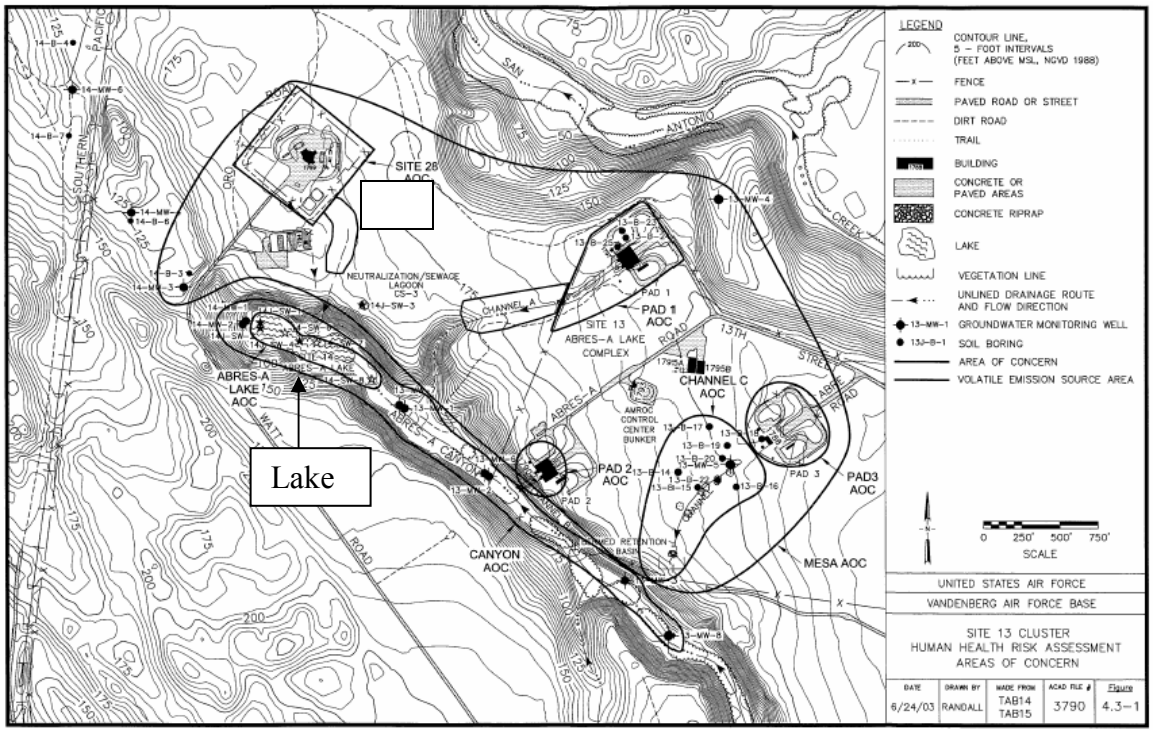

Figure 3.1 Vandenberg Air Force Base Site 13C

The area modeled begins in the southeast end of the canyon and follows the canyon northwest toward ABRES-A lake. The model continues in the northwest direction as the groundwater travels along this direction in a subsurface paleochannel. Figure 3.2

illustrates how the unique layout of the bedrock at Site 13C creates a river-like flow of groundwater along the paleochannel.

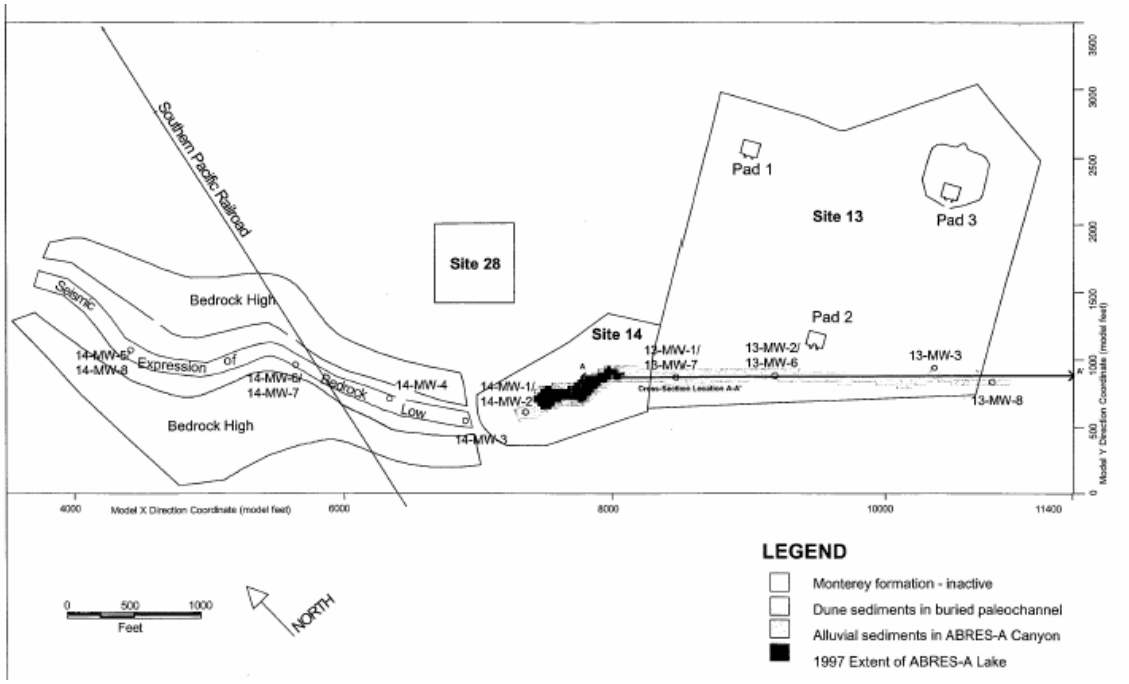

Figure 3.2 Site 13C Geological Conditions

Site 13C is located on the east side of Figure 3.2, and consists of three rocket launch pads (Pad 1, 2, and 3). A canyon travels along the southwest edge of site 13C towards ABRES-A lake. The paleochannel follows the seismic expression of bedrock that runs between the areas of high bedrock from ABRES-A lake to the northwest.

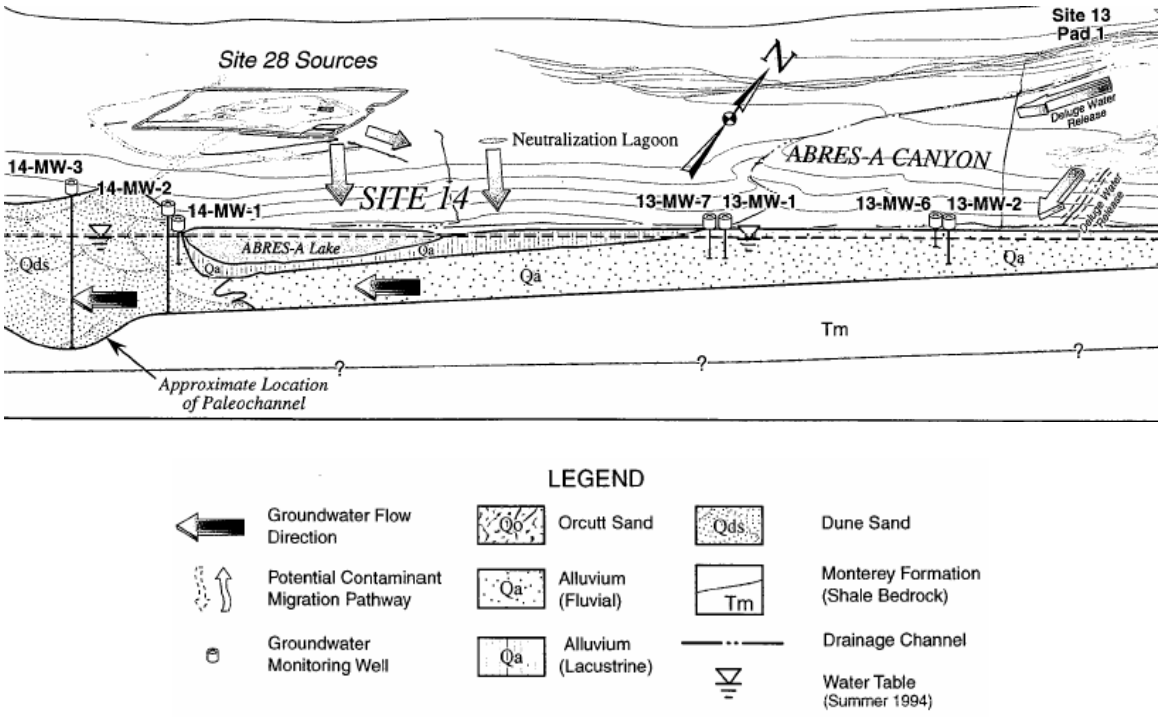

Figure 3.3 Cross section of site geology

In Figure 3.3 it can be seen that the low bedrock creates a paleochannel which funnels the groundwater in a river-like manner as it moves to the north-west away from ABRES-A lake. The model of the site simulates groundwater flow from south-east to north-west, showing how groundwater follows the canyon to the lake, and then flows through the paleochannel to the northwest. A model grid was created using the actual site as a guide. Each grid block is 6 meters square. The grid consists of two layers each about 10 meters thick. Based on concentration data that will be provided subsequently, two layers were chosen for the model. Upgradient of ABRES-A Lake the two layers were also used to model the different hydraulic conductivities found in the two layers of aquifer materials there (Figure 3.3). Downgradient of ABRES-A Lake the soil matrix is uniform dune

sand; therefore the hydraulic conductivity is the same in both layers. Figure 3.4 shows a plan view of the model grid layout.

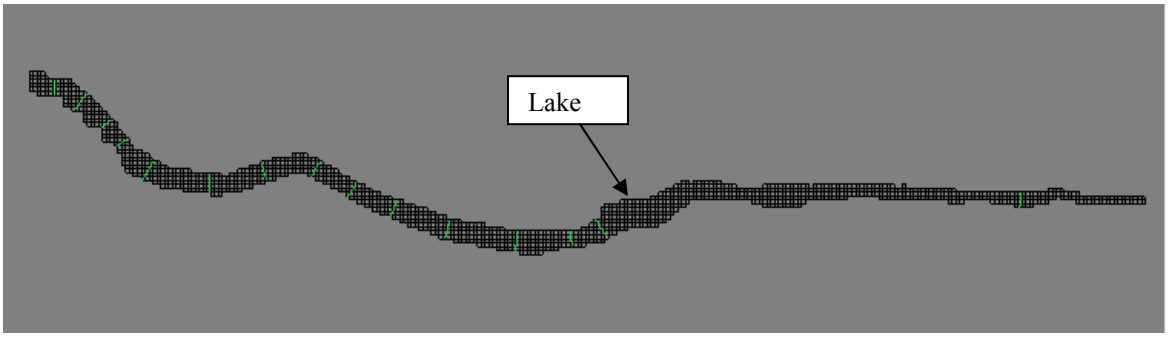

Figure 3.4 Model site grid

3.3.1.1 Site Hydrology

The model described above was used with the program MODFLOW to calculate hydraulic heads and groundwater fluxes in each cell. The boundary conditions for the flow model were a combination of constant head and no flow conditions. The boundaries along the side of the paleochannel aquifer are bedrock and were defined as no flow boundaries. The boundaries at the upgradient and downgradient limits of the paleochannel aquifer were defined as constant head boundaries. The upgradient boundary condition was set to a constant head of 83 feet above mean sea level (MSL) based on the head measured at monitoring well 13-MW-8. The downgradient boundary condition was set to a constant head of 15 feet above MSL based on the head measured at monitoring well 14-MW-5. The location of these monitoring wells can be seen in Figure 3.2. Table 3.1 lists the input parameters used in MODFLOW. The resulting output, shown in Figure 3.5, was then used by RT3D to perform contaminant transport calculations.

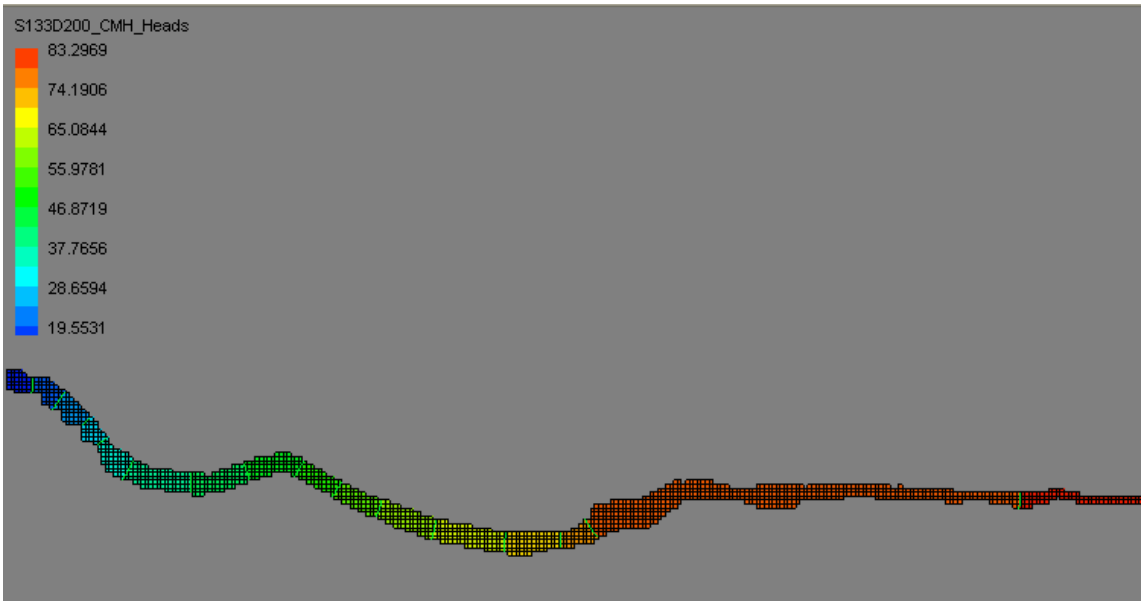

Figure 3.5 MODFLOW output

Table 3.1 Groundwater flow model input parameters (TetraTech, 2003)

Parameter	Value	Source
Flow		
For Alluvial Sediments		
Hydraulic Conductivity	13 ft/day	Average of slug test hydraulic conductivities of wells screened in alluvium
Total Porosity	0.376	Average of alluvial sediments
Effective Porosity	0.251	2/3 of total porosity for alluvial sediments
For Dune Sand Sediments		
Hydraulic Conductivity	45 ft/day	Average of slug test hydraulic conductivities of wells screened in dune sand
Total Porosity	0.323	Average of dune sand sediments
Effective Porosity	0.215	2/3 of total porosity for dune sand sediments

3.3.1.2 Contaminant Fate and Transport

RT3D was used to model the transport and reductive dehalogenation of TCE and its daughter products, DCE and VC, through the Site 13C aquifer. There are two components to this modeling effort. Initially, the historical data were used to approximate the first-order biological decay constants for TCE, DCE, and VC. The

approximated first-order decay constants were kept within reasonable ranges as determined from BIOCHLOR studies as shown in Figure 2.8. These first-order decay constants were then used as input parameters to RT3D to predict the extent of biodegradation that would have occurred at the site since the start of the HRC® pilot study had the HRC® not been injected. This provided a baseline to compare to the actual results of the pilot study in order to assess the success or failure of the HRC® to accelerate biodegradation of the contaminants beyond what was occurring naturally. The second part of the modeling effort simulated the effect on biodegradation rates of the HRC® injection. The model was calibrated using sampling data obtained over the first three months after HRC® injection. The calibration step will be discussed further in section 3.4.2 below. For validation, the model is then used to predict chlorinated ethene concentrations that were measured at sampling events that occurred six and nine months after HRC® injection.

Table 3.2 Contaminant fate and transport model input parameters (TetraTech, 2003)

Parameter	Value	Source
Transport		
Longitudinal Dispersivity (αL)	50 ft	Gelhar et al. 1985
Transverse Dispersivity	1/8 * αL	Gelhar et al. 1985
Vertical Dispersivity	1/160 * αL	Gelhar et al. 1985
Dry Bulk Density	1.80 g/cm3	Average of dune sand sediments
Fraction Organic Carbon	0.0017	Average of dune sand sediments
TCE retardation factor	6.32	Estimated using the site organic carbon data and the VOC organic carbon partition coefficients.
DCE retardation factor	3.06	
VC retardation factor	2.16	
Decay		
TCE degradation rate	0.001 yr^{-1}	Estimated using historical data
DCE degradation rate	0.008 yr^{-1}	Estimated using historical data
VC degradation rate	0.07 yr^{-1}	Estimated using historical data

3.3.1.2.1 Simulating Site Conditions in the Absence of HRC® Application

Table 3.2 lists all parameters used in the contaminant fate and transport model. The transport parameters listed were either taken from the literature or calculated using data from the site. The first-order decay constants provided by TetraTech (2003) were found to produce unrealistic results when used in our model. For this reason, as previously mentioned, the first-order decay constants were estimated by using them to calibrate RT3D to CAH concentration measurements at the site over four years of active monitoring. Once the model was calibrated, it was used in a predictive mode to simulate CAH fate and transport from the time just prior to HRC® injection to the present, under the assumption that HRC® had not been injected. This provided a prediction of CAH concentrations that would be found had the HRC® treatability study never taken place. This prediction was used for comparison with actual post-HRC® site data, in order to answer research questions 1 and 2 and determine the impact the HRC® application had.

3.3.3 Modeling Remediation by HRC®

In order to simulate the HRC® pilot study area, where data were collected over relatively short distances and timeframes, it was necessary to construct a detailed local model of the area. This was accomplished by taking the regional model and refining it in the area of the pilot study. The grid size of this local model was 0.6 meter square (Figure 3.5). The local model used the parameters determined in the regional model. The local model was oriented in such a way that the top and bottom boundaries were parallel to flow and were considered no-flow boundaries. The right and left boundaries were set as constant head

boundaries. Figure 3.6 shows the local model along with the three HRC® injection wells and three monitoring wells.

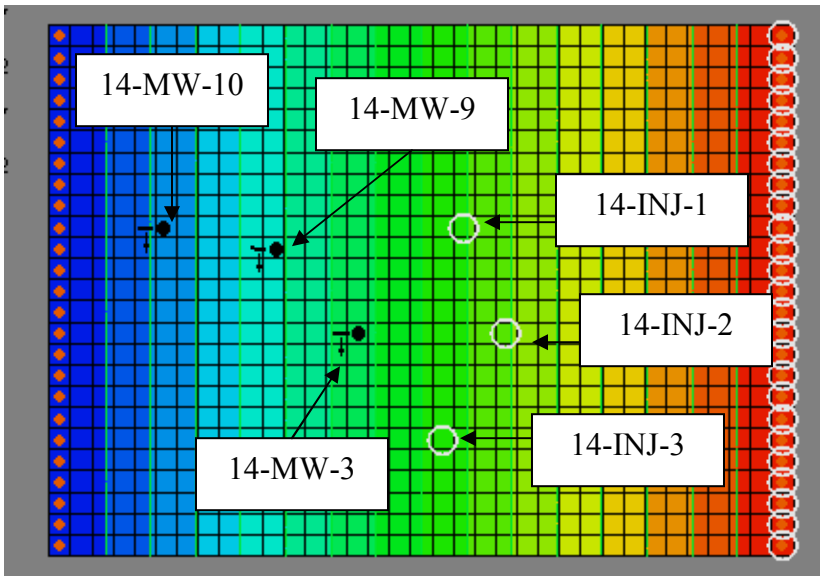

Figure 3.6 Local model with injection (INJ) and monitoring (MW) wells

HRC® was modeled as a constant source of hydrogen in the subsurface at the points of injection. From laboratory studies, we know that at the HRC®-water interface the concentration of lactate can reach levels around 110 mM (Regenesis, personal correspondence). Using this concentration of 110 mM lactate, and knowing the mass of HRC® injected per well (203 kg which is approximately 170 liters of HRC®), we were able to calculate the lactate mass loading rate at each well as follows. The injection well was screened over 6.1 m and we assumed that the well was purged after HRC® injection, meaning there was no residual HRC® inside the well. We assumed the HRC® would move away from the injection well evenly in all directions forming a hollow cylinder of HRC® with the hollow center being the injection well. The porosity of the soil was assumed to be 0.3. Using the equation for the volume of a hollow cylinder, and knowing

that 170 liters of HRC® was emplaced outside a 0.05 m radius well into an aquifer of porosity 0.3, we can determine that the HRC® will approximate a hollow cylinder of height 6.1 m and outer radius 0.164 m. The next step was calculating the area perpendicular to flow, which was the length of the cylinder, 6.1 m, multiplied by the diameter. This value then had to be modified to find the effective area of flow. The cross sectional area of the well was subtracted out and the remaining area was multiplied by the porosity to result in an effective area of HRC® perpendicular to flow of 0.41 m^2 at each injection well. The groundwater pore velocity was calculated to be 0.046 m/d using a hydraulic conductivity of 13.7 m/d, a hydraulic gradient of 0.001 m/m, and a porosity of 0.3. Using this pore velocity, flow was calculated as 18.9 liters/d through the effective area of HRC. Multiplying 18.9 liters/day by 110 mM lactate gave us the mass of lactate leaving the source area as 2.079 moles lactate/day. By stoichiometry, when fermented, 1 mole of lactate produces 2 moles of H_2. Thus, if we assume rapid fermentation of lactate, we find that the H_2 mass loading near the HRC® injection zone is 4.158 moles H_2/day. This value was used for the mass loading of hydrogen at each well.

As the hydrogen is transported by the groundwater it will create the reducing conditions that are necessary to accelerate the reductive dehalogenation of the CAHs. We assume that CAH degradation kinetics can be simulated using a dual-Monod model, where the rate of dechlorination is a function of both the contaminant concentration and the H_2 concentration. The Clapp *et al.* (2004) model presented in section 2.3.3.2 was used in this modeling effort. The Clapp *et al.* (2004) model assumed there were two different populations of microorganisms, one that fed on PCE/TCE and another that fed on

DCE/VC. The model also assumes methanogens play a significant role in competing for the electron donor (H_2). Although PCE is not present at Site 13C, it was included in the model so that the model can be used at other sites where PCE is present. Since there is no PCE present at Site 13C, it was turned off during simulation by setting the initial PCE concentration to zero. Competitive inhibition was included in this model. Competition by methanogens was accounted for using the method described by Clapp *et al.* (2004). The following transport equations are modified from equations 2.16 – 2.20 to simulate advective/dispersive transport of chlorinated ethenes affected by linear equilibrium sorption and reductive dehalogenation with the dehalogenation rate described by dual-Monod kinetics:

$$R_{PCE}\frac{\partial C_{PCE}}{\partial t} = D_{ij}\frac{\partial^2 C_{PCE}}{\partial x^2} - v_i\frac{\partial C_{PCE}}{\partial x} - r_{PCE} \tag{3.2}$$

$$R_{TCE}\frac{\partial C_{TCE}}{\partial t} = D_{ij}\frac{\partial^2 C_{TCE}}{\partial x^2} - v_i\frac{\partial C_{TCE}}{\partial x} - r_{TCE} + F_{TCE/PCE} * r_{PCE} \tag{3.3}$$

$$R_{DCE}\frac{\partial C_{DCE}}{\partial t} = D_{ij}\frac{\partial^2 C_{DCE}}{\partial x^2} - v_i\frac{\partial C_{DCE}}{\partial x} - r_{DCE} + F_{DCE/TCE} * r_{TCE} \tag{3.4}$$

$$R_{VC}\frac{\partial C_{VC}}{\partial t} = D_{ij}\frac{\partial^2 C_{VC}}{\partial x^2} - v_i\frac{\partial C_{VC}}{\partial x} - r_{VC} + F_{VC/DCE} * r_{DCE} \tag{3.5}$$

$$R_{H_2}\frac{\partial C_{H_2}}{\partial t} = D_{ij}\frac{\partial^2 C_{H_2}}{\partial x^2} - v_i\frac{\partial C_{H_2}}{\partial x} - r_{H_2,dech} - r_{H_2,meth} \tag{3.6}$$

$$r_{PCE} = k_{PCE,dech1}X_{dech1}\left(\frac{C_{PCE}}{K_{s,PCE,dech1}\left(1+\frac{C_{TCE}}{K_{x,TCE,dech1}}\right)+C_{PCE}}\right)\times\left(\frac{C_{H_2}-C_{H_2,th,dech}}{K_{s,H_2,dech1}+\left(C_{H_2}-C_{H_2,th,dech}\right)}\right) \tag{3.7}$$

$$r_{TCE} = k_{TCE,dech1} X_{dech1} \left(\frac{C_{TCE}}{K_{s,TCE,dech1}\left(1 + \frac{C_{PCE}}{K_{x,PCE,dech1}}\right) + C_{TCE}} \right) \times \left(\frac{C_{H_2} - C_{H_2,th,dech}}{K_{s,H_2,dech1} + \left(C_{H_2} - C_{H_2,th,dech}\right)} \right) \tag{3.8}$$

$$r_{DCE} = k_{DCE} X_{dech2} \left(\frac{C_{DCE}}{K_{s,DCE,dech2}\left(1 + \frac{C_{VC}}{K_{s,VC,dech2}}\right) + C_{DCE}} \right) \times \left(\frac{C_{H_2} - C_{H_2,th,dech}}{K_{s,H_2,dech2} + \left(C_{H_2} - C_{H_2,th,dech}\right)} \right) \tag{3.9}$$

$$r_{VC} = k_{VC} X_{dech2} \left(\frac{C_{VC}}{K_{s,VC,dech2}\left(1 + \frac{C_{DCE}}{K_{s,DCE,dech2}}\right) + C_{VC}} \right) \times \left(\frac{C_{H_2} - C_{H_2,th,dech}}{K_{s,H_2,dech2} + \left(C_{H_2} - C_{H_2,th,dech}\right)} \right) \tag{3.10}$$

H_2 utilization by the two dechlorinating microbial populations was described using the following equation which is modified from equation 2.21 in order to keep the units in terms of hydrogen concentration per time.

$$r_{H_2,dech} = F_{H_2/PCE} r_{PCE} + F_{H_2/TCE} r_{TCE} + F_{H_2/DCE} r_{DCE} + F_{H_2/VC} r_{VC} \tag{3.11}$$

H_2 utilization by methanogens was described using the following equation, which is similar to equation 2.22:

$$r_{H_2,meth} = k_{meth} X_{meth} \left(\frac{C_{H_2} - C_{H_2,th,meth}}{K_{s,H_2,meth} + \left(C_{H_2} - C_{H_2,th,meth}\right)} \right) \tag{3.12}$$

The parameters in the above equations are identical to those described in chapter 2. In equation 3.12, the inhibition term from equation 2.22 has been removed because it has

been shown that inhibition to methanogens occurs only within 2 mm of the NAPL contaminant source and therefore can be considered negligible throughout the contaminant plume (Chu *et al.,* 2003). The microorganism population growth/decay was described using the following equations:

$$r_{X,dech1} = Y_{dech}(r_{PCE} + r_{TCE}) - b_{dech1}X_{dech1}; X_{dech1} > X_{dech1,\min}$$
$$r_{X,dech1} = 0; X_{dech1} \le X_{dech1,\min} \quad (3.13)$$

$$r_{X,dech2} = Y_{dech}(r_{DCE} + r_{VC}) - b_{dech2}X_{dech2}; X_{dech2} > X_{dech2,\min}$$
$$r_{X,dech2} = 0; X_{dech2} \le X_{dech2,\min} \quad (3.14)$$

$$r_{X,meth} = Y_{meth}r_{H_2,meth} - b_{meth}X_{meth}; X_{meth} > X_{meth,\min}$$
$$r_{X,meth} = 0; X_{meth} \le X_{meth,\min} \quad (3.15)$$

Equations 3.13-3.15 include a "switch" to keep the population of microorganisms from completely disappearing in areas where electron donor or acceptor is depleted (Parr, 2002).

3.3.4 Model Assumptions

(1) Dehalogenating microorganisms were assumed to be ubiquitous at some relatively low, initial spatially constant concentration.

(2) In order not to build an overly complex model, the effect of competing electron acceptors like nitrate and sulfate on CAH biodegradation was not simulated. Although sampling data confirms the presence of some competing electron acceptors, we feel justified in not explicitly simulating their effect as the calibrated first-order CAH degradation rate constants that we are using implicitly account for their impact on CAH biodegradation.

(3) Groundwater flow was assumed to be steady state. The soil matrix will be assumed to consist of two layers, which are each homogeneous and isotropic.

(4) HRC® acts as a constant source of hydrogen. The actual process involves the breakdown and fermentation of a number of acids to produce hydrogen, as discussed in chapter 2. For the sake of simplicity, we do not simulate these fermentation reactions, and assume HRC® generates hydrogen directly. In essence, we are assuming that the rate of fermentation is fast compared to the rate of dechlorination.

(5) Cell yield ($Y_{biomass}$) and biomass decay (b) did not change with the presence of HRC®. Cell yield was also assumed to be the same for each contaminant being degraded.

(6) Dissolved hydrogen was assumed to be nonsorbing. That is, R_{H_2} in equation 3.5 equals 1.0.

3.4 Model Application

3.4.1 Validation

The first step in validating the model was creating a batch model, with transport turned off, to verify that the biodegradation portion of the model is behaving correctly. The batch model was used to simulate the behavior of the contaminants, microorganisms, and hydrogen as a function of time. In their study, Lee *et al.* (2004) developed a model for the reductive dehalogenation of PCE to ethene. The model included fermentors that convert the primary donor used (glucose) into byproducts including hydrogen. Methanogens and two dehalogenator groups were also included. The dehalogenators used the hydrogen as an electron donor and the different CAH contaminants as electron acceptors. The results of the batch model simulations were compared to simulations

presented in Lee *et al.* (2004). Comparing model simulations with published results serves to confirm that the biological process equations are accurately represented in the model code.

As described below, the model of HRC® performance was calibrated using monitoring data taken over the initial three months (baseline, 10, 30, 60, and 90 days) of the treatability study. The calibrated model was then used to predict data from the subsequent six months (180 and 270 days) as a validation step.

3.4.2 Calibration

The model was calibrated to the pilot study results by varying certain parameters (Table 3.3) in order to obtain the best visual fit of model output to measured CAH concentrations, while keeping the parameters within ranges reported in the literature. An important note is that by varying the longitudinal dispersivity, the transverse and vertical dispersivities were varied as well. In the model, it was assumed the longitudinal:transverse dispersivity ratio was constant at 1:8, and that the longitudinal:vertical dispersivity ratio was constant at 1:160 (Gelhar *et* al., 1985). The model was run to simulate a three-month period and model CAH concentrations simulated at three monitoring wells (14-MW-3, 14-MW-9, and 14-MW-10) were compared to the actual monitoring data taken at those same monitoring wells during the first three months of the treatability study. Concentrations were obtained at 0 days, 10 days, 30 days, 60 days, and 90 days. The actual and modeled data were compared side by side on graphs and parameters were adjusted to obtain the best visual fit at all three

wells. The parameters used in the calibration that produced the best fit are shown in the "used" column in Table 3.3.

Table 3.3 Parameters used in model calibration

Parameter	Description	Units	Tested	Used
k_{TCE}	Maximum specific dechlorination rate of TCE to DCE	µmol TCE/ mg biomass-d	2.4 – 365.8	365.8
k_{DCE}	Maximum specific dechlorination rate of DCE to VC	µmol DCE/ mg biomass-d	1.7 - 48	1.65
k_{VC}	Maximum specific dechlorination rate of VC to ethene	µmol VC/ mg biomass-d	2.6 - 48	2.56
$k_{H2,meth}$	Maximum H_2 utilization by methanogens	µmol H_2/ mg biomass-d	27 - 1500	1500
$K_{S(TCE)}$	Half-velocity coefficient for TCE dehalogenation	µM	0.049 - 1.44	0.76
$K_{S(cDCE)}$	Half-velocity coefficient for DCE dehalogenation	µM	0.54 - 3.3	3.3
$K_{S(VC)}$	Half-velocity coefficient for VC dehalogenation	µM	2.6 - 360	320
$K_{sH2,dech}$	H2 utilization by both dechlorinator populations	µM	0.015 - 0.1	0.072
K	Hydraulic conductivity	m/day	1.5 - 30.5	15.2
α_L	Longitudinal dispersivity	m	4.27 - 98.5*	13.7

* Varying the longitudinal dispersivity resulted in simultaneously varying the transverse and vertical dispersivities (see text).

3.4.3 Comparison of site with and without HRC®

The output for the site model that does not incorporate HRC® injection (using the first-order degradation rate constants calculated from historical data) was compared to the actual data obtained during the treatability study in order to approximate the effect of HRC® injection on CAH concentrations. This analysis can also help answer research question #2 regarding the potential of the HRC® to produce harmful byproducts such as vinyl chloride. If the amount of VC actually present at the site is significantly greater

than what was predicted had the HRC® not been employed, this is an indicator that the HRC® injection resulted in greater accumulation of VC.

3.5 HRC® Injection System Design

In order to help determine which parameters are most important to consider when designing an HRC® EISB system, a sensitivity analysis was run. The sensitivity analysis was conducted in two parts. The first part consisted of varying eight environmental parameters to determine how changes in these parameters affected the contaminant concentrations simulated by the model. The second part consisted of varying an engineered parameter, the HRC® injection well spacing, to determine how this spacing affects contaminant concentrations. The results of the well spacing analysis could also be used in designing an HRC® injection system to ensure hydrogen reaches all areas of the contaminant plume. In this study, it is assumed that if hydrogen has reached an area of the plume in sufficient concentration, dechlorination will occur. A full-scale system could then be designed and modeled and the simulated CAH concentrations in the plume could be compared to the MCLs to determine system effectiveness. The results of both parts of this analysis are presented in Section 4.5.

3.5.1 Sensitivity Analysis

In order to answer research question 3 and determine what conditions favor the use of HRC® to accelerate natural attenuation, a sensitivity analysis was conducted. The first part of the analysis consisted of varying eight environmental parameters to determine how changing these parameters affected the contaminant concentration simulated by the

model. The parameters varied were the longitudinal dispersivity, α_L, the hydraulic conductivity, K, the maximum specific utilization rate, k, of TCE, DCE, and VC, and the half-saturation and inhibition constant K_s, of TCE, DCE, and VC. These parameters were varied, one at a time, within reasonable ranges (Table 3.3), while all other parameters were held constant, to evaluate the impact each parameter had on simulated performance of the HRC® EISB system.

The sensitivity analysis was conducted following the methodology of Rong *et al.* (1998). The model was run by varying the input parameter values, one at a time, within reasonable ranges. Then model outputs from various input values are compared with the respective "baseline" case. The baseline values are labeled as "Used" in Table 3.3. Sensitivity was measured using relative sensitivity (S), where relative sensitivity is calculated using equation (3.16):

$$S = \left| \left(\frac{df}{f} \right) \left(\frac{x}{dx} \right) \right| \tag{3.16}$$

where x and f are baseline input and model output values, and dx and df are input and model output range, respectively.

The next step in the sensitivity analysis was to see how the HRC® injection well spacing affects system performance. The Regenesis HRC® design software discussed in Chapter 2 (Regenesis, 2002) recommends a 3 meter on-center spacing of injection wells for the average case, with spacing increased to as much as 4.5 meters on-center for sites with high groundwater flow and dispersivity (such as gravelly or rocky soils), and decreased to 2.4 meters on-center for sites with low hydraulic conductivities and dispersivity (such as

silty or clayey soils). By modeling the injection of HRC® and subsequent transport of hydrogen through the aquifer matrix, the area of influence of a single injection well can be seen. Knowing the area of influence of a single injection well under specific hydrogeologic conditions will allow the user to design a full-scale treatment system to ensure that hydrogen is fully mixed across the CAH plume. In this study, the hydrogen plume resulting from a single HRC® injection well was modeled over a period of 180 days. The model was run multiple times for varying values of hydraulic conductivity and dispersivity. The remaining parameters were set to those determined in the model calibration. They are listed in Table 3.3 as values used. The object was to find the maximum separation between injection wells that could be achieved while meeting the following criteria: (1) hydrogen concentrations must be at least 1.5 nM (which is the minimum hydrogen concentration at which dechlorinating microorganisms gain energy (Clapp *et al.,* 2004)) in the area of aquifer needing treatment within 180 days of injection of HRC®, and (2) the plume of hydrogen produced from the HRC® injection well must intersect the plume of hydrogen produced from the adjacent HRC® injection well within 20 meters downgradient of the injection site. Adherence to these criteria helps ensure that no contaminated groundwater flows past the HRC® injection zone without being in contact with sufficient hydrogen for the dechlorinators to effectively treat the contaminants. The results of this exercise are presented in Section 4.5.

3.5.2 Error Analysis

An analysis of the error between the measured concentrations at the site and the simulated values resulting from both the calibration and validation steps was run.

Pebesma *et al*. (2004) showed that observed and predicted values can be represented as a continuous time series over the simulation period τ as follows:

$$\{o(t), p(t)\}, t \in \tau \tag{3.17}$$

where o(t) and p(t) are, respectively, the observed and predicted values at time t. The residual, or error, time series e(t) can be defined as:

$$\{e(t) = o(t) - p(t)\}, t \in \tau \tag{3.18}$$

As defined in equation 3.18, negative and positive errors indicate over prediction and under prediction, respectively. In this thesis, we sampled observed and simulated concentrations at discrete intervals. Equation 3.18 can be rewritten as follows:

$$e(i) = o(i) - p(i), i = 1,...n \tag{3.19}$$

One of the most commonly used measures for the average size of errors is the mean square error (MSE) (Pebesma *et al*., 2004),

$$MSE = \frac{1}{n}\sum_{i=1}^{n} e(i)^2 \tag{3.20}$$

and its square root, the root mean square error (RMSE). To compare RMSE values across different variables or across events with different magnitude, they can be divided by the mean of the observed values over the entire event, $\overline{o}$ (Pebesma *et al*., 2004). This yields the relative RMSE, given by:

$$RMSE_r = \sqrt{MSE} / \overline{o} \tag{3.21}$$

RMSE and $RMSE_r$ are always positive, with smaller values indicating a smaller error or in other words, the predicted value matched the observed value well.

3.5.3 Design of an HRC® EISB System

In order to answer research question number 4, concerning how an HRC® injection system should be designed to ensure a CAH-plume is effectively treated to meet remediation goals, it was necessary to determine the criteria that could be measured and used to signify success. The most obvious criterion for a successful design is achieving downgradient contaminant concentrations below the maximum contaminant levels (MCLs) in a reasonable timeframe. The results from the sensitivity analysis of injection well spacing were used to design an HRC® injection system for the Vandenberg site. The assumption here was that the most complete coverage of hydrogen provided by the injection wells would produce the greatest reduction in CAH concentrations. A system that was designed to ensure full hydrogen coverage across the CAH plume was then modeled for a period of one year and the simulated downgradient CAH concentrations compared with MCLs to determine effectiveness. The results of this study are in Section 4.5.1.

4.0 Results and Analysis

4.1 Introduction

In this chapter we present and discuss the results obtained by applying the numerical flow model coupled with the dual-Monod biochemical fate and transport model developed in chapter 3 to the site conditions at the Vandenberg AFB site. We begin the chapter by using first-order decay parameters to estimate contaminant concentrations that would exist at the Vandenberg site had the HRC® pilot study not taken place. Then, in order to quantify the effects of the HRC® pilot study, we compare the 9-month pilot study results to the simulated "no HRC® added" results for the same 9 month period. In Section 4.3 we verify the general behavior of the model by running the model in a batch mode by "turning off" groundwater flow and comparing the results to published results where virtually the same biochemical model was run to simulate batch experimental results. When the biochemical portion of the model has been verified, we apply the full model to the Vandenberg site in Section 4.4, using the first three months of sampling data from the HRC® pilot study to calibrate the model. The 6- and 9-month data from the pilot study are then used to validate that the model. In Section 4.5, we conducted a sensitivity analysis, varying environmental and engineered parameters to see how these factors influence the effectiveness of HRC® at accelerating reductive dehalogenation of CAH-contaminated groundwater. Finally, it is shown how the model can be applied to design an HRC® injection treatment system for a site.

4.2 HRC® Effectiveness

As discussed in Chapter 3, a simple method was devised to approximately quantify the effect of HRC® on the degradation of the CAHs. RT3D, with its sequential decay module (as described in Section 2.3.3.5), which assumes sequential first-order decay, was used to predict CAH concentrations at the site had the HRC® never been injected. These results could then be compared to the actual monitoring data collected at the site over the 9 months subsequent to HRC® injection.

4.2.1 Contaminant Concentrations Simulated without the HRC® Pilot Study Compared to Pilot Study Results

There are three wells in the vicinity of the pilot study at Vandenberg AFB. These wells are designated 14-MW-3, 14-MW-9, and 14-MW-10 as seen in Figure 3.6. The pilot study began October 2003 and went through June 2004. Thus, for this comparison, the estimate of contaminant concentrations without HRC® uses the CAH concentrations measured in the wells in October 2003 as an initial condition. Using GMS's inverse distance weighted method of 3D interpolation, the measured concentrations were input in their respective well locations, and then extrapolated to obtain a contaminant concentration value at each grid location in the model. Using these initial concentration values, GMS was then run to simulate CAH concentrations over a 9 month period, using the parameters listed in Table 3.2 with RT3D and its chain decay module. The first-order rate parameter values used were obtained by running RT3D's chain decay module and varying the first-order rate parameter until the best achievable visual fit was obtained between the model results and the historical monitoring data from many wells throughout

the Vandenberg site. The model was then run with these best-fit first-order parameter values to simulate CAH concentrations at the three monitoring wells over the 9-month pilot study. Simulation results are presented in Figures 4.1 – 4.9, along with the concentrations actually measured during the HRC® pilot study.

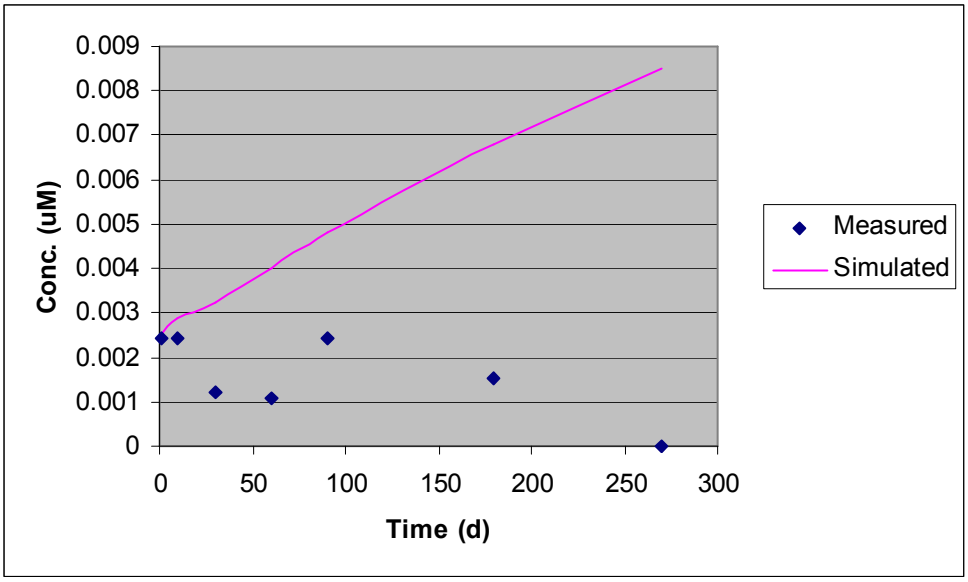

Figure 4.1 Measured and simulated TCE values at 14-MW-3

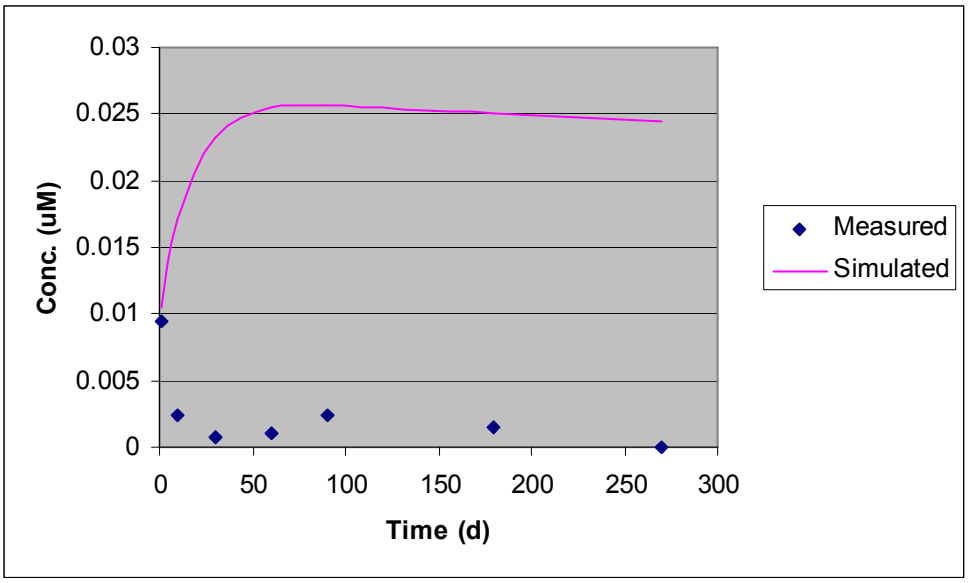

Figure 4.2 Measured and simulated TCE values at 14-MW-9

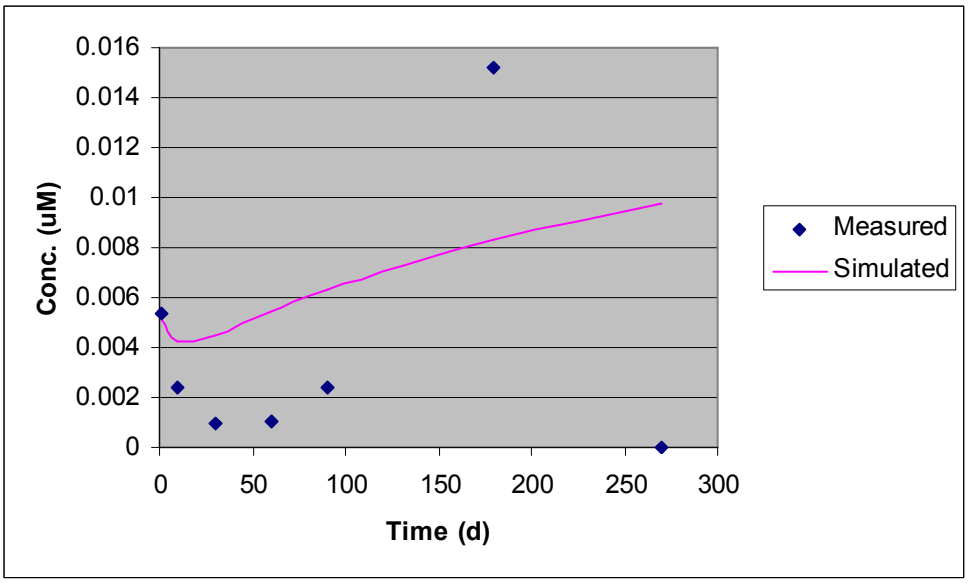

Figure 4.3 Measured and simulated TCE values at 14-MW-10

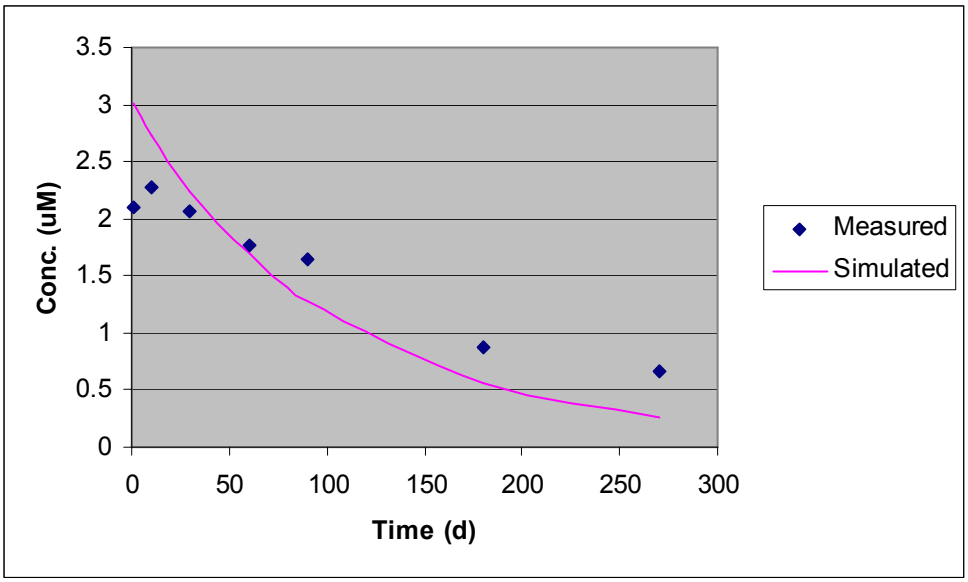

Figure 4.4 Measured and simulated DCE values at 14-MW-3

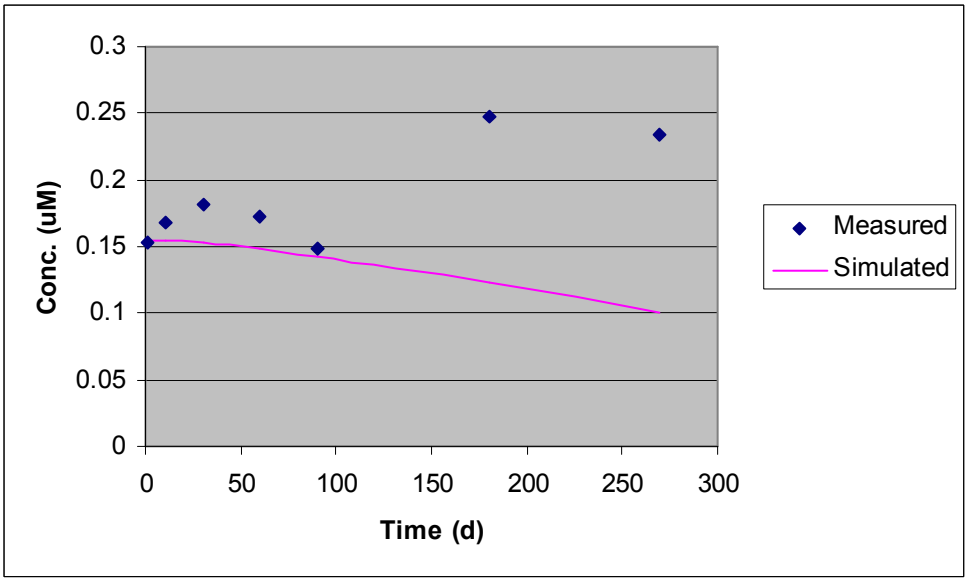

Figure 4.5 Measured and simulated DCE values at 14-MW-9

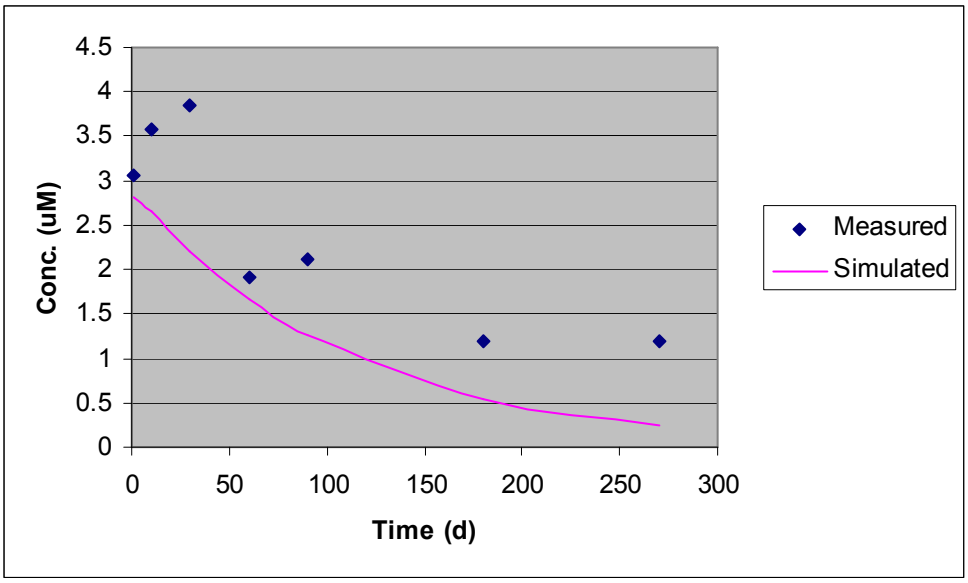

Figure 4.6 Measured and simulated DCE values at 14-MW-10

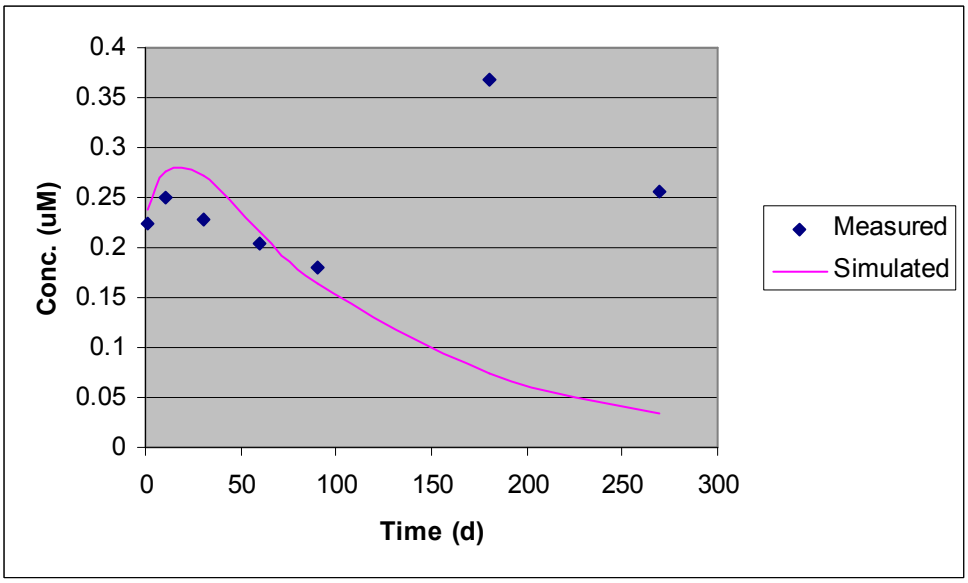

Figure 4.7 Measured and simulated VC values at 14-MW-3

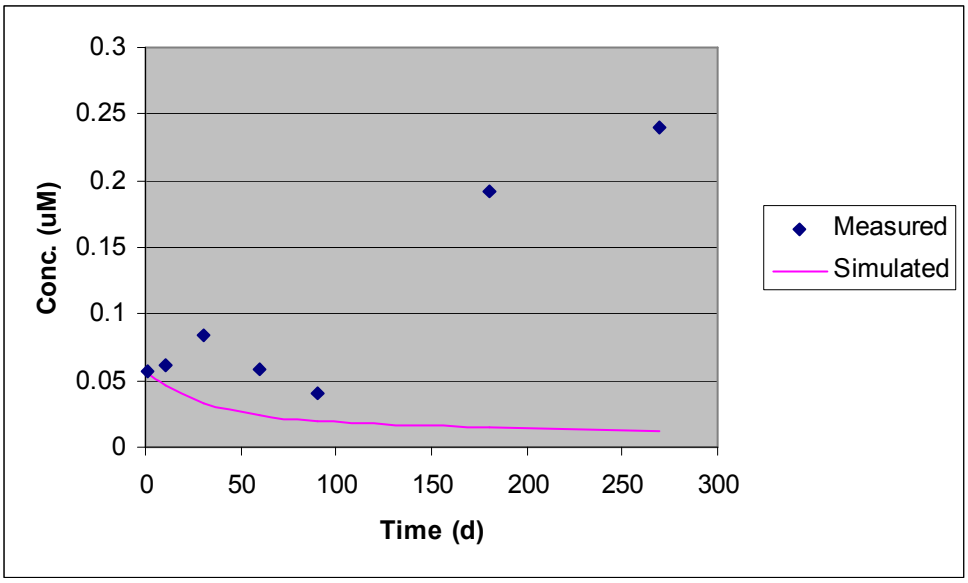

Figure 4.8 Measured and simulated VC values at 14-MW-9

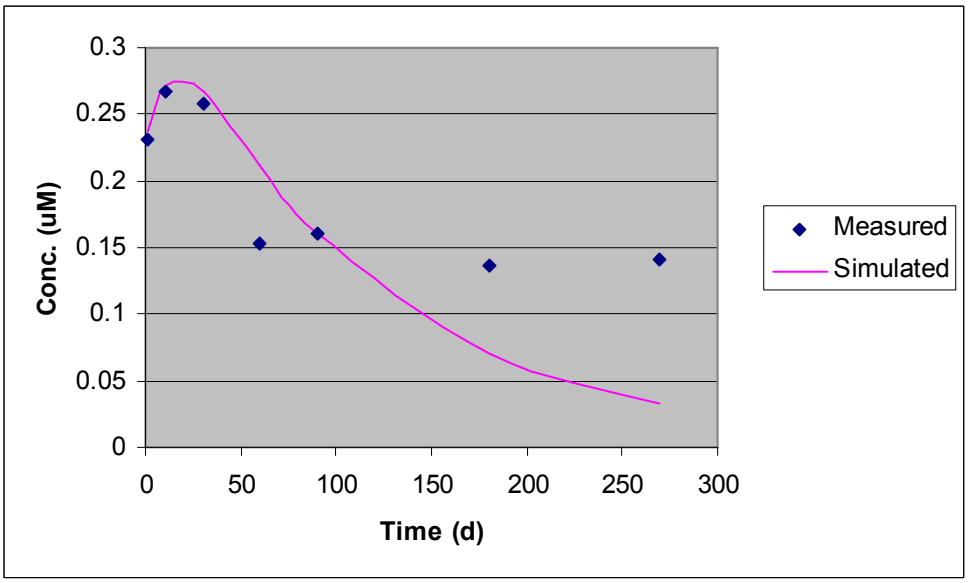

Figure 4.9 Measured and simulated VC values at 14-MW-10

4.2.2 Discussion

Looking at figures 4.1 – 4.3, it can be observed that the measured TCE concentrations were lower than the simulated concentrations at all wells. This is

consistent with the assumption that the HRC® is accelerating the conversion of TCE to DCE. Figures 4.4 – 4.9 show measured DCE and VC concentrations equal to or greater than those predicted using RT3Ds first-order decay module. This may be due to the fact that the HRC® has accelerated biodegradation of TCE, resulting in increased production of DCE and VC daughter products.

4.3 Model Verification

At this point we will discuss the dual-Monod kinetics submodel, which was developed for use in this study to describe CAH biodegradation kinetics. The submodel was incorporated as a user-defined module in RT3D. In order to gain confidence that the submodel was working correctly, we tested it by verifying the mass balance of the model output and also by comparing model output to published results of a similar study.

4.3.1 Mass Balance

The submodel was run in a batch mode by disabling the transport (advection and dispersion) functions in GMS in order to more easily track the mass of each reactant. The results of the simulation are shown in Figure 4.10. The figure shows that the submodel correctly conserves mass, and that every mole of PCE is ultimately converted to ethene.

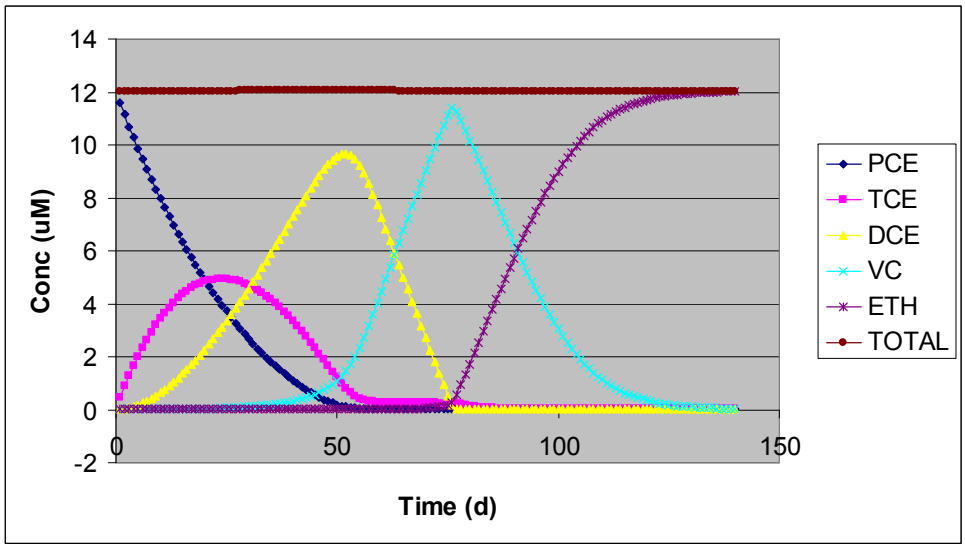

Figure 4.10 Biochemical submodel mass balance

4.3.2 Comparison to Published Results

The next step in verifying the biochemical submodel was to compare its results to similar published results. Lee *et al*. (2004) performed a similar study in which they modeled the reductive dehalogenation of PCE using different sources of hydrogen. The equations used in the glucose model by Lee *et al*. (2004) (as seen in Section 2.3.3.3) are the same as ours. In order to obtain similar results, our submodel was run in a batch mode using initial concentrations of PCE and DCE that matched the initial concentrations of the CAHs that were used in the Lee *et al.* (2004) study. The hydrogen source of the glucose model varied, because the model included fermentation to provide hydrogen. For comparison, we matched the hydrogen source behavior as best we could by varying the hydrogen mass loading over time. Side-by-side comparisons of their results (top) and our results (bottom) are shown in Figures 4.11 and 4.12 for TCE and DCE respectively.

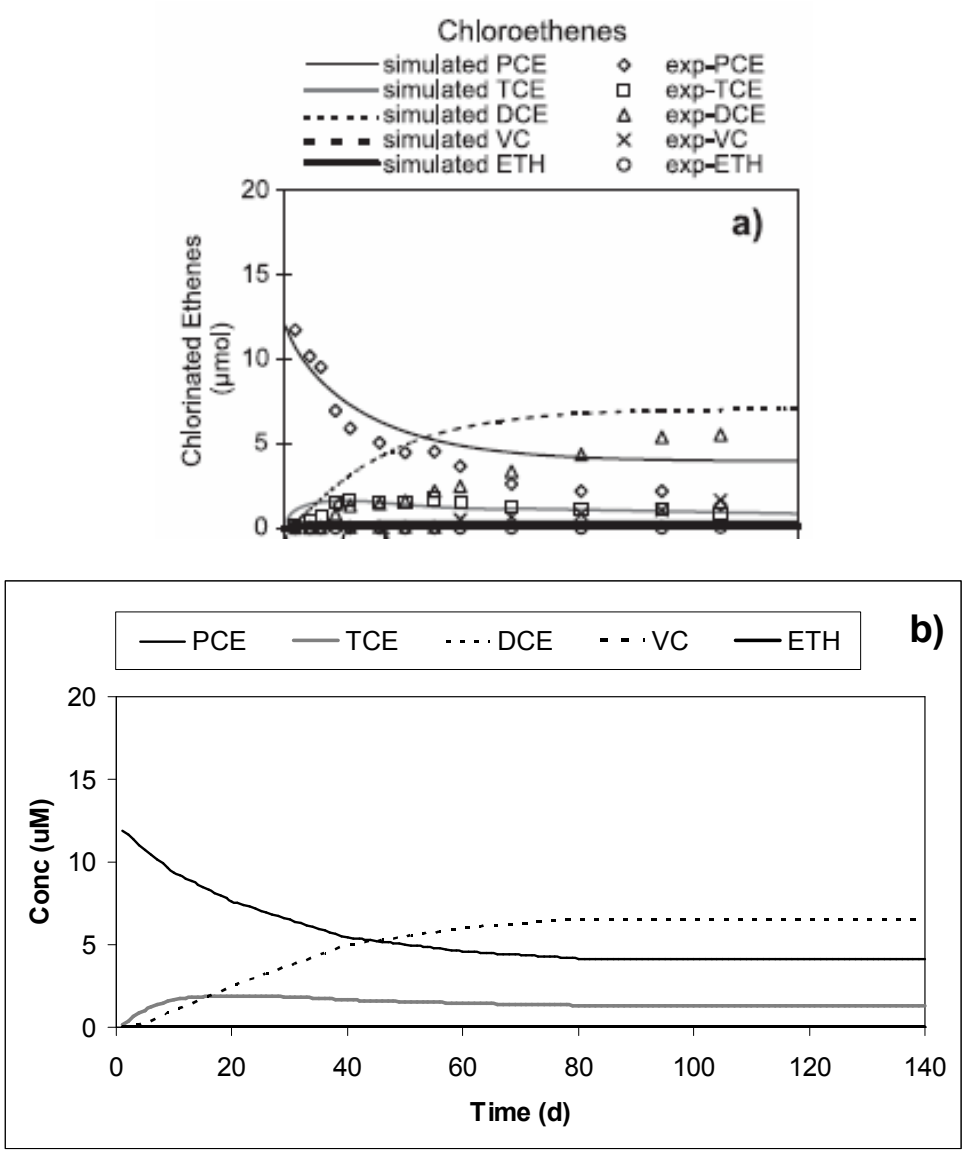

Figure 4.11 Modeled and simulated reductive dehalogenation of PCE from (a) Lee et al. (2004) compared with (b) batch simulations of the dual-Monod kinetic submodel developed for this study

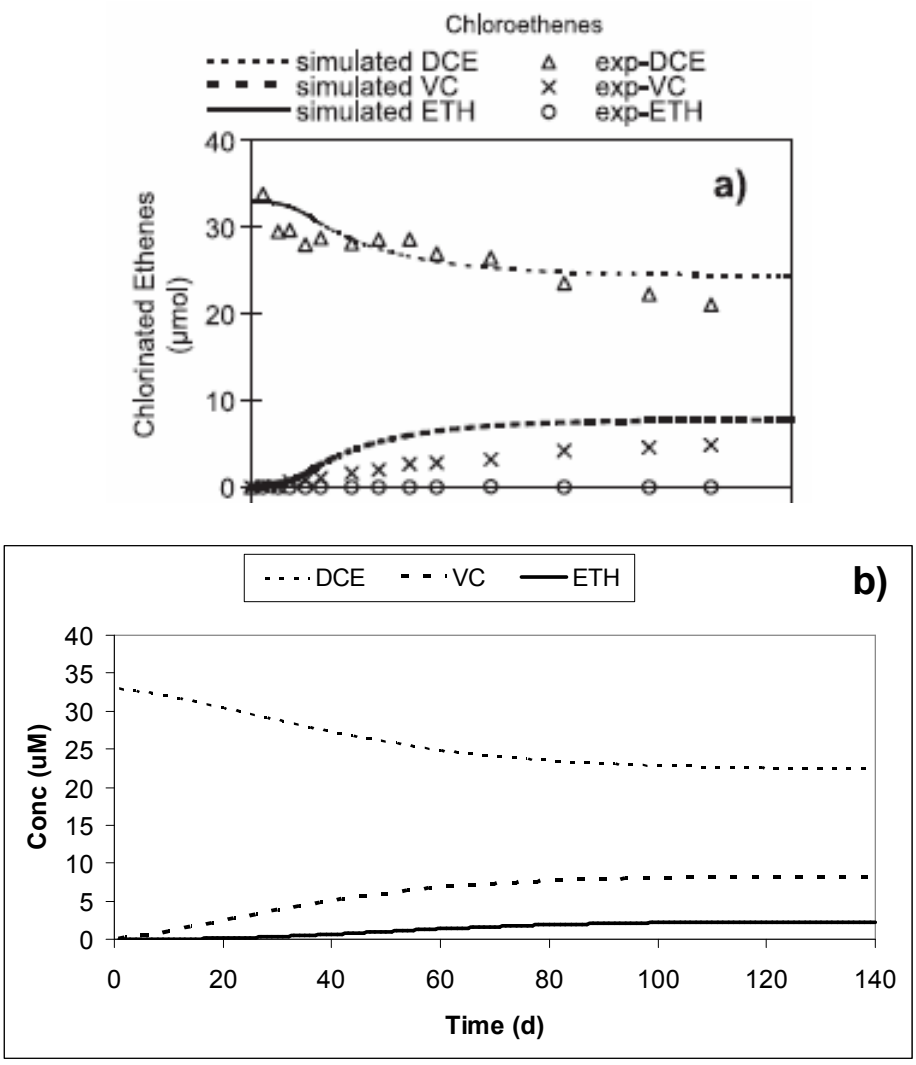

Figure 4.12 Modeled and simulated reductive dehalogenation of DCE from (a) Lee et al. (2004) compared with (b) batch simulations of the dual-Monod kinetic submodel developed for this study

The results of this comparison give us confidence that the submodel is properly simulating the dual-Monod kinetics and other biochemical processes (competition, etc.).

4.4 Model Application to the Vandenberg Site

4.4.1 Calibration Results

Using the procedures discussed in Section 3.4.2, dual-Monod model parameters were selected to obtain a visual best fit of model simulations to the CAH concentration data at the three monitoring wells of interest. Figures 4.13 through 4.21 compare these model simulations to the CAH concentration data at the three monitoring wells of interest, 14-MW-3, 14-MW-9, and 14-MW-10. .

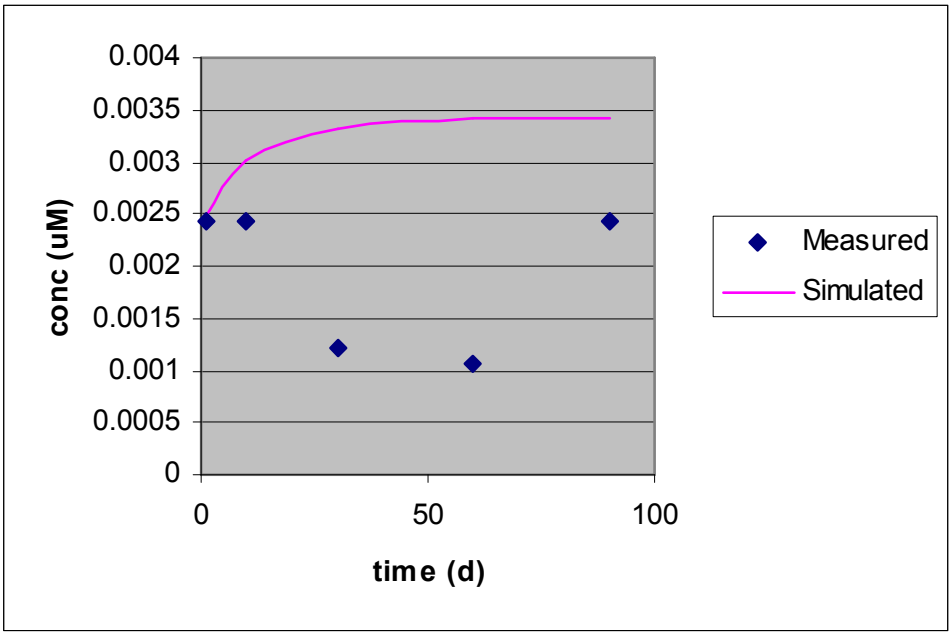

Figure 4.13 Measured and simulated TCE values at 14-MW-3

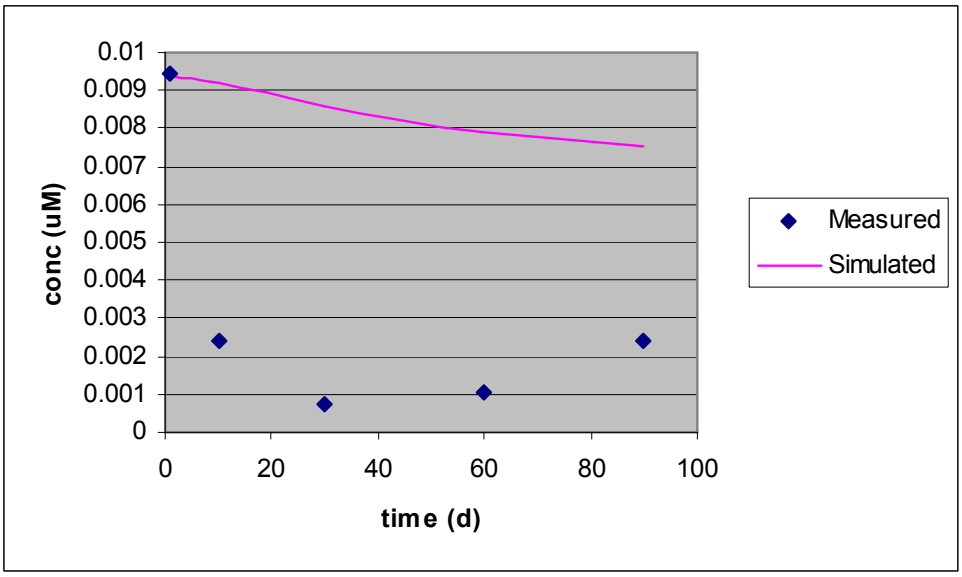

Figure 4.14 Measured and simulated TCE values at 14-MW-9

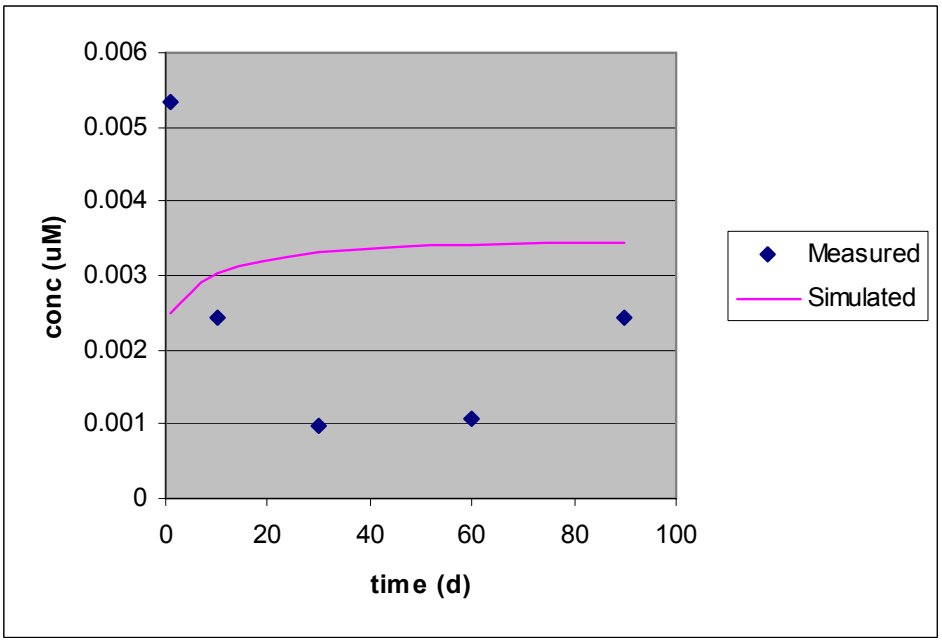

Figure 4.15 Measured and simulated TCE values at 14-MW-10

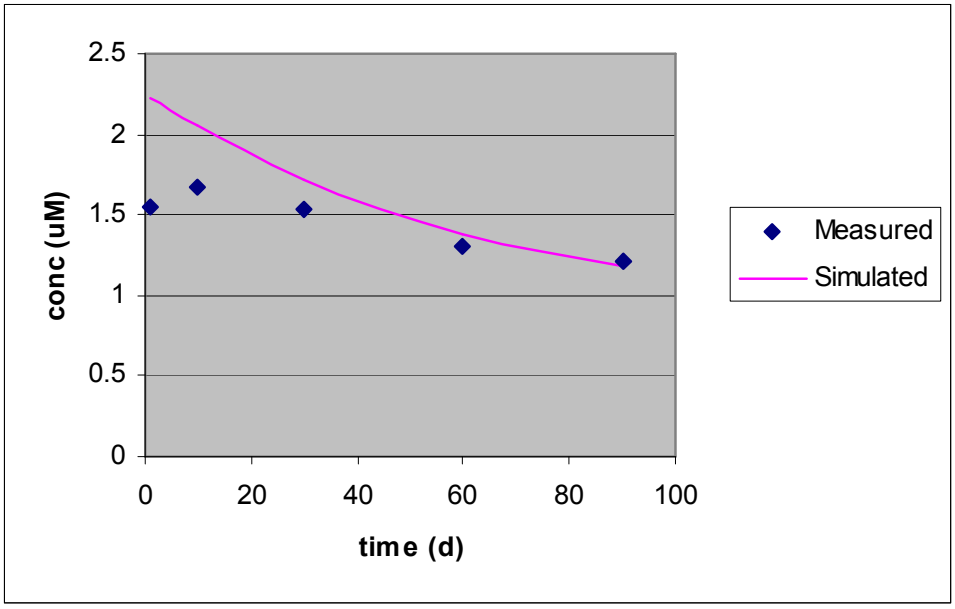

Figure 4.16 Measured and simulated DCE values at 14-MW-3

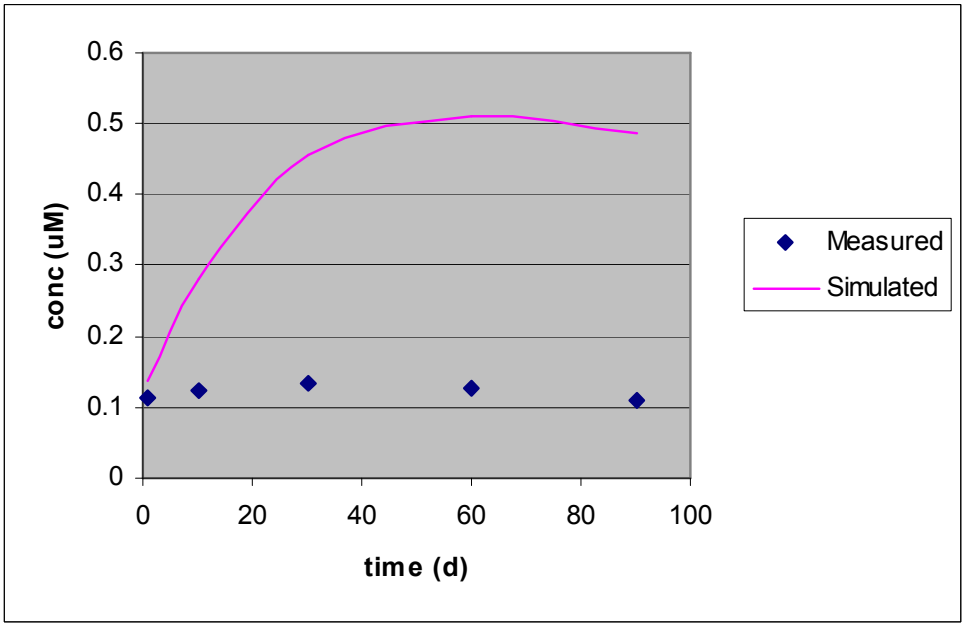

Figure 4.17 Measured and simulated DCE values at 14-MW-9

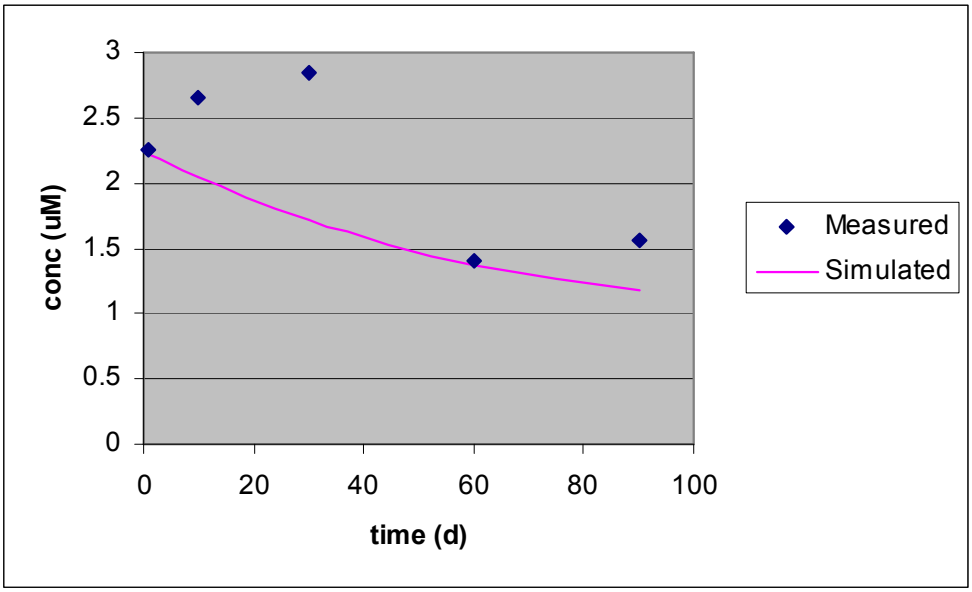

Figure 4.18 Measured and simulated DCE values at 14-MW-10

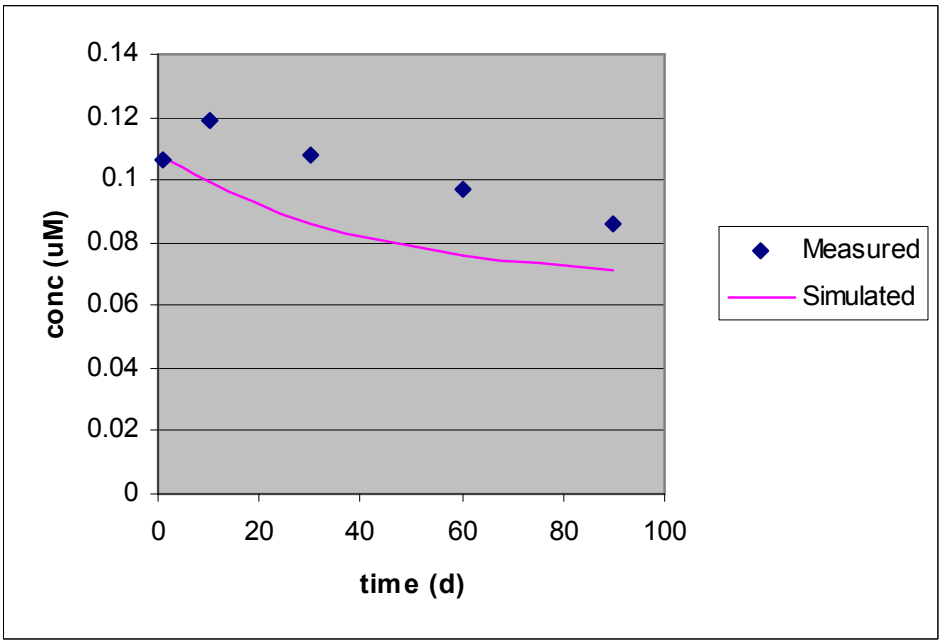

Figure 4.19 Measured and simulated VC values at 14-MW-3

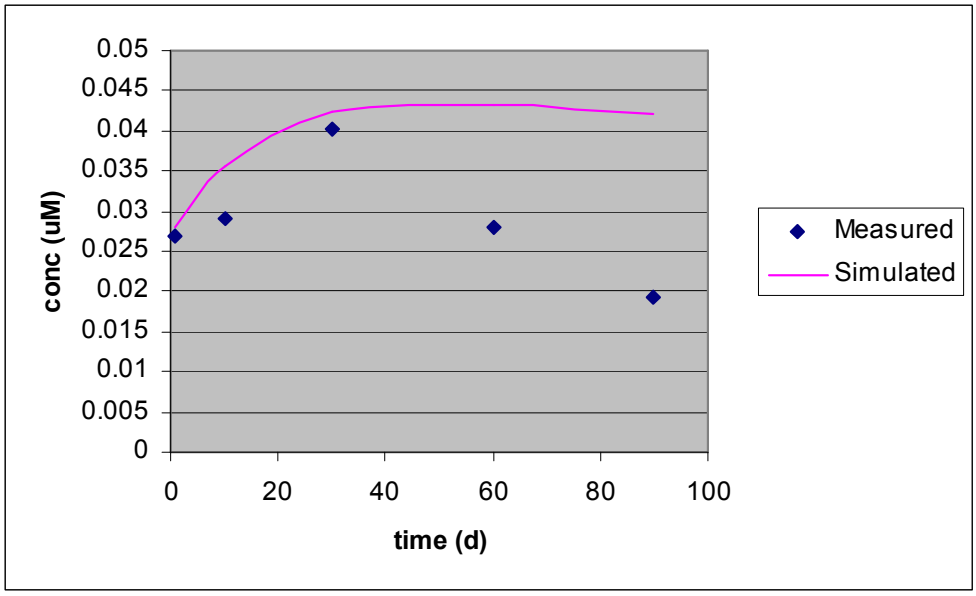

Figure 4.20 Measured and simulated VC values at 14-MW-9

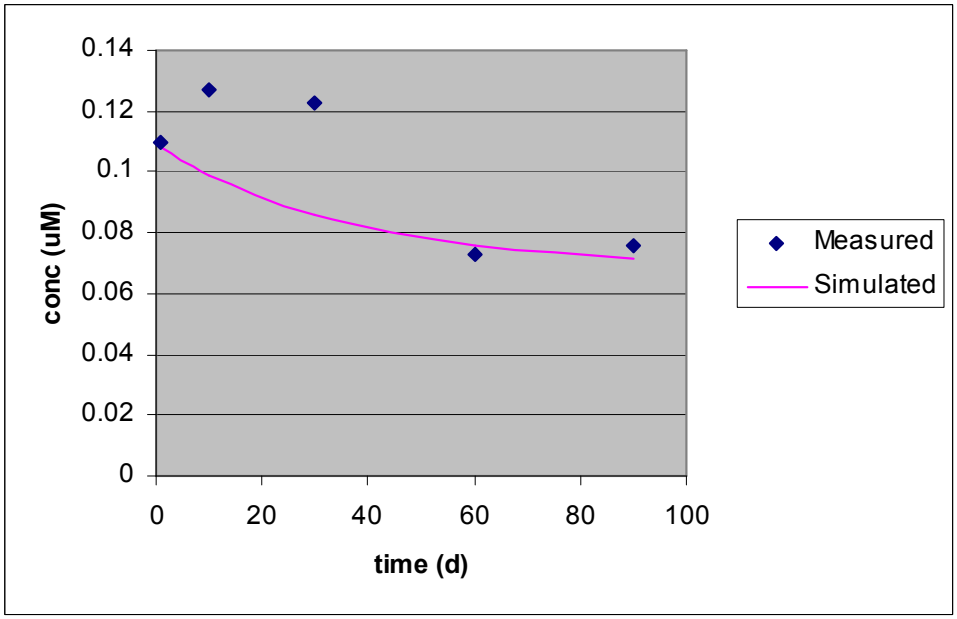

Figure 4.21 Measured and simulated VC values at 14-MW-10

4.4.2 Validation

The calibrated model was next run for a period of 270 days to assess its performance in predicting measured concentrations. Results of these simulations are shown in Figures 4.22 through 4.30. The initial 90-day results shown in the figures are the same as those in figures 4.13 – 4.21, but were included for comparison purposes. The 180-day and 270-day results show the difference between the measured CAH concentrations and the model predictions.

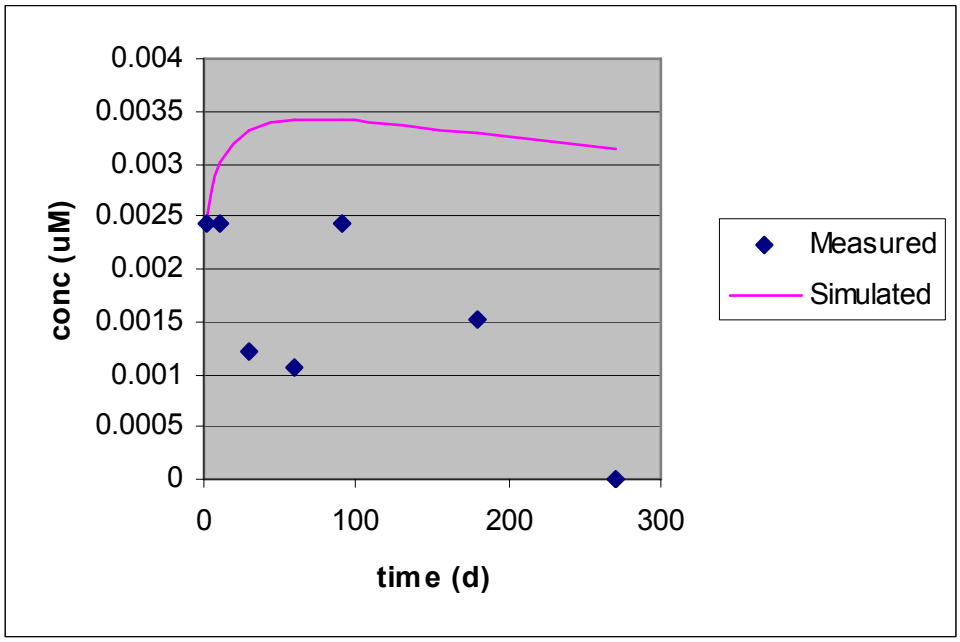

Figure 4.22 Measured and simulated TCE values at 14-MW-3

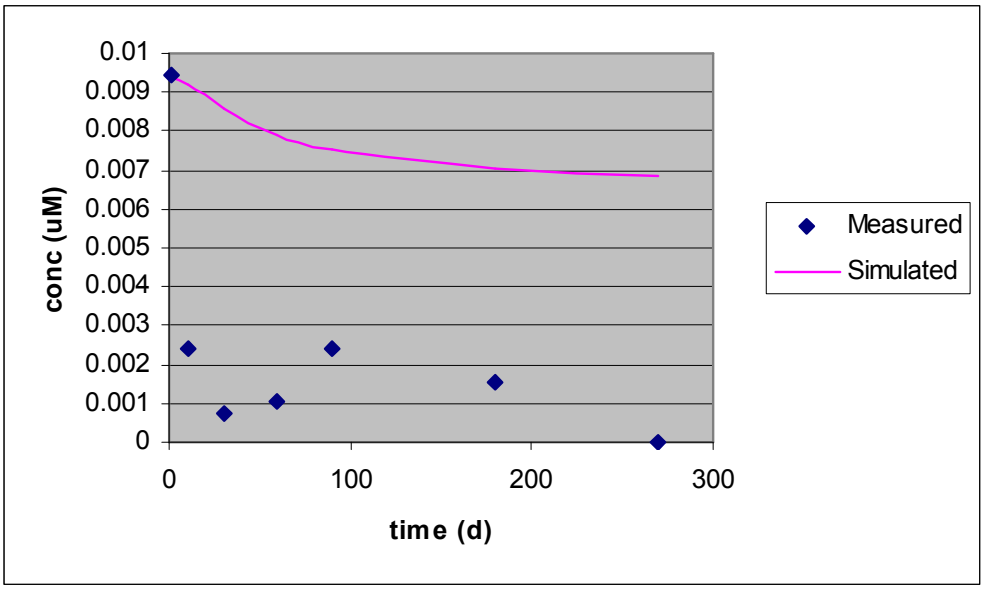

Figure 4.23 Measured and simulated TCE values at 14-MW-9

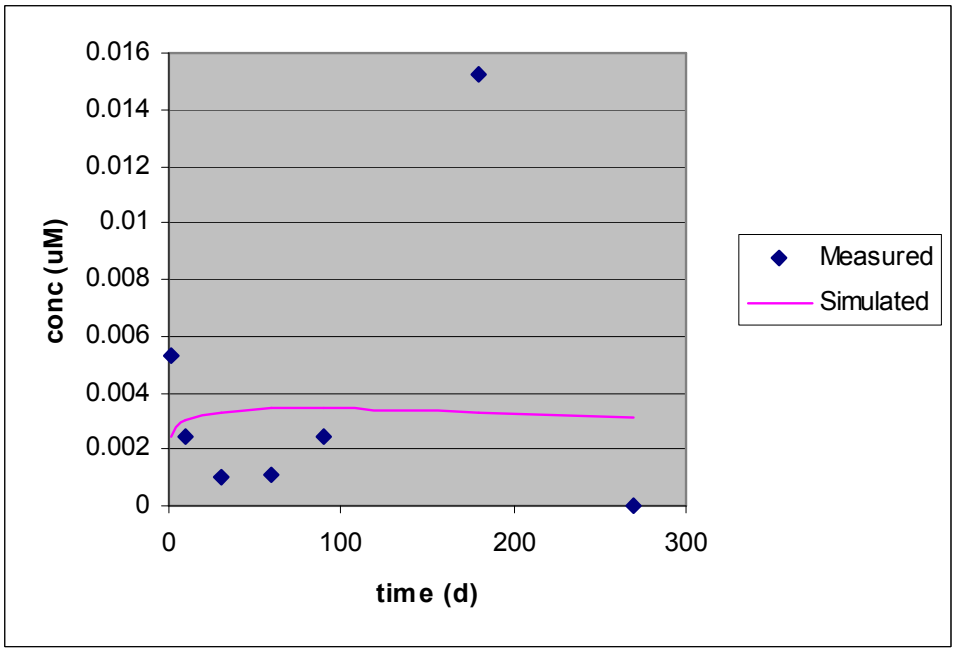

Figure 4.24 Measured and simulated TCE values at 14-MW-10

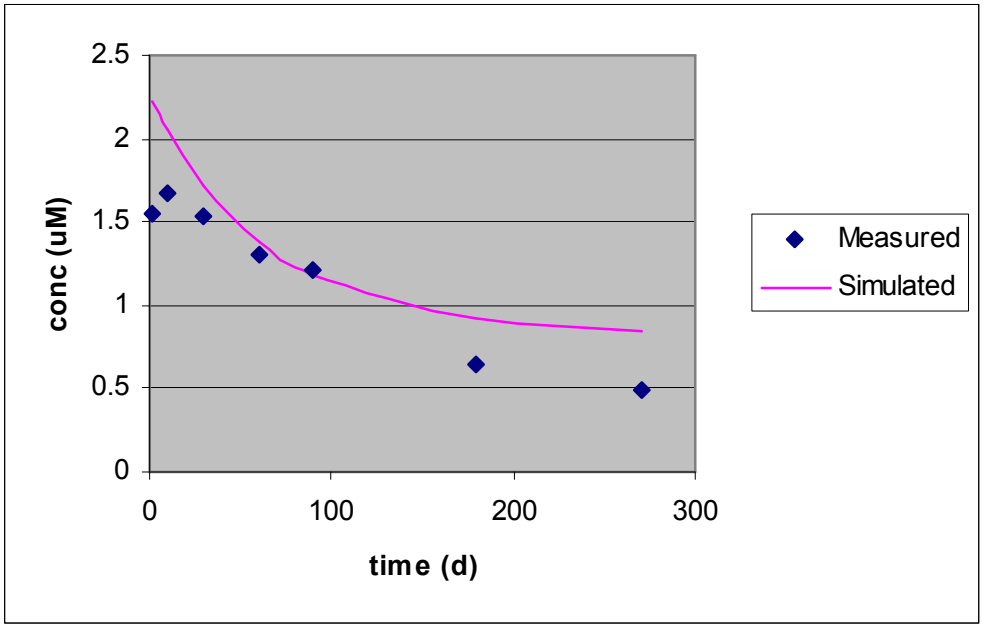

Figure 4.25 Measured and simulated DCE values at 14-MW-3

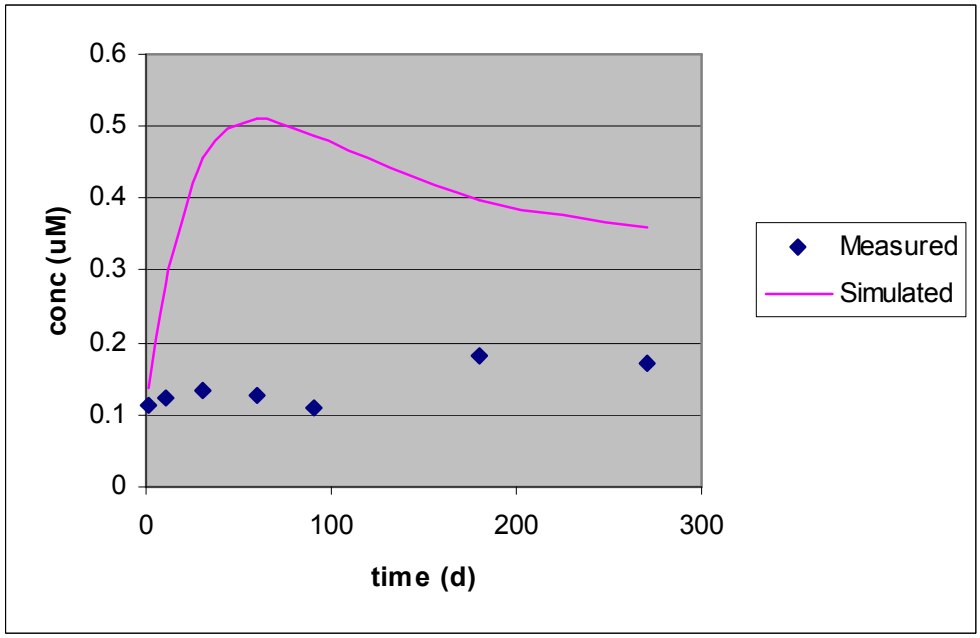

Figure 4.26 Measured and simulated DCE values at 14-MW-9

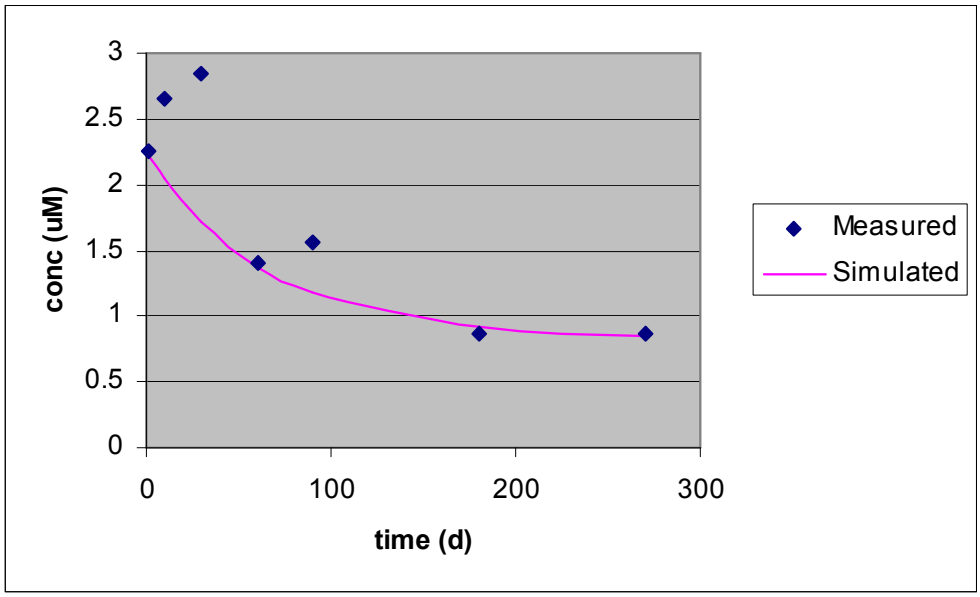

Figure 4.27 Measured and simulated DCE values at 14-MW-10

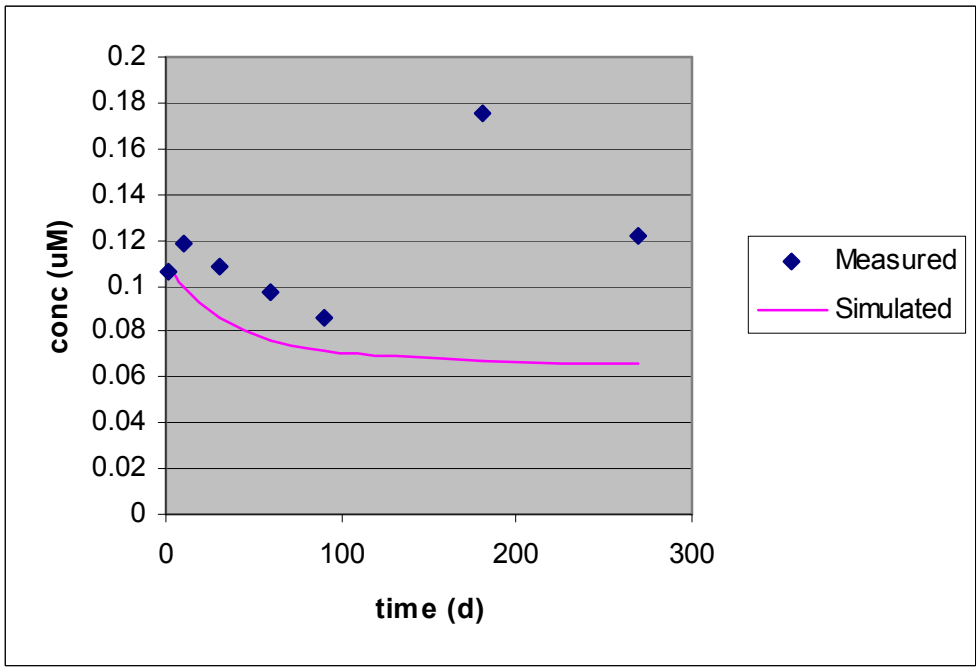

Figure 4.28 Measured and simulated VC values at 14-MW-3

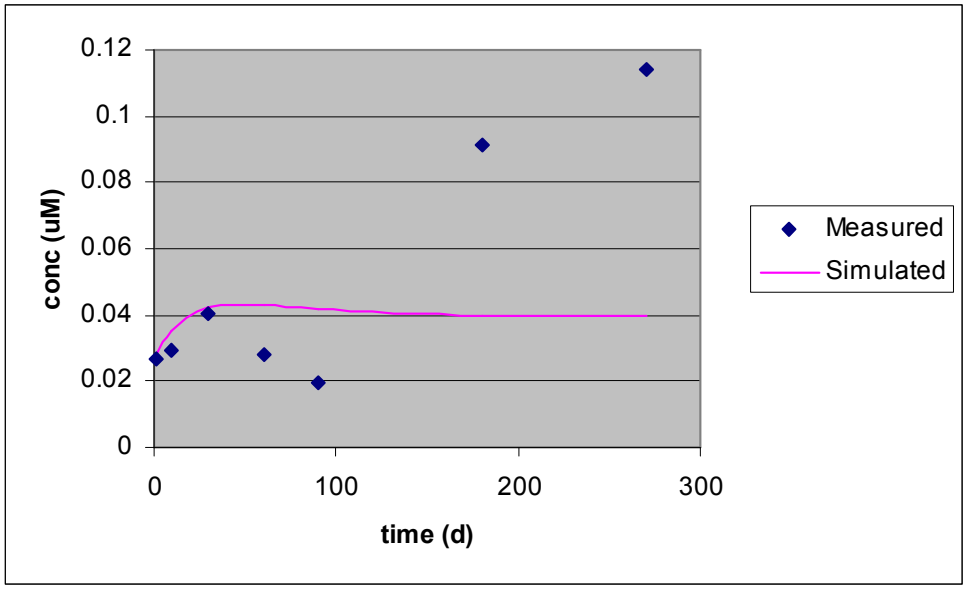

Figure 4.29 Measured and simulated VC values at 14-MW-9

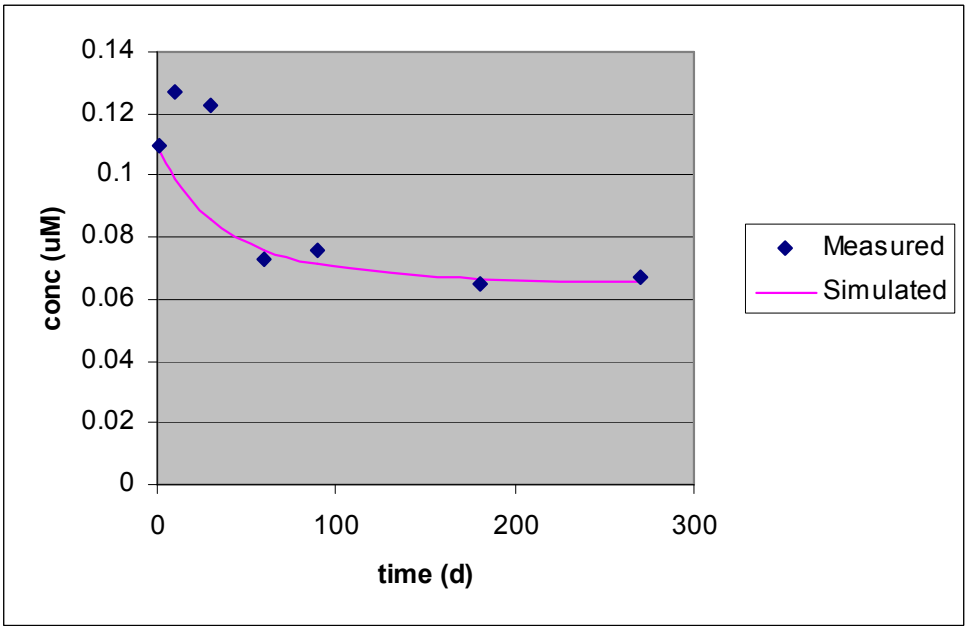

Figure 4.30 Measured and simulated VC values at 14-MW-10

In order to determine how well the model simulates measured data, the RMSEr was calculated. The RMSEr values for the calibration results (0 – 90 days) were then

compared to those for the validation data (180 – 270 days). As described in Section 3.5.3, the smaller the RMSEr, the better the simulations match the measured data. Figures 4.31 – 4.33 show the results of this comparison at each monitoring well. The RMSEr is graphed as a percentage of error, meaning the model simulation is within a certain percentage of the measured value. From these graphs, it can be seen that the fit of the model to the data used for validation (180 - 270 days), where no fitting was done, was generally as good, if not better, than the fit of the model to the data used for calibration (0 - 90 days) for both DCE and VC. This is a good indicator that the model will continue to perform favorably beyond the calibrated range. In each case, the fit of the model to the validation data for TCE was not as good as the fit to the calibration data. This would suggest that the model does a better job modeling DCE and VC than it does TCE. Note, however, that even the worst RMSEr, over 800%, indicates the simulated value is within an order of magnitude of the measured value. Considering the many assumptions and unknowns inherent in modeling a complex subsurface system, the model predictions are surprisingly good.

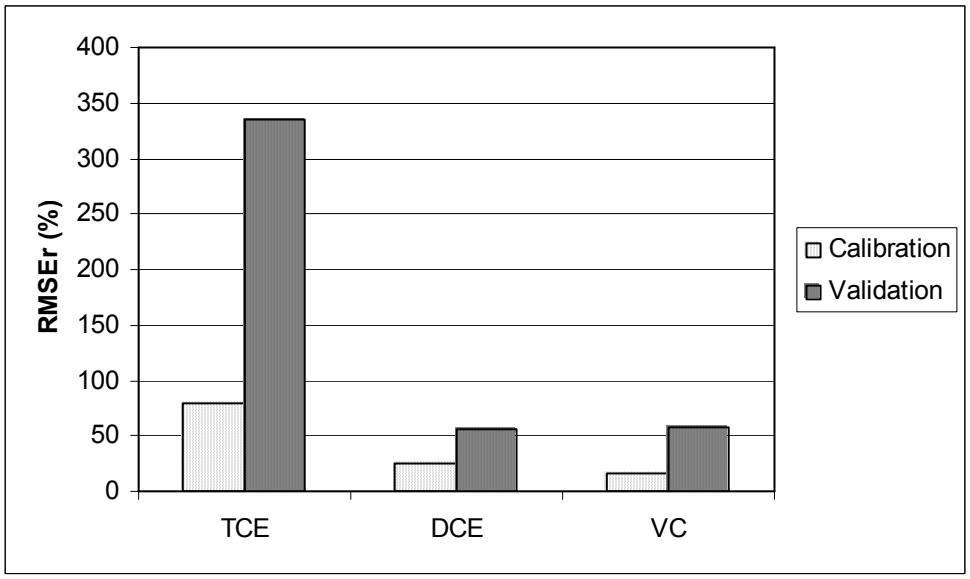

Figure 4.31 RMSEr of data at 14-MW-3

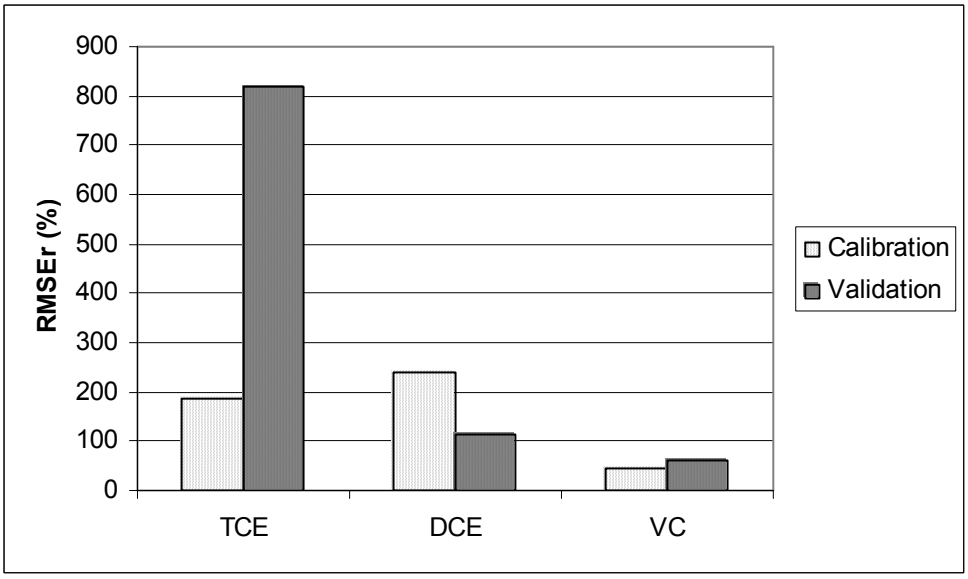

Figure 4.32 RMSEr of data at 14-MW-9

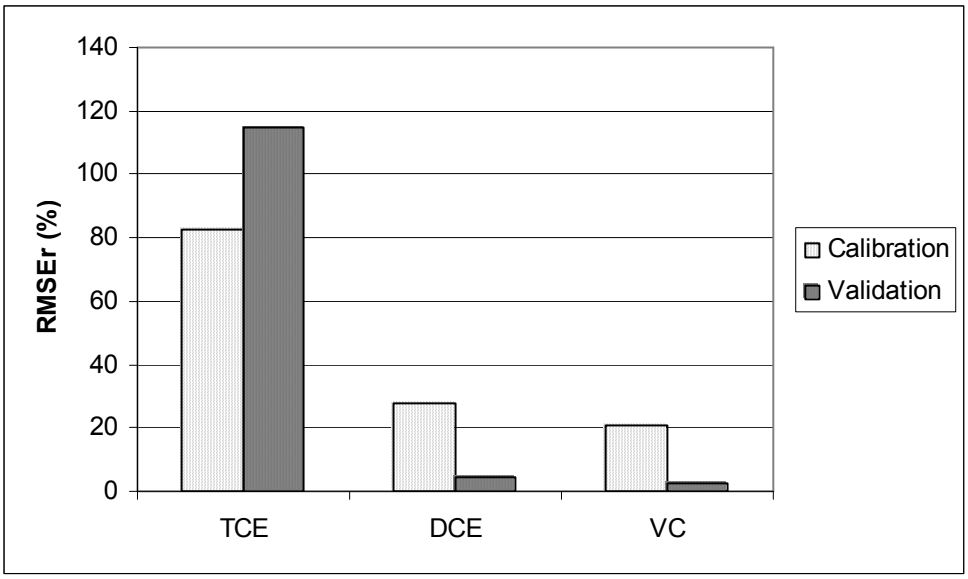

Figure 4.33 RMSEr of data at 14-MW-10

4.5 HRC® Injection Plan Design

The hydrogen plume produced from HRC® injection wells was simulated for nine different hydrogeological scenarios. For each scenario, multiple simulations were run, in order to determine the maximum separation distance between HRC® injection wells that could be achieved without violating the design criteria specified in Section 3.5.1. Results of this sensitivity analysis are presented in Table 4.1. A couple of observations can be made from Table 4.1. First, with low hydraulic conductivity, the maximum separation distance increases as the longitudinal (as well as transverse and vertical) dispersivity increases. Next, at a higher hydraulic conductivity value, (13.7 m/d), the opposite occurs. As the dispersivity increases, the maximum separation distance decreases. Finally, at the highest hydraulic conductivity considered, the maximum separation distance also decreases with increasing dispersivity, with the extent of decrease even greater than it

was at the lower hydraulic conductivity. The criterion that specified that the hydrogen concentration in the plume must reach a level of 1.5 nM in order to be effective plays a role in the results reported in Table 4.1. The hydrogen plume spread is quantified by the dispersion coefficient, which is proportional to the product of conductivity and dispersivity. Thus, it'd be expected that as this product increases, transverse spread of the hydrogen plumes would increase and the maximum separation would also increase. However, we observed that the separation distance decreased even though spreading increased. This seems to be due to the fact that at the higher conductivities and dispersivities the plume hydrogen concentrations rapidly fall below the specified concentration of 1.5 nM.

Table 4.1 Maximum HRC® injection well separation

Hydraulic Conductivity	*Longitudinal Dispersivity*	*Maximum HRC Injection Well Separation*
K (m/day)	α_L (m)	L (m)
1.5	4.27	6.1
	15.24	11
	98.5	12.8
13.7	4.27	10.4
	15.24	3.7
	98.5	1.2
30.5	4.27	7.3
	15.24	1.2
	98.5	1.2

4.5.1 Vandenberg Site HRC® Injection Design

Table 4.1 was next used to determine the maximum well spacing that could be used at the Vandenberg AFB Site 13C. The hydraulic conductivity at the site is 13.7 m/day and the longitudinal dispersivity is 15.24 m. The maximum separation was calculated to be 3.7

m for these conditions. In the model application we used 80% of this value to allow for a safety factor. Thus, a value of 3.0 m was used as the well separation distance. Injection wells were placed across the contaminated zone at a spacing of 3.0 m on center in order to model a full scale treatment application at Site 13C. The results of this study are presented in Table 4.2. The model output concentrations of the contaminants TCE, DCE, and VC are presented over a period of 360 days at wells 14-MW-3, 14-MW-9, and 14-MW-10. The maximum contaminant level (MCL) is also shown for each contaminant. The contaminant concentrations are approaching the MCLs at the monitoring wells. Note, though, that after 360 days, none have reached the MCLs (except for those cases where the concentration was already below the MCL at 0 days). Also note from the table that concentration trends at different wells vary. At some wells, concentrations initially increase with time before decreasing while at other wells concentrations monotonically decrease. This behavior can be explained by the heterogeneity of the initial contaminant distribution in the subsurface, as well as the production of daughter products as their parent compounds are reductively dehalogenated.

Table 4.2 Dechlorination effectiveness of HRC® at Vandenberg AFB for baseline design

		Concentration (µg/L)							
Well	Contaminant	0 days	30 days	60 days	90 days	180 days	270 days	360 days	MCL
14-MW-3	TCE	0	0.398	0.372	0.341	0.264	0.222	0.202	5
14-MW-9	TCE	1.24	1.1	0.985	0.909	0.794	0.75	0.73	5
14-MW-10	TCE	0.7	0.624	0.573	0.523	0.396	0.32	0.281	5
14-MW-3	DCE	213.02	225.1	180.9	155.1	121.8	111.9	108.7	70
14-MW-9	DCE	15.48	60.2	67.3	64.2	52.2	47.5	45.9	70
14-MW-10	DCE	297.04	229.7	184.7	153.9	110.4	97.1	93	70
14-MW-3	VC	14.3	11.3	10.1	9.5	8.9	8.8	8.8	2
14-MW-9	VC	3.53	5.6	5.7	5.6	5.3	5.2	5.2	2
14-MW-10	VC	14.4	11.1	9.6	8.8	8.1	7.9	7.9	2

4.5.2 Sensitivity Analysis

Equation 3.16 was used to perform the following sensitivity analysis. The sensitivity analysis results, as presented in Table 4.2, indicate, by the relatively high value of S, that model output C_k (aqueous phase concentration of the k^{th} species) is relatively sensitive to the model input parameters dispersivity (α_L) and hydraulic conductivity (K). The maximum specific utilization rates caused very little, if any, change in model output, while the half-saturation and inhibition constants also caused minimal change in model output. These results provide some insight to research question number 3 regarding subsurface conditions favorable or unfavorable to the use of HRC®. From Table 4.3, it appears that the physical characteristics of the site, such as hydraulic conductivity and dispersivity, are very important to the effectiveness of HRC®. I believe this relates directly to the obvious limitation of using substrates like HRC®, which is the problem of delivery. Section 4.5.3 below further investigates the importance of K and α_L on the effectiveness of HRC®.

Table 4.3 Sensitivity analysis results

Input Parameter		*Factor of Input Change from Baseline*	*Model Output C (μM)*			*Factor of C difference from Baseline*			*Relative Sensitivity, S*		
			C_{TCE}	C_{DCE}	C_{VC}	C_{TCE}	C_{DCE}	C_{VC}	C_{TCE}	C_{DCE}	C_{VC}
longitudinal dispersivity											
α_L (m)											
15.2	baseline	---	0.62	154.9	11.18	---	---	---			
4.27		0.28	0.491	177.6	12.7	0.79	1.15	1.136	0.042	0.028	0.027
98.5		6.46	0.653	150.5	10.8	1.05	0.97	0.966			
hydraulic conductivity											
K (m/day)											
13.7	baseline	---	0.62	154.9	11.18	---	---	---			
1.5		0.11	0.53	190.5	12.6	0.85	1.23	1.127	0.088	0.122	0.076
30.5		2.22	0.645	150.5	10.8	1.04	0.97	0.966			
Max. specific utilization rate, k (mg/mg biomass-day)											
k_{TCE}											
5.68	baseline	---	0.62	154.9	11.18	---	---	---			
0.32		0.56	0.63	154.9	11.19	1.02	1	1.001	0.010	0.000	0.001
48.1		8.46	0.578	154.9	11.13	0.93	1	0.996			
k_{DCE}											
1.28	baseline	---	0.62	154.9	11.18	---	---	---			
0.16		0.125	0.597	154.9	11.1	0.96	1	0.993	0.014	0.000	0.003
4.65		3.63	0.627	154.9	11.2	1.01	1	1.002			
k_{VC}											
1.38	baseline	---	0.62	154.9	11.18	---	---	---			
0.16		0.12	0.62	154.9	11.18	1	1	1	0.000	0.000	0.000
3		2.17	0.62	154.9	11.18	1	1	1			
Half-saturation and inhibition constant, Ks(μM)											
$K_{s,TCE}$											
0.07	baseline	---	0.62	154.9	11.18	---	---	---			
0.0065		0.09	0.573	155	11.13	0.92	1	0.996	0.033	0.000	0.002
0.19		2.71	0.626	154.9	11.19	1.01	1	1.001			
$K_{s,DCE}$											
0.22	baseline	---	0.62	154.9	11.18	---	---	---			
0.05		0.23	0.624	154.9	11.2	1.01	1	1.002	0.009	0.000	0.002
0.32		1.45	0.617	154.9	11.17	1	1	0.999			
$K_{s,VC}$											
20.3	baseline	---	0.62	154.9	11.18	---	---	---			
0.1625		0.008	0.621	154.8	11.14	1	1	0.996	0.001	0.001	0.003
22.5		1.11	0.62	154.8	11.18	1	1	1			

4.5.3 Treatment Effectiveness

In order to determine the effect of dispersivity (α_L) and hydraulic conductivity (K) on treatment effectiveness as simulated by the model, the model was run for 365 days for each of the nine combinations of these two parameters. Except for dispersivity and conductivity, baseline values were used for all other parameters and the wells were spaced at 3 m. The maximum contaminant concentration at the end of the 365 days at the model boundary was recorded. The results are presented in Table 4.4.

Table 4.4 Simulated maximum concentration at model boundary after 1 year

Parameters Varied		Contaminant Concentration (µg/L)		
K (m/day)	α_L (m)	TCE	DCE	VC
1.5	4.27	1.09	245.7	15.2
1.5	15.24	0.335	176.4	13.6
1.5	98.5	0.042	149.4	12.8
13.7	4.27	0.202	162.4	12.6
13.7	15.24	0.408	142.2	10.6
13.7	98.5	0.574	138.7	10.3
30.5	4.27	0.592	162.8	11.8
30.5	15.24	0.765	142.2	10.4
30.5	98.5	0.851	138.5	10.2

It can be observed that as the dispersivity (α_L) increases, the boundary DCE and VC concentrations decrease for a constant hydraulic conductivity, and for the same dispersivity, the boundary concentrations of DCE and VC decrease slightly with increasing hydraulic conductivity. The response of TCE boundary concentrations to conductivity and dispersivity changes is not as systematic. Since TCE concentrations are extremely low to begin with, we cannot generalize regarding the response of TCE boundary concentrations to changes in conductivity and dispersivity. Based on the DCE and VC results, it appears that as conductivity and dispersivity increase, treatment effectiveness increases. This makes intuitive sense, since mixing, as determined by the

dispersion coefficient, is proportional to the product of dispersivity and conductivity and we would expect that as mixing between the electron donor and acceptors increase, treatment effectiveness increases.

5.0 Conclusions

5.1 Summary

In this thesis, equations for a biological submodel developed by Fennell and Gossett (1998), Clapp et al. (2004), and Lee et al. (2004), which incorporated dual-Monod kinetics, competition, and methanogenesis to describe the kinetics of PCE and TCE reductive dehalogenation to ethene, were coupled with the three-dimensional advective-dispersive transport equations simulated in the program RT3D by means of the user-defined module. The resultant model was used to simulate a real-world pilot study of the electron donor-producing substrate, HRC®, being conducted at a TCE-contaminated site at Vandenberg AFB. Simulations of the model for DCE and VC were able to reproduce the pilot study results to a degree of accuracy generally as good as the calibrated model. Values simulated in the validation step varied from 2.4% to 113% from the observed values, while those for calibration varied from 17% to 239%, as shown in Figures 4.31 – 4.33. The validation results for TCE were not as good, varying from 114% to 817%, though still surprisingly accurate considering the uncertainties when predicting contaminant concentrations in a heterogeneous, complex, subsurface system. The biological submodel successfully simulated the increase in electron donor resulting from the injection of HRC® as well as the increased reductive dehalogenation of CAHs in the vicinity of increased electron donor.

5.2 Conclusions

This modeling exercise has shown how the hydrogen produced by HRC® can be an effective additive to stimulate the degradation of CAHs. This study showed the potential

benefit of using HRC® to provide molecular hydrogen as an electron donor to accelerate the reductive dehalogenation of CAHs. This study also showed how much of an impact the groundwater velocity, hydraulic conductivity, and dispersivity can have on the ability of HRC® to disperse and reach all contaminated areas of the aquifer. This reemphasized a shortfall common to techniques requiring delivery to the subsurface, which is mixing.

Based on the kinetic parameters used in this research (Table 3.3), HRC® facilitates the complete reduction of PCE or TCE to ethene via DCE and VC. We observed that based on these parameters, daughter product build-up may be a problem under certain circumstances. The instances when daughter product build-up is problematic are scenario dependent. For instance, in this study, a transient build-up of VC was noticed within the time- and distance-scales being modeled. However, if compliance boundaries are far away, this build-up would not create a problem.

Based on the sensitivity analyses, it was seen that kinetic parameters such as the half-saturation constant and the maximum specific utilization rate had little impact on model performance, so long as these parameters were kept within reasonable ranges. Longitudinal dispersivity and hydraulic conductivity, on the other hand, had a much greater impact on simulated performance of the technology. This would suggest that when designing an HRC® system, it would be best to spend greater effort determining the most accurate measures of longitudinal dispersivity and hydraulic conductivity.

Even with HRC® injection wells placed to ensure full coverage of hydrogen to the contaminant plume, it may still prove difficult to reach MCLs. It was seen with our model that even with full hydrogen coverage for 1 year, the contaminants were not degraded below their respective MCLs. This does not indicate a failure of the system as the compliance boundaries are well beyond the boundary of the modeled area. The MCLs may very well have been reached by the time the groundwater moved across the compliance boundary. The ability to reach MCLs depends on many things including the starting concentrations of the contaminants, the influx of additional contaminant from sources upstream, and the groundwater velocity. A great advantage of modeling is the ability to predict whether or not the contaminants will reach their respective MCLs before crossing the compliance boundary, and the ability to use these predictions to design a system to help ensure compliance at the boundaries.

5.3 Recommendations for Further Research

1. Develop a procedure to optimize HRC® injection scheme design so that cost is minimized while achieving MCLs downgradient.

2. Use 12-18 month monitoring data when available from the pilot study to further calibrate and validate as well as refine the model. HRC® has the ability to release hydrogen for many months after injection. The short scale of the monitoring data used in this study (9 months) does not provide a full picture of the performance of the HRC®. It would be valuable to use the data collected at 12 and 18 months further calibrate the

model. A better understanding of the performance of the HRC® pilot study will be gained by investigating the 12-18 month data.

3. Incorporate donor fermentation and NAPL dissolution into the model. A critical process in the ability of HRC® to accelerate the reductive dehalogenation of CAHs is the dissolution and subsequent fermentation of the HRC®, creating hydrogen. If these processes are slow, the HRC® would be ineffective. Some of the models reviewed in this study (Glucose/production and competition models) included fermentation reactions. The dissolution and fermentation processes were not included in our model; for simplicity we assumed dissolution and fermentation occurred instantaneously compared to dehalogenation and the other kinetic processes that were simulated in the model. This assumption may be unrealistic. The kinetics of dissolution and fermentation may occur at such a rate as to limit the dehalogenation process. Thus, addition of NAPL dissolution and fermentation kinetics into the model could provide us with further insight into how these processes may affect overall technology performance.

4. Experiment with other electron donor delivery methods such as colloids. There are many different natural and man-made products available for use as substrates providing electron donors. The delivery of these donors is limited by the mixing occurring in the groundwater. New ways of donor delivery would be valuable to the field of EISB. Research in this area could help to quantify the difference in performance between the available substrates helping project managers decide if a more expensive engineered product is worth the money at their site.

6.0 Bibliography

Air Force Center for Environmental Excellence (AFCEE). Principles and Practices of Enhanced Anaerobic Bioremediation of Chlorinated Solvents. The Parsons Corporation, 2004.

AFCEE. Natural Attenuation of Chlorinated Solvents Performance and Cost results from Multiple Air Force Demonstration Sites, Technology Demonstration Technical Summary Report. Parsons Engineering Science, Inc., 1999.

American Society for Testing and Materials (ASTM). Standard Guide for Remediation of Ground Water by Natural Attenuation at Petroleum Release Sites. E 1943-98, West Conshohocken, PA. 1998.

Anderson, M. P., Woessner, W. W. Applied Groundwater Modeling. Academic Press: San Diego. 1992.

Aziz, C. E., Newell, C. J., Gonzales, A. R., Haas, P., Clement, T. P., Sun, Y. BIOCHLOR Natural Attenuation Decision Support System User's Manual. Prepared for the Air Force Center for Environmental Excellence, Brooks AFB, San Antonio, TX. 1999.

Bagley, D. M. Systematic approach for modeling tetrachloroethene biodegradation. *Journal of Environmental Engineering, Vol 124,* No. 11. 1076-1086, 1998.

Ballapragada, B.S., Stensel, H. D., Puhakka J. A., Ferguson, J. F. Effect of Hydrogen on Reductive Dechlorination of Chlorinated Ethenes. *Environmental Science & Technology*, *Vol 31,* No. 6. 1728-1734, 1997.

Bradley, P.M., Chapelle, F.H. Anaerobic mineralization of vinyl chloride in Fe(III)-reducing aquifer sediments: *Environmental Science and Technology*, *Vol 30*, 2084-2086. 1996.

Chu, M., Kitanidis, P. K., McCarty, P. L. Effects of Biomass Accumulation on Microbially Enhanced Dissolution of a PCE Pool: A Numerical Simulation. *Journal of Contaminant Hydrology, Vol 65*. 79-100, 2003.

Clapp, L. W., Semment, M. J., Novak, P. J., and Hozalski, R. M. Model for In Situ Perchloroethene Dechlorination via Membrane-Delivered Hydrogen. *Journal of Environmental Engineering, Vol 130,* No. 11. 1367-1381, 2004.

Clark, M. M. Transport Modeling for Environmental Engineers and Scientists. New York: John Wiley & Sons, Inc, 1996.

Clement, T. P., Truex, M. J., Lee, P. A Case Study for Demonstrating the Application of U.S. EPA's Monitored Natural Attenuation Screening Protocol at a Hazardous Waste Site. *Journal of Contaminant Hydrology, Vol 59.* 133-162, 2002.

Clement, T.P., Johnson, C.D., Sun, Y., Klecka, G.M., Bartlett, C. Natural attenuation of chlorinated ethene compounds: model development and field-scale application at the Dover site, *Journal of Contaminant Hydrology*, *Vol 42.* 113-140, 2000.

Clement, T.P., Sun, Y., Hooker, B.S., Petersen, J.N. Modeling multi-species reactive transport in groundwater aquifers. *Ground Water Monit. Rem. Vol 18*, No. 2. 79-92, 1998.

Clement, T. P. RT3D - A Modular Computer Code for Simulating Reactive Multi-species Transport in 3-Dimensional Groundwater Systems. PNNL-SA-11720. Richland, Washington: Pacific Northwest National Laboratory, 1997.

Domenico, P. A., Schwartz, F. W. Physical and Chemical Hydrogeology. 2nd Ed. Wiley and Sons, New York, 1998.

Faron, W. A., Koenigsberg, S. S., Hughes, J. A Chemical Dynamics Model for CAH Remediation with Polylactate Esthers. In: A. Leeson and B. C. Alleman (Eds.), Engineering Approaches for In Situ Bioremediation of Chlorinated Solvent Contamination. Columbus: Battelle Press, 1999.

Fennell, D. E., Gossett, J. M. Modeling the Production of and Competition for Hydrogen in a Dechlorinating Culture. *Environmental Science and Technology, Vol 32,* No. 16. 2450-2460, 1998.

Fennell, D. E., Stover, M. A., Zinder, S. H., Gossett, J. M. Comparison of alternative electron donors to sustain PCE anaerobic reductive dechlorination, *in* Hinchee, R.E., Leeson, A., and Semprini, L., eds., Bioremediation of chlorinated solvents. Columbus: Battelle Press, 1995.

Flynn, S. J., Loffler, F. E., Teidje, J. M. Microbial community changes associated with a shift from reductive dechlorination of PCE to reductive dechlorination of *cis*-DCE and VC. *Environmental Science and Technology, Vol 34*, No. 6. 1056-1061, 2000.

Freeze, R. A., Cherry, J. A. Groundwater. Prentice-Hall, Englewood Cliffs, NJ. 1979.

Gelhar, L. W., Montoglou, A., Welty, C., Rehfeldt, K. R. A Review of Field Scale Physical Solute Transport Processes in Saturated and Unsaturated Porous Media. Final Project Report. EPRI EA-4190. Electric Power Research Institute, Palo Alto, California. 1985.

Gossett, J. M., Zinder, S. H. Microbial aspects relevant to natural attenuation of chlorinated ethenes. Proceedings from the Symposium on Natural Attenuation of Chlorinated Organics in Ground Water. EPA/540/R-96/509. Dallas, TX. 1996.

He, J., K. M. Ritalahti, K. Yang, S. S. Koenigsberg, Löffler, F. E. Detoxification of Vinyl Chloride to Ethene Coupled to Growth of an Anaerobic Bacterium. *Nature, Vol 424*. 62-65. 2003.

Hendrickson, E. R., Payne, J. A., Young, R. M., Starr, M. G., Perry, M. P., Fahnestock, S., Ellis, D. E., Ebersole, R. C. Molecular Analysis of *Dehalococcoides* 16S Ribosomal DNA from Chloroethene-Contaminated Sites throughout North America and Europe. *Applied Environmental Microbiology*, *Vol 68,* No. 2. 485-495, 2002.

Holliger, C., Schraa, G., Stams, A. J. M., Zehnder, A. J. B. A highly purified enrichment culture couples the reductive dechlorination of tetrachloroethene to growth. *Applied Environmental Microbiology*, *Vol 59*. 2991-2997, 1993.

Klier, N. J., West, R. J., Donberg, P. A. Aerobic biodegradation of dichloroethylenes in surface and subsurface soils. *Chemosphere, Vol 38*, No 5. 1175-1188, 1999.

Koenigsberg, S. S. Facilitated Desorption and Incomplete Dechlorination Observations From 350 Applications of HRC®. Proceedings of the Battelle sponsored Third International Conference on Remediation of Chlorinated and Recalcitrant Compounds, Monterey, California, May 20-23, 2002. Batelle Press, 2002.

LaGrega, M.D., Buckingham, P.L., Evans, J.C. Hazardous Waste Management. McGraw-Hill, Inc., New York, 1994.

Lee, M. D., Odom, J. M., Buchanan, R. J., Jr. New Perspectives on Microbial Dehalogenation of Chlorinated Solvents: Insights from the Field. *Annual Review of Microbiology, Vol 52*. 423-425, 1998.

Lee, I., Bae, J., Yang, Y., McCarty, P. Simulated and experimental evaluation of factors affecting the rate and extent of reductive dehalogenation of chloroethenes with glucose, *Journal of Contaminant Hydrology*, *Vol 74,* 313-331, 2004.

Major, D. W., McMaster, M. L., Cox, E. E., Edwards, E. A., Dworatzek, S. M., Hendrickson, E. R., Starr, M.G., Payne, J. A., Buonamici, L. W. Field Demonstration of Successful Bioaugmentation to Achieve Dechlorination of Tetrachloroethene to Ethene. *Environmental Science & Technology, Vol 36*. 5106-5116, 2002.

Maymo-Gatell, X., Nijenhuis, I., Zinder, S. H. Reductive Dechlorination of *cis*-1,2-Dichloroethene and Vinyl Chloride by "*Dehalococcoides ethenogenes.*" *Environmental Science and Technology, Vol 35,* No. 3. 516-521, 2001.

McCarty, P. L. Breathing with Chlorinated Solvents. *Science, Vol 276,* No. 5318. 1521-1522, 1997.

McCarty, P.L., Semprini, L. Groundwater Treatment for Chlorinated Solvents. In: Handbook of Bioremediation. R.D. Norris and others, eds. Lewis Publishers, Boca Raton, pp 87-116, 1994.

National Research Council, (NRC). Alternatives for Ground Water Cleanup. Washington: National Academy Press, 1994.

NRC. Natural Attenuation for Groundwater Remediation. Washington: National Academy Press, Washington, 2000.

Newell, C. J., McLeod, R. K., Gonzales, J. BIOSCREEN Natural Attenuation Decision Support System, EPA /600/R-96/ 087, August, 1996.

Niederer, U. In Search of Truth: The Regulatory Necessity of Validation. In: Safety Assessment of Radioactive Waste Repositories: Validation of Geosphere Flow and Transport Models GEOVAL-1990. Swedish Nuclear Power Inspectorate (SKI) and the OECD Nuclear Energy Agency, Stockholm, 1990.

Nyer, E. K., Payne, F., Suthersan, S. Environment vs. Bacteria or Let's Play 'Name That Bacteria.' *Ground Water Monitoring & Remediation, Vol 23,* No. 1. 36-48, 2003.

Pankow, J., Cherry, J. Dense Chlorinated Solvents and other DNAPLs in Groundwater. Portland: Waterloo Pres, 1996.

Parr, J. C. *Application of Horizontal Flow Treatment Wells for* In Situ *Treatment of Perchlorate Contaminated Groundwater.* MS Thesis, AFIT/GEE/ENV/02M-08. School of Engineering and Management, Air Force Institute of Technology, (AU), Wright-Patterson AFB OH, March 2002.

Pebesma, E. J., Switzer, P., Loague, K. Error Analysis for the Evaluation of Model Performance: Rainfall-Runoff Event Time Series Data. *Hydrological Processes, in press.* Published online in Wiley InterScience (www.wiley.interscience.com), 2004.

Richardson, J. P., Nicklow, J. W. *In Situ* Permeable Reactive Barriers for Groundwater Contamination. *Soil and Sediment Contamination, Vol 11*, No. 2. 241-268, 2002.

Rittman, B.E., McCarty P.L. Environmental Biotechnology: Principles and Applications. McGraw Hill, 2001.

Regenesis, Inc. Personal correspondence. 2005.

Regenesis, Inc. ORC and HRC® Design Software for Barriers Using Slurry Injection. Available online at www.regenesis.com. 2002.

Rong, Y., Wang, R.F., Chou, R. Monte Carlo simulation for a groundwater mixing model in soil remediation of tetrachloroethylene. *Journal of Soil Contamination, Vol 7*, No. 1. 87-102, 1998.

Schlesinger, S., Crosbie, R. E., Gagne, R. E., Innis, G. S., Lalwani, C. S., Loch, J., Sylvester, R. J., Wright, R. D., Kheir, N., Bartos, D. Terminology for model credibility. *Simulation, Vol* 32. 103-104, 1979.

Schwartzenbach, R. P., Gschwend, P. M., Imboden, D. M. Environmental Organic Chemistry. John Wiley and Sons, 1993.

Semprini, L., McCarty, P. L.. Comparison between Model Simulations and Field Results for *In Situ* Biorestoration of Chlorinated Aliphatics: Part 1. Biostimulation of Methanotrophic Bacteria. *Groundwater, Vol* 29, No. 3, 365-374, 1991.

Sleep, B. E. Modeling Fate and Transport of Chlorinated Organic Compounds in the Subsurface. In: Contaminated Ground Water and Sediment. C.C. Chien and others, eds. Lewis Publishers, Boca Raton, pp 179-245, 2004.

Smatlak, C. R., Gossett, J. M., Zinder, S. H. Comparative kinetics of hydrogen utilization for reductive dechlorination of tetrachloroethene and methanogenesis in and anaerobic enrichment culture. *Environmental Science and Technology, Vol 30.* 2850-2858, 1996.

Stiber, N.A., Pantazidou, M., Small, M. J. Expert System Methodology for Evaluating Reductive Dechlorination at TCE Sites. *Environmental Science and Technology, Vol* 33, No. 17. 3012-3020, 1999.

Suthersan, S.S. Natural and Enhanced Remediation Systems. Lewis Publishers, Boca Raton, 2002.

TetraTech, Inc. Personal correspondence. 2004.

TetraTech, Inc. Groundwater Treatability Study Work Plan: Site 13 Cluster – Site 13 (ABRES-A Launch Complex), Site 14 (ABRES-A Lake), Site 28 (Missile Silo 395-B) Operable Unit 4. May 2003.

Travis, C. C., Doty, C. B. Can Contaminated Aquifers at Superfund Sites be Remediated? *Environmental Science and Technology*, *Vol 24,* No. 10. 1464-1466, 1990.

United States Environmental Protection Agency, (U.S. EPA). "Commonly Asked Questions Regarding the Use of Natural Attenuation for Chlorinated Solvent Spills at Federal Facilities," 20 May 1999.

U.S. EPA. "Technical Protocol for Evaluating Natural Attenuation of Chlorinated Solvents in Ground Water." EPA/600/R-98/128, September, 1998.

U.S. EPA. "Use of Bioremediation at Superfund Sites," Office of Solid Waste and Emergency Response Directive 542-R-01-019, 2001.

U.S. EPA. "Calculation and Use of First-Order Rate Constants for Monitored Natural Attenuation Studies," EPA/540/S-02/500, 2002.

United States Geological Survey (USGS). "Methodology for Estimating Times of Remediation Associated with Monitored Natural Attenuation," Water Resources Investigations Report 03-4057, 2003.

Vique, B. W., Koenigsberg, S. S. Bioremediation on the Fast Track. Water and Wastewater Products, July/August, 2003.

Vogel, T. M., Criddle, C. S., McCarty, P. L. Transformation of halogenated aliphatic compounds. *Environmental Science and Technology*, *Vol* 21, 722-736, 1987.

Vogel, T. M., McCarty, P. L. Biotransformation of tetrachloroethylene to trichloroethylene, dichloroethylene, vinyl chloride, and carbon dioxide under methanogenic conditions. *Applied Environmental Microbiology, Vol* 49, 1080-1083, 1985.

Wiedemeier, T. H., Rifai, C. J., Newell, J. T., Wilson, J. T. Natural Attenuation of Fuels and Chlorinated Solvents in the Subsurface. New York: John Wiley & Sons, Inc, 1999.

Vita

1st Lt Ryan C. Wood hails from Mission Viejo, California. He graduated from Mission Viejo High School in June, 1995 and entered undergraduate studies at the United States Air Force Academy in Colorado Springs, Colorado. He took a two year absence from the Academy to serve as a church missionary in Samara, Russia. After returning to the Academy, he graduated with a Bachelor of Science degree in Environmental Engineering in May 2001. He received his commission as an Air Force officer on 30 May 2001. He then spent two years with the 99th Civil Engineer Squadron at Nellis Air Force Base, Nevada. In August 2003, he entered the Graduate Engineering Management program of the Graduate School of Engineering and Management, Air Force Institute of Technology.

REPORT DOCUMENTATION PAGE

Form Approved
OMB No. 074-0188

1. REPORT DATE *(DD-MM-YYYY)*	**2. REPORT TYPE**	**3. DATES COVERED** *(From – To)*
21-03-2005	**Master's Thesis**	Sep 2003 – Mar 2005

4. TITLE AND SUBTITLE

Modeling Application of Hydrogen Release Compound to Effect *in situ* Bioremediation of Chlorinated Solvent-Contaminated Groundwater

5a. CONTRACT NUMBER

5b. GRANT NUMBER

5c. PROGRAM ELEMENT NUMBER

6. AUTHOR(S)

Wood, Ryan C., 1st Lt, USAF

5d. PROJECT NUMBER
If funded, enter ENR #

5e. TASK NUMBER

5f. WORK UNIT NUMBER

7. PERFORMING ORGANIZATION NAMES(S) AND ADDRESS(S)
Air Force Institute of Technology
Graduate School of Engineering and Management (AFIT/EN)
2950 Hobson Way
WPAFB OH 45433-7765

8. PERFORMING ORGANIZATION REPORT NUMBER

AFIT/GEM/ENV/05M-14

9. SPONSORING/MONITORING AGENCY NAME(S) AND ADDRESS(ES)
AFCEE/TD
Attn: Lt Col Mark Smith
3300 Sidney Brooks
Brooks City-Base
TX 78235 DSN: 240-3332

10. SPONSOR/MONITOR'S ACRONYM(S)

11. SPONSOR/MONITOR'S REPORT NUMBER(S)

12. DISTRIBUTION/AVAILABILITY STATEMENT
APPROVED FOR PUBLIC RELEASE; DISTRIBUTION UNLIMITED.

13. SUPPLEMENTARY NOTES

14. ABSTRACT
This study investigates how application of Hydrogen Release Compound (HRC®) might be implemented to remediate a site contaminated with tetrachloroethene (PCE) or its daughter products, under varying site conditions. The 3-D reactive transport model RT3D was coupled with a dual-Monod biodegradation submodel to simulate the effect of the hydrogen generated by HRC® on accelerating the biodegradation of dissolved chlorinated solvents. Varying site conditions and injection well configurations were investigated to determine the effect of these environmental and design conditions on overall treatment efficiency. The model was applied to data obtained at a chlorinated solvent contaminated site at Vandenberg AFB, where a pilot study of HRC® injection was conducted. Historical data were initially used to calibrate the model, under the assumption that natural reductive dehalogenation processes are occurring at the site. The model was then applied to predict how HRC® injection enhances natural attenuation processes. Model predictions were compared to the results of the pilot study. The model-simulated concentrations were relatively consistent with concentrations measured at the site, indicating the model may be a useful design tool, as well as an aid to help us better understand how HRC® injection may enhance natural attenuation of chlorinated solvents.

15. SUBJECT TERMS
Chlorinated solvents, reductive dehalogenation, TCE, hydrogen release compound, bioremediation, HRC

16. SECURITY CLASSIFICATION OF:			**17. LIMITATION OF ABSTRACT**	**18. NUMBER OF PAGES**	**19a. NAME OF RESPONSIBLE PERSON**
REPORT	**ABSTRACT**	**c. THIS PAGE**			Mark N. Goltz (ENV)
U	**U**	**U**	**UU**	134	**19b. TELEPHONE NUMBER** *(Include area code)* (937) 255-3636, ext 4638; e-mail: Mark.Goltz@afit.edu

Standard Form 298 (Rev: 8-98)
Prescribed by ANSI Std. Z39-18